THE UNIVERSITY
of EDINBURGH

Neuroepigenetics of Preterm White Matter Injury

Sarah Anne SPARROW

Doctorate of Medicine
The University of Edinburgh
2017

Table of Contents

Chapter 2: Materials and Methods

Declaration

I declare that this thesis is a presentation of my own original research.

Where others have contributed, I have made every effort to indicate this clearly.

The data presented has not been submitted for any other degree.

Dr Sarah A SPARROW

Edinburgh, UK

Acknowledgements

I would firstly like to thank my supervisors Dr James P Boardman and Amanda J Drake, for their hard work and endless support throughout this project. They provided me with the opportunity to initiate this work as well as wisdom and patience to help me complete it.

I would also like to extend a large thank you to Dr Jonathan Manning, for his hard work with the Bioinformatics processing of the epigenetic array data. A whole section of my work could not have been possible without his skills and knowledge.

I would like to thank Dr Jessy Cartier with her guidance and help with the pyrosequencing processing as well as Dr Yan Zeng for teaching me the PCR techniques.

The team at the Edinburgh Clinical Research Facility also have my gratitude for their excellent work in the processing of my methylation array. Receiving meaningful data after years spent collecting saliva was quite a special moment.

The members of 'Team Drake' including Dr Catherine Rose, Dr Khulan Batbayar, Dr Marcus Lyall and Dr Tom Chambers were so important over the last 4 years, for giving me inspiration, answering all my idiotic questions and keeping me laughing throughout my time in the laboratory. Dr Chinthika Piyasena, was a key member of this team, and I am so grateful to her for 'paving the way' with her earlier neonatal epigenetic work, for her help and support and for the use of some extra term control DNA when it was needed.

I'd like to thank all the members of the Clinical Research Imaging Centre, a vast team of people who are driven to ensuring high quality imaging based research. I am endlessly impressed by their knowledge and expertise. In particular, Dr Devasuda Anblagan, Dr Mark Bastin and Dr Scott Semple for teaching my inferior brain about physics and MRI data processing as well as their support with the logistics of MRI scanning.

The radiographers at the CRIC also deserve a special mention, particularly for their patience and humour when another baby had decided that a MRI scan was not on his/her list of priorities for the day.

In relation to this, there are two people who worked tirelessly alongside me - recruiting, organising and rocking babies back to sleep and these are Dr Rozalia Pataky and Dr Emma Telford. I cannot thank them enough for their enthusiasm and hard work.

I am also immensely grateful to my funders, Theirworld and Simpson's Special Care Babies. This work would not have been possible without their support.

I'd like to thank my husband Pete for his endless optimism, humour and ongoing efforts to keep me off junk food. Thank you for listening to my tales of work related woes and understanding when I'm too grumpy to talk in the morning.

To my colleagues in the Neonatal Transport team, my day and night (and day and night) job whilst researching, what can I say? Thank you for all the fun, food, midnight trips to Glasgow

and above all the immense professionalism you display looking after Scotland's smallest patients.

Lastly, I'd like to thank all the parents who consented to this research, and their precious cargo - the babies. Thank you for your faith in us and your time. Without these special families, there would be no data to write about.

List of Tables

List of Figures

4.2a Agreement of FA measurements in right PLIC

4.2b Agreement of FA measurements in left PLIC

4.2c Agreement of FA measurements in genu CC

4.3a Agreement of MD measurements in right PLIC

4.3b Agreement of MD measurements in Left PLIC

4.3c Agreement of MD measurements in genu CC

4.4a Agreement of FA in right PLIC/CST (PNT versus ROI)

4.4b Agreement of FA in left PLIC/CST (PNT versus ROI)

4.4c Agreement of FA in genu CC (PNT versus ROI)

4.5a Agreement of MD in right PLIC/CST (PNT versus ROI)

4.5b Agreement of MD in left PLIC/CST (PNT versus ROI)

4.5c Agreement of MD in genu CC (PNT versus ROI)

5.1 Qualification of optimal annealing temperature for F and R primers with gel electrophoresis

5.2 Differential Methylation between preterm infants at TEA and term controls at CpG sites in protein coding genes with neural function identified by Methylation Array

5.3 Pyrosequencing validation of selected neural genes: percentage methylation in preterm versus term control subjects

5.4 Illustration of segmented tracts overlaid on FA maps

List of Abbreviations

ADC mean diffusivity
ADHD attention deficit hyperactive disorder
AF arcuate fasciculus
AgCC agenesis of corpus callosum
ALS amyotrophic lateral sclerosis
APOL1 Apolipoprotein L1
ART artificial reproductive therapy
ASD autistic spectrum disorder
AuCD autophagic cell death
BA Bland Altman
BBB Blood-brain-barrier
BDNF brain derived neurotrophic factor
BMI body mass index
BPD bronchopulmonary dysplasia/chronic lung disease
BSID Bayley scale of infant and toddler development
CB cingulum bundle
CCG cingulum cingulate gyrus
CGA corrected gestational age
CNS central nervous system
CP cerebral palsy
CpG Cytosine-phosphate-guanine
CRF corticotrophin-releasing factor
CRIC clinical research imaging centre
CSF cerebrospinal fluid
CST corticospinal tract
Dav mean diffusivity
DCE-MRI dynamic contrast enhanced MRI
DHESI diffuse excessive high intensity
DMR differentially methylated regions
DNA Deoxyribonucleic acid
DNAm DNA methylation
DNMT DNA methyl transferase
DTI diffusion tensor imaging
DWI diffusion weighted image
DQ developmental quotient
ECG electrocardiogram
EDTA disodium ethylenediamine tetraacetate.$2H_2O$
ELBW extremely low birth weight (less than 1000 grams)
EPT extremely preterm (less than 26 weeks' gestation at birth)
EtOH ethanol
EWAS Epigenome-wide association study
FA fractional anisotropy
FDR false discovery rate
5mC 5-methylcytosine

FOF fronto-occipital fasciculus
GA gestational age
gCC genu of corpus callosum
G-CSF granulocyte colony-stimulating factor
GD Gestational diabetes
GM-CSF granulocyte-macrophage colony-stimulating factor
GR glucocorticoid receptor
GRIK5 Glutamate Ionotropic Receptor Kainate Type Subunit 5
HCA histological chorioamnionitis
HDAC histone deacetylase
HPA hypothalamic–pituitary–adrenal axis
HPI haemorrhagic parenchymal infarction
ICC Intraclass Correlation Coefficients
IFN Interferon
ILF inferior longitudinal fasciculus
IUGR intrauterine growth restriction
IVH intraventricular haemorrhage
KO knockout
LOS late onset sepsis
LPS Lipopolysaccharide
LRG1 Leucine-rich alpha-2-glycoprotein 1
LTP Long term potentiation
MCHR1 Melanin-concentrating hormone receptor 1
MD Mean diffusivity
$MgSO_4$ Magnesium Sulphate
MLF middle longitudinal fasciculus
MRI magnetic resonance imaging
NEC necrotising enterocolitis
NPBWR1 Neuropeptides B/W Receptor 1
OFC occipital-frontal circumference of head
PBMC peripheral blood mononuclear cells
PC principle component
PCR polymerase chain reaction
PLIC posterior limb of internal capsule
PLOSL Polycystic Lipomembranous Osteodysplasia with Sclerosing Leukoencephalopathy
PMA post menstrual age
PNT probabilistic neighbourhood tractography
pre-OL premyelinating oligodendrocyte
PRPH Peripherin
PVL periventricular leukomalacia
QPRT quinolinate phosphoribosyltransferase
R goodness-of fit of the segmented tract to the reference
RF radiofrequency
RNS reactive nitrogen species
RNA ribonucleic acid
ROI regions of interest

ROS reactive oxygen species
RTT Rett Syndrome
SAM S-adeosylmethionine
SD standard deviation
SEN Special Educational Needs
SGA small for gestational age
SLC1a2 Solute Carrier Family 1 (Glial High Affinity Glutamate Transporter), Member 2
SLC7a5 Solute Carrier Family 7 (Amino Acid Transporter Light Chain, L System), Member 5
SLF superior longitudinal fasciculus
TBE Tris/Borate/EDTA
TE Tris-EDTA
TEA term equivalent age
TPN total parenteral nutrition
TREM2 Triggering receptor expressed on myeloid cells 2
UF uncinate fasciculus
VLBW very low birth weight (less than 1500 grams)
VPT very preterm (less than 32 weeks' gestation at birth)
VTA Ventral tegmental area
WM white matter

Abstract

Introduction: Preterm birth is increasing worldwide and is a major cause of neonatal death. Survivors are at increased risk of neurodisability, cognitive, social and psychiatric disorders in later life. Alterations to the white matter can be assessed using diffusion tensor imaging (DTI) MRI and are associated with poor neurodevelopmental outcome. The pathogenesis of white matter injury is multifactorial and several clinical risk and resilience factors have been identified. DNA methylation (DNAm) is an epigenetic process which links stressful early life experience to later life disease and is associated with normal brain development, neuronal processes and neurological disease. Several studies have shown DNAm is altered by the perinatal environment, however its role in preterm white mater injury is yet to be investigated.

Aims: 1. To examine the relationship between preterm birth and white matter integrity 2. To investigate the effect of neuroprotective treatments and deleterious clinical states on white matter integrity in preterm infants 3. To assess the best DTI method of quantifying white matter integrity in a neonatal population 4. To investigate the effect of preterm birth on DNA methylation and 5. To determine the clinical and imaging factors that contribute to the variance in DNA Methylation caused by preterm birth

Methods: DTI data was acquired from preterm infants (< 32 weeks' gestation or < 1500 grams at birth) at term equivalent age (TEA) and term controls (> 37 weeks' gestation at birth). Region-of-interests (ROI) and tract-averaged methods of DTI analysis were performed to obtain measurements of fractional anisotropy (FA) and mean diffusivity (MD) in the genu of corpus callosum, posterior limb of internal capsule and centrum semiovale. Clinical data was collected for all infants and the effect of prematurity, neuroprotective agents and clinical risk

factors on white matter integrity were analysed. 8 major white matter tracts were segmented using probabilistic neighbourhood tractography (PNT), a tract-averaged technique which also allowed the calculation of tract shape. The two DTI techniques were compared to evaluate agreement between results. DNA was collected from preterm infants and term controls at TEA, and a genome-wide analysis of DNAm was performed. DTI parameters from probabilistic neighborhood tractography (PNT) methodology and clinical risk and resilience factors were used to inform a principal components analysis to investigate the contribution of white matter integrity and clinical variables to variance in DNAm.

Results: FA and MD were significantly affected by preterm birth on ROI analysis. In addition, DTI parameters were affected by clinical factors that included antenatal magnesium sulphate, histological chorioamnionitis and bronchopulmonary dysplasia. Evaluation of DTI methodology revealed good accuracy in repeated ROI measurements but limited agreement with tract-averaged values. Differential methylation was found within 25 gene bodies and 58 promoters of protein-coding genes in preterm infants, compared with controls. 10 of these genes have a documented association with neural function or neurological disease. Differences detected in the array were validated with pyrosequencing which captured additional differentially methylated CpGs. Ninety-five percent of the variance in DNAm in preterm infants was explained by 23 principal components (PC); corticospinal tract shape associated with 6th PC, and gender and early nutritional exposure associated with the 7th PC.

Conclusions: Preterm birth is associated with alterations in white matter integrity which is modifiable by clinical risk factors and neuroprotective agents. ROI analysis may not provide sufficient representation of white matter tracts in their entirety. Prematurity is related to alterations in the methylome at sites that influence neural development and function.

Differential methylation analysis has identified several promising candidate genes for future work and contributed to the understanding of the pathogenesis of preterm brain injury.

Lay Summary

Introduction: Preterm birth, defined as being born less than 37 weeks' gestation is increasing worldwide. Preterm infants are at increased risk of disability including cerebral palsy and problems with behavior, learning and mood in later life. A specialised imaging technique (DTI-MRI) can assess the microscopic brain injury associated with preterm birth and results are linked to how an infant develops and learns. There are many underlying reasons which lead to brain injury in preterm infants but there are also 'neuroprotective' treatments which can improve brain development. DNA methylation (DNAm) is a genetic process which allows the environment we experience to alter how our genes are 'read' and therefore causes changes in how our bodies function. The role of DNAm in premature brain injury is yet to be investigated.

Aims: To investigate the relationship between preterm birth and microscopic changes to specific regions of the brain and to investigate how neuroprotective treatments and harmful clinical experiences affect this. To assess two different methods of analysing DTI-MRI to determine which was preferable for use in newborn infants. To investigate the effect of preterm birth on DNA methylation and to determine if any clinical factors and microscopic brain changes will affect DNAm in preterm infants.

Methods: Parental consent was given before enrolment in to the study. Preterm infants were defined as <32 weeks' gestation or <1500g at birth, with term control infants being >37 weeks' gestation. They underwent MRI imaging at term-equivalent age (between 38 and 42 weeks) and had saliva collected for DNA. Two methods (ROI and PNT) for assessing the brain white matter changes were used for analysis and their results were compared. DNAm was assessed

using a technique which looks at the entire genetic code. Statistical analysis was used to compare clinical factors and results from the PNT analysis with DNAm.

Results: Preterm birth was negatively associated with microscopic changes in brain development, which also may be negatively affected by intrauterine infection or lung disease in the preterm infants but improved by an antenatal neuroprotective treatments - magnesium sulphate. When I compared two different DTI techniques they produced results with limited agreement and I concluded that PNT gave a better representation of the brain microscopic development. DNA methylation was different between preterm infants and term controls in the middle of 25 genes and the starting sequence of 58 others. 10 of these genes have a documented association with brain function or disease. There was a subtle effect on DNAm from some clinical factors.

Conclusions: Preterm birth is associated with microscopic changes to the brain which may be affected by infection, lung disease and the neuroprotective therapy – magnesium sulphate. PNT analysis may be preferable over ROI analysis to investigate the newborn brain. Preterm birth is related to changes in DNA methylation in several genes involved in brain development and function. This work has contributed to the understanding of preterm brain injury and may lead to future therapies which will improve outcome.

Chapter 1: Introduction

1.1 Prematurity and Brain injury

1.1.1 Definition, Incidence and Clinical burden of Preterm Birth

Preterm birth, by definition being born at less than 37 weeks' gestation, is increasing with recent data showing that worldwide over 1 in 10 infants are born prematurely (Blencowe H et al, 2012). It is the single most important cause of death within the first month of life (Liu L et al, 2012), with 2/3^{rds} of UK neonatal deaths being attributable to prematurity (Wolfe I et al, 2014).

With advances in neonatal medicine, survival to discharge rates have improved dramatically from 40% in 1995 to 53% in 2006, in UK infants born at less than 26 weeks' gestation (Costeloe K et al, 2012). However, the survivors of preterm birth have an increased risk of neurodevelopmental problems, with 19-21% of <26 weeks gestation infants having severe disability and 12-14% developing cerebral palsy (Moore T et al, 2012; Marlow N et al, 2005).

As well as severe disability, preterm survivors have increased risk of cognitive, social, behavioural and later life psychiatric disorders. This is evidenced by literature which shows the following:

1. Gestational age at birth has a significant dose-dependent relationship with special educational needs (SEN) (MacKay DF et al, 2010), with 57% of extreme preterm infants (gestational age < 25 weeks) having SEN and 13% requiring special school provision (Johnson S et al, 2009).

2. Children who are born at less than 33 weeks have been shown to have reduced social competence including more peer relationship difficulties (Ritchie K et al, 2015).

3. There is an increased risk of screening positive for autism or autistic spectrum disorder (ASD) in both extreme preterm (EPT <26 weeks gestation) (Johnson S et al, 2010a) and late

preterm (32 to 36 weeks' gestation) infants (Guy A et al, 2015), with other studies quoting a 65-fold increase in the prevalence of ASD compared to the general population in extremely preterm children (Johnson S et al, 2011).

4. There is a gestational effect related to the most common behavioural deficit found in preterm infants, attention deficit (Sucksdorff M et al, 2015) with a prevalence of 9 to 11% in VPT (very preterm, <32 weeks gestation at birth) or VLBW (very low birthweight, <1500 grams) which rises to 17 to 20% in EPT or ELBW (extremely low birthweight, <1000 grams) infants (Johnson S et al, 2011).

5. And finally, individuals who were born preterm have an increased risk of developing psychiatric problems including anxiety (OR 3.5) and emotional disturbances (OR 4.6), (Johnson et al, 2010b) depression, psychosis and need for psychiatric hospitalisation (Nosarti C et al, 2012).

1.1.2 Preterm Brain Injury

There is a wide range of brain injury associated with preterm birth and altered neurodevelopmental outcome. Depending on their pathology, these changes may be diagnosed by neuroimaging techniques such as cranial ultrasound and MRI and may be seen on macroscopic and microscopic pathological examination of the brain. They include intraventricular haemorrhage (IVH), post haemorrhagic cystic degeneration and periventricular leukomalacia (PVL).

1.1.2.1 Haemorrhagic Injury

IVH is a common occurrence in preterm infants with 20-25% of VLBW infants developing some degree of IVH (McCrea HJ & Ment LR, 2008). It can be categorised as grade I – haemorrhage within the germinal matrix, grade II – intraventricular blood without ventricular dilatation,

grade III – intraventricular blood with ventricular dilatation and grade IV – parenchymal haemorrhage (Papile LA et al, 1978). IVH most often occurs within the 24 hour period after delivery, with most lesions reaching full extent by 7 days of age (McCrea HJ & Ment LR, 2008). The risk of developing IVH is altered by perinatal characteristics including gestational age, intrauterine growth restriction (IUGR), exposure to antenatal steroids, male gender, foetal distress and intrauterine infection (Heuchan A et al, 2002; Linder N et al, 2003 & Alexander JM et al, 1998). It is significantly associated with altered neurodevelopmental outcome, which worsens according to its severity, with an increased risk of cerebral palsy (OR 1.72 for grades I-II & 5.99 for grades III-IV) and with neurosensory impairment (OR 2.06 for grades I-II & 5.49 for grades III-IV) found in infants born at less than 28 weeks' gestation (Bolisetty S et al, 2014). IVH, in particular grade IV, may be associated with subsequent cystic degeneration of the white matter, which sees deletion of neurons, axons and glia within these necrotic lesions (Back SA & Miller SP, 2014). However, the pathophysiology of neurological damage as a consequence of IVH is not completely understood and may include iron activation of reactive oxygen species (Savman K et al, 2001) and alterations in neuronal precursor cell proliferation within the germinal matrix (Del Bigio MR, 2011).

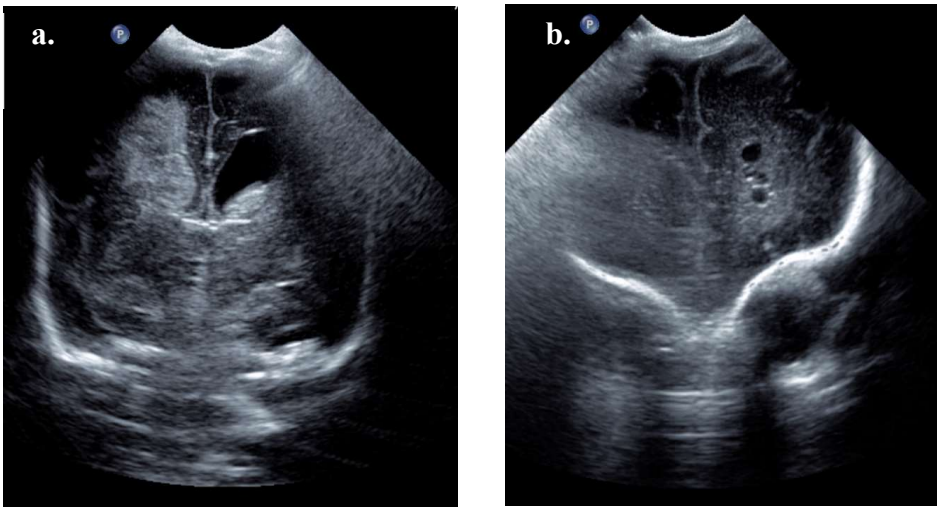

Figure 1.1 (A) Cranial ultrasound appearance of grade IV intraventricular haemorrhage and dilated ventricles and (B) left sided porencephalic cysts (anonymised images from Simpson Centre for Reproductive Health, Edinburgh UK)

1.1.2.2 White Matter Injury

Injury to the developing white matter in preterm infants and animal models presents as a spectrum where myelination failure is associated with diffuse white matter changes as well as macroscopic and microscopic focal cystic lesions. It generally occurs near the lateral ventricles and is therefore described as periventricular leukomalacia (PVL).

Macroscopic cystic PVL involves the degeneration of all cell types including glia and axons however it is less common than other types, being diagnosed in <5% of MRI studies (Black SA & Miller SP, 2014).

Microscopic cystic PVL, with lesions measuring <1mm in diameter are not visualised on MRI but may be diagnosed on neuropathological examination. Analysis of these lesions demonstrate their association with axonal degeneration and phagocytic macrophages (Black SA & Miller, 2014).

The most prevalent form of white matter injury (WMI) diffuse PVL is characterised by loss of pre-myelinating oligodendrocytes with subsequent hypomyelination, astrogliosis and microglial infiltration (Khwaja O & Volpe JJ, 2008). The forms of PVL are shown in figure 1.2 below.

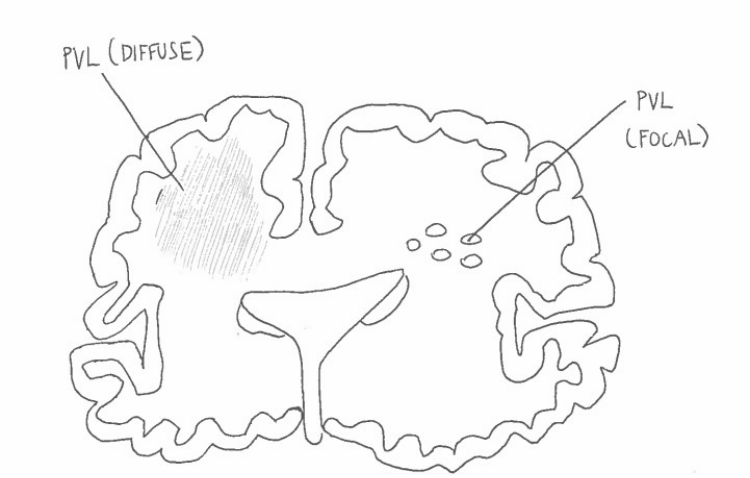

Figure 1.2 Cross sectional drawing of cerebrum depicting cystic (focal) PVL – white dots and non-cystic (diffuse) PVL as grey shading

In the initial phase of white matter injury, there can be damage to 2 important cell types, the premyelinating oligodendrocyte (pre-OL) a glial cell precursor, and the neuronal axon.

1.1.2.2a Axonal Degeneration

Axonal injury and degeneration is a prominent feature where there is necrosis of the white matter, such as occurs in microscopic and macroscopic cystic PVL. It is thought that more severe hypoxic-ischaemic insult may select this pathologically distinct form of PVL. In contrast, milder hypoxic-ischaemic events may lead to diffuse PVL, which is less associated with axonal degeneration and more with dysregulation of the pre-OL (Black SA & Miller SP, 2014).

1.1.2.2b Pre-Oligodendrocyte Dysregulation and Diffuse WMI

The pathogenesis of diffuse white matter injury is multifactorial and involves upstream mechanisms including hypoxia/ischaemia and infection/inflammation as well as downstream mechanisms including microglia activation, excitotoxic processes and free radical attack (Khwaja O & Volpe JJ, 2008).

Preterm infants are particularly susceptible to these mechanisms as a result of their clinical environment. Foetal distress around the time of birth, instability due to lung immaturity or

subsequent infections may lead to periods of hypoxia. These insults occur during a time period where the development of cerebral arteries is incomplete and may ultimately subject areas of the brain to severe ischaemia (Volpe JJ, 2001). Furthermore, infection and inflammatory processes are common events; chorioamnionitis affecting 40-70% of spontaneous onset preterm births (Yoon BH et al, 2001) and up to 25% of VLBW infants having at least one episode of late onset sepsis (Dong Y & Speer CP, 2015).

During the preterm period, pre-OLs are the dominant oligodendrocyte cell lineage and this compounds the susceptibility of the preterm brain to white matter injury. Maturity-dependent intrinsic properties of the pre-OL include an increased vulnerability to free radical attack (Khwaja O & Volpe JJ, 2008) and an increase in glutamate receptor expression (which mediates excitotoxic apoptosis) compared to more mature oligodendrocytes (Volpe JJ et al, 2011). Additionally, microglia are particularly concentrated in white matter during the third trimester (Billiards SS et al, 2006) and their activation causes release of free radicals, harmful cytokines and augmentation of excitoxicity (Volpe JJ et al, 2011). These processes are summarised in figure 1.3 below.

Figure 1.3 Upstream and downstream mechanisms in the pathogenesis of periventricular leukomalacia

(IVH = Intraventricular Haemorrhage, RNS = Reactive Nitrogen Species, ROS = Reactive Oxygen Species). Adapted from Volpe JJ et al, Int J Dev Neurosci 2011 & Fields RD, Nature Reviews Neuroscience 2015)

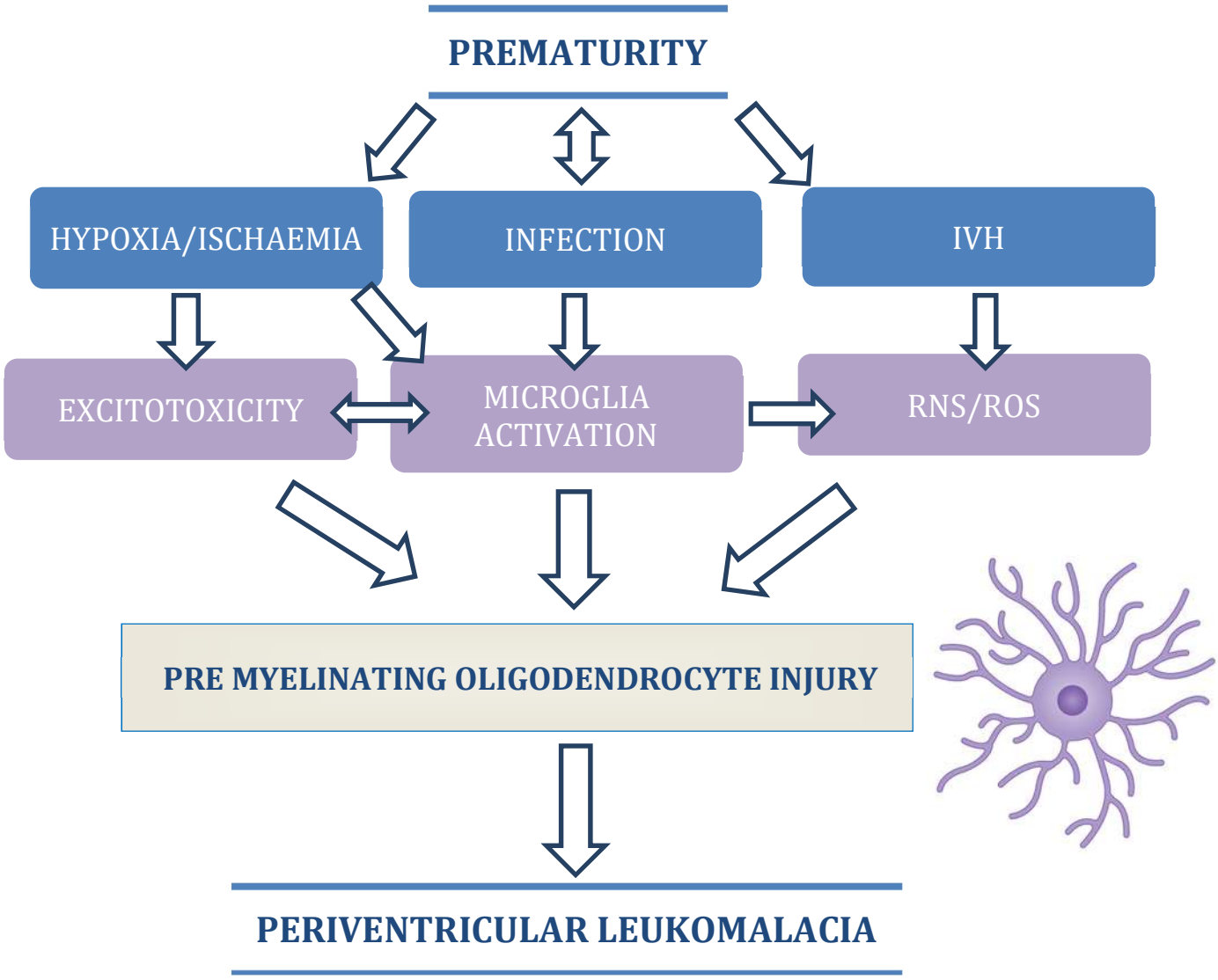

1.1.3 White Matter Structures and their Role in Disease

The dysregulation of myelination associated with preterm WMI is not only manifest as PVL but also as abnormal growth and development of major white matter structures throughout the brain. The most widely studied white matter areas in preterm research being the major white matter fasciculi of the corpus callosum, the posterior limb of the internal capsule, the corticospinal tracts, the inferior longitudinal fasciculi, the cingulate and the white matter of the centrum semiovale. Before examining the role of these structures in preterm white injury, it is worth understanding their normal structure and function.

1.1.3.1 The Corpus Callosum

The corpus callosum is the largest white matter structure in the brain and the major transverse interhemispheric commissure (Thompson DK et al, 2011).

It was first classified into seven geometric dissectible regions by Witelson (Witelson SF, Brain 1989). The anterior section is known as the genu, the posterior as the splenium and the middle is referred to as the midbody (which is further divided in to anterior, middle and posterior midbody). Between the body and the splenium, there is a thinner segment known as the isthmus. The rostrum is anterior to the genu but curves backwards in posterior/inferior position. The structure of the corpus callosum is demonstrated in figure 1.4.

The basic structure of the corpus callosum is thought to be complete by 18-20 weeks gestation, but continues to grow in size over the 3rd trimester (Malinger G and Zakut H, 1993). Although the number of fibres is fixed by full term (Lunders E et al, 2010), growth and maturation continues in to early adulthood (Giedd JN et al, 1996 & Tanaka-Arakawa MM et al, 2015). Studies have shown that maturational changes include increasing size of the whole structure but decreasing MRI signal intensity, which at a microstructural level may be related

to maturation of the axonal cytoskeleton increasing axonal size and myelination (Keshavan M et al, 2002).

Figure 1.4 Regions of the Corpus Callosum

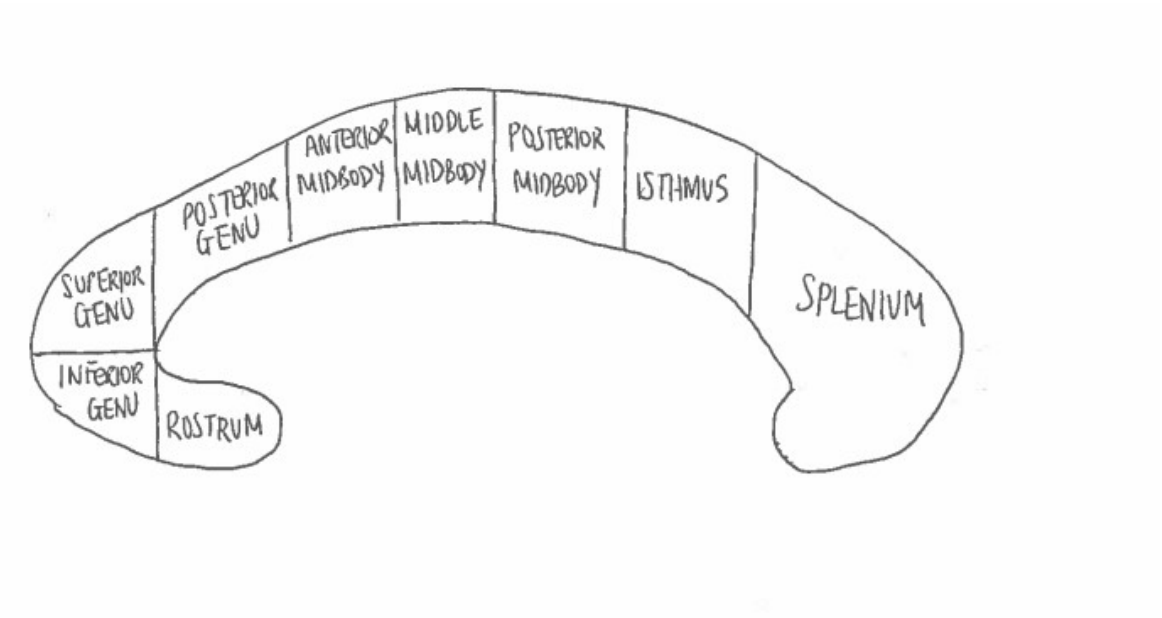

Congenital abnormalities of the corpus callosum, including complete agenesis (AgCC) occur in 1.8 in 10,000 live births (Glass HC et al, 2008). Although AgCC does not affect IQ scores or overall cognitive ability, it may cause problems with more sophisticated language skills and complex problem solving. Individuals with AgCC have been shown to have problems with understanding non-literal language and humour and may have poor conversational skills and difficulty verbalising emotions (Paul LK, 2011). These individuals also may have problems with attention; have difficulties with social self-awareness and display aggressive behaviour. This may lead to complications with social interactions and indeed there are similarities with individuals who are on the autistic spectrum (**Badaruddin DH, 2007)**.

1.1.3.2 The Corticospinal Tract

The posterior limb of the internal capsule (PLIC) lies between the thalamus and the lentiform nucleus of the basal ganglia. It contains corticospinal (CST) tract fibres (Gan C & Maingard J, Radiopedia) as well as descending tract fibres from the parietal, temporal, and occipital lobes (Schmahmann JD et al, 2008).

With regards to development, myelination of the CST occurs in the cranial direction, with posterior portions of the PLIC showing increased signal on T1 weighted images by 38-40 weeks (Counsell SJ et al, 2002) and continues until 14 months of age (Deoni SCL et al, 2011). The absence of any myelination at term equivalent age (visualised using structural MRI, T1 weighted sequence) has implications for neurodevelopment and is a risk for the development of hemiplegia (de Vries LS, 1999). Additionally, both macrostructural and microstructural asymmetry of the PLIC after periventricular haemorrhage, is significantly associated with unilateral spastic cerebral palsy, demonstrating that the CST has a major role in voluntary motor function (Roze E et al, 2015).

1.1.3.3 The Centrum Semiovale

The centrum semiovale (CSO) lies superiorly to the lateral ventricles and inferiorly to the cerebral cortex. It contains projection, commissural and association fibres (Gan C & Maingard J, Radiopedia).

Projection fibres include striatal fibres that pass to the basal ganglia, pontine fibres which project to lower brain structures and the spinal cord and thalamic fibres. The commissural fibres are those which connect contralateral hemispheric regions, whereas association fibres travel between ipsilateral cortical areas and include local, neighbourhood and long association fibres (Schmahmann JD et al, 2008).

From disconnection observational studies, animal work and more recently advanced imaging techniques, the long association fibres can be characterised and functions elucidated. They include: The superior longitudinal fasciculus (SLF) and its three subcomponents, which are involved in proprioception, the initiation of motor activity, attention, visual awareness and articulating language. The arcuate fasciculus (AF) and the extreme capsule, both important for language and the middle longitudinal fasciculus, (MLF) which also deals with spatial organisation and memory. The uncinate fasciculus (UF) and inferior longitudinal fasciculus, (ILF) which appear to be significant in emotional visual processing. The fronto-occipital fasciculus (FOF) that is involved in visual spatial information and finally, the cingulum bundle (CB) that assists the emotional reaction to somatic sensation and nociception as well as having a role in attention, motivation, and memory (Schmahmann JD et al, 2008).

Compared to the PLIC and corpus callosum, the centrum semiovale is later to mature and myelinate (Huppi PS et al, 1998). Measurements relating to microstructural maturation and myelination begin to increase in the MLF and UF at birth, the IFOF and ILF at 4 months of age and SLF by 12 months of age (Welker KM & Paton A, 2012).

1.2 Imaging Preterm Brain Injury

Currently, standard practice for imaging of the preterm brain within the UK involves sequential cranial ultrasound. This imaging modality can reliably detect gross lesions such as IVH, cystic PVL and ventricular dilatation or hydrocephalus (Stewart AL et al, 1983 & de Vries LS et al, 2004), however the use of MRI at term equivalent age (TEA, 38 -42 weeks corrected gestation) allows closer inspection of diffuse white matter injury (Maalouf EF et al, 2001 & Inder TE et al, 2003).

Conventional MRI allows qualification of brain maturation and injury at a macroscopic level, however advanced MRI techniques including diffusion tensor imaging (DTI) enables examination of brain tissue at the microstructural level and quantification of its development and organisation.

1.2.1 Physics of Conventional MRI and Diffusion Tensor Imaging

Before exploring the role of conventional and advanced MRI imaging in mapping preterm brain injury, it is worth having a basic understanding of the physics involved with these imaging processes.

1.2.1.1 Conventional MRI

The soft tissue of the body is composed mostly of water (H_20), and each molecule contains two ^1H which have a net magnetic moment capable of interacting with the MRI scanner. During MR imaging, a radiofrequency (RF) pulse is applied causing a change in the eigenstate of the ^1H protons from spin up (low energy) to spin down (high energy). As they relax after excitation and return from spin down to spin up, they precess about the static magnetic field and induce a current in the receiver coil, which can be measured. The ^1H protons in different

tissues relax at different rates and this causes the contrast which creates the MRI image we see (Hendee WR & Rietnour ER, 2002 and Graham DT et al, 2006).

T1 Weighted MRI Sequence

Within the brain, T1 sequences give good differentiation between white matter and grey matter. This sequence shows the differences in the 'spin-lattice relaxation time'. Spin-lattice relaxation occurs as the protons release the energy they absorbed from a RF pulse. The 'lattice' is the surrounding tissue, and this is heated up as the spins recover from a high energy state to a low energy state, which re-establishes thermal equilibrium. T1 relaxation time is different in every tissue and in general is longer where the magnetic field strength (measured in units of Tesla from 0.5 to 3) is higher (NessAvier M, 2008)

T2 Weighted MRI Sequence

In T2 sequences of the brain, cerebrospinal fluid (CSF) shows up lighter than the surrounding brain matter. T2 describes the signal decay, or the loss of coherence (MRI signal) between spins after the initial RF pulse. It is due to spin to spin as well as spin-lattice interactions but does not take in to account magnetic field inhomogeneities. Similarly to T1, it is different in every type of tissue and is less affected by the magnetic field strength (NessAvier M, 2008).

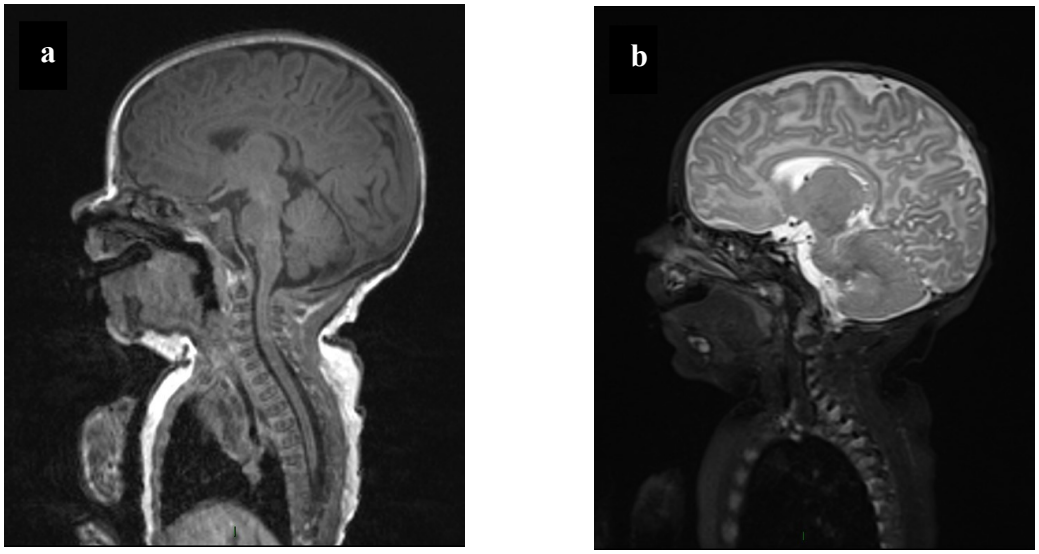

Figure 1.5 MRI imaging of the normal neonatal brain with a. T1w sequence and b. T2w sequence shown (anonymised images from Clinical Research Imaging Centre, Edinburgh UK)

1.2.1.2 Diffusion Tensor Imaging

Diffusion tensor imaging was first introduced in to clinical practice in the 1990s. It is based on the theory of 'Brownian motion' which describes the random motion of molecules due to heat (Mukherjee P et al, 2008). The movement of water molecules by Brownian motion can be described graphically by a 3D ellipsoid. Diffusion of water molecules is restricted by the tissue microstructure, reducing the apparent rate of diffusion; the axes of the ellipsoid indicate the apparent diffusion coefficient in each direction. The orientations of the axes of the ellipsoid are dependent on eigenvectors and their length on eigenvalues (λ1, λ2 and λ3) which represent diffusion along the tensor axes (Huppi PS & Dubois JS, 2006). Within biological matter, water molecules will diffuse differently according to tissue type, its underlying architecture and microstructural barriers (Soares JM et al, 2013). For example, in the brain CSF water diffuses equally in all directions (termed isotropic motion) and hence the ellipsoid is spherical in shape. In white matter, the diffusion of water has a directional quality (termed anisotropic). White matter is organised into bundles and the neuronal fibres are surrounded by myelin which insulates by decreasing the membrane permeability. As such, diffusion of water is faster parallel to the fibres than perpendicular. The more organised the white matter is, the higher the anisotropy will be. In this situation, the diffusion tensor is cigar shaped (Huppi PS & Dubois JS, 2006). This is shown in more detail in figure 1.6.

Figure 1.6 The diffusion tensor ellipsoid

a. Eigenvectors determining direction and eigenvalues length of each axis. b. In CSF the ellipsoid is spherical and in c. white matter it is cigar shaped

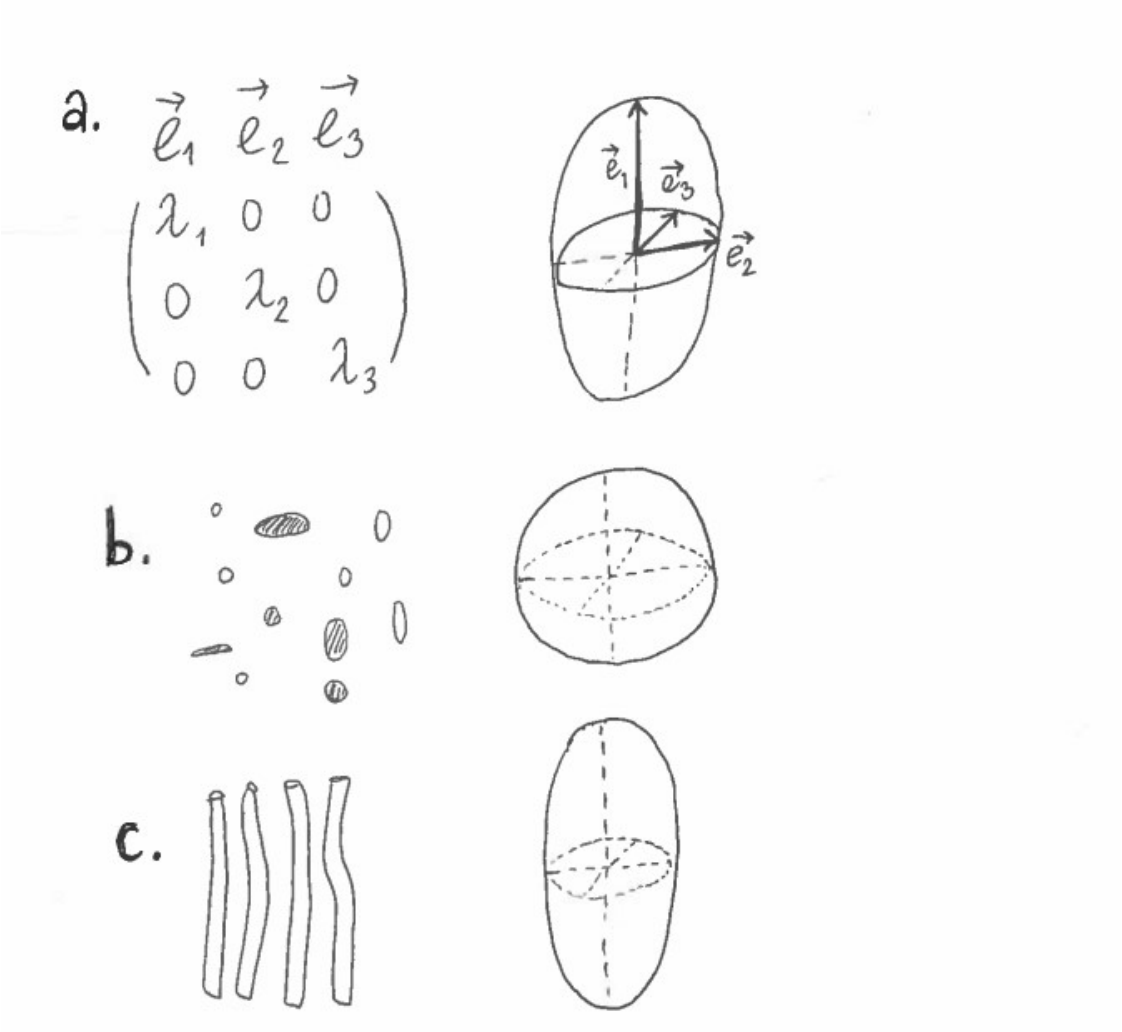

To measure this diffusion of water using MRI, the Stejskal-Tanner imaging sequence is used. This applies two equally strong but opposite gradient pulses around a 180 degree refocusing pulse. The first pulse causes a phase shift for all spins; the second cancels this out if there has been no net movement of water. However, if there is movement due to Brownian motion the spins are not completely refocused and there is signal loss which can be measured (Westin CF et al, 2002).

Within a particular voxel, quantitative measures of diffusion can be calculated – the fractional anisotropy and mean diffusivity. Mean diffusivity (ADC, Dav, MD) is the mean of the 3 eigenvalues and describes the directionally averaged diffusivity of water with higher rates reflecting more water diffusion in a particular tissue (MD in free water at body temperature is approximately 3.0×10^{-3} mm^2/s) and lower signal intensity in the diffusion weighted image (Mukherjee P et al, 2008, Huppi PS & Dubois JS, 2006). Fractional anisotropy (FA), describes the overall directionality of the water diffusion and an indication of the ellipsoid shape (Alexander AL et al, 2007). FA is 0 in tissues where the diffusion is completely isotropic and moves towards 1 where there is total anisotropy (Huppi PS & Dubois JS, 2006).

There are several methods for analysing the quantitative measures of diffusion and these include region-of-interest based and tract-based approaches. Region-of-interest is the more traditional DTI approach which may be the only option in some clinical software packages. It performs calculations on the original MRI slice, this eliminating post processing errors (Hakulinen U et al, 2012). However, it has been shown to have low repeatability (Bisdas S et al, 2008) and high variability (Bonekamp D et al, 2007). Tract-based approaches average FA and MD for the entire white matter fibre bundle however data can be affected by image artefact or crossing tracts (Alexander AL et al 2007).

MD and FA are not fixed in a particular tissue throughout development and within the brain, alterations in their values are felt to reflect changes in water content, myelination, growth and organisation of neuronal tissue. Generally, MD values fall with increasing age and this is related to the water content of the brain lessening as an individual matures. In addition, structures that restrict water movement - such as axons - become more densely packed and organised. FA values increase with age and this is observed in line with myelination of a particular white matter structure. It is also seen pre-myelination where it is explained by histological changes including axonal membrane permeability, the presence of microtubule-associated proteins, increases in axonal calibre and increases in oligodendrocytes (Huppi PS & Dubois JS, 2006).

1.2.2 Imaging the Developing Brain in relation to Neurodevelopmental Outcome

1.2.2.1 Conventional MRI

MRI of preterm infants at TEA allows closer inspection of white matter changes such as diffuse WMI and allows examination of the posterior limb of internal capsule and cerebellum which are difficult to visualise on cranial ultrasound (Maalouf EF et al, 2001 & Inder TE et al, 2003).

In a study of 167 VPT infants, Woodward et al categorised the preterm MRI brain phenotype into categories of white matter abnormalities and showed that moderate to severe changes were highly predictive of cognitive delay (OR 3.6), motor delay (OR 10.3), cerebral palsy (OR 9.6) and neurosensory impairment (OR 4.2) (Woodward LJ et al, 2006).

However, the specificity of conventional MRI to predict survival without cerebral palsy is similar to cranial ultrasound (85 to 96%) where no major abnormalities are present (Valkama AM et al, 2000; Mirmiran M et al, 2004; Woodward LJ et al, 2006; de Vries LS et al, 2011) and although it is more sensitive (60 to 92%) than cranial ultrasound to predict survival with CP, reported confidence intervals are wide (Valkama AM et al, 2000; Mirmiran M et al, 2004; Woodward LJ et al, 2006; Skiold B et al, 2012).

Therefore, current British Association of Perinatal Medicine guidance is to obtain a structural MRI for preterm infants at TEA only if there is evidence of parenchymal injury on cranial ultrasound scans or in the context of unexplained abnormal neurological signs (BAPM, 2015).

Figure 1.7 Classification of white matter abnormalities on T2 weighted MRI.

a. Normal MRI appearance b. Mild WM abnormalities c. Moderate WM abnormalities and d. Severe WM abnormalities characterised by 'increasing ventricular size, decreasing white-matter volume and increasing intensity of white-matter signal' (Reproduced with permission from Woodward LJ et al, NEJM 2006, Copyright Massachusetts Medical Society).

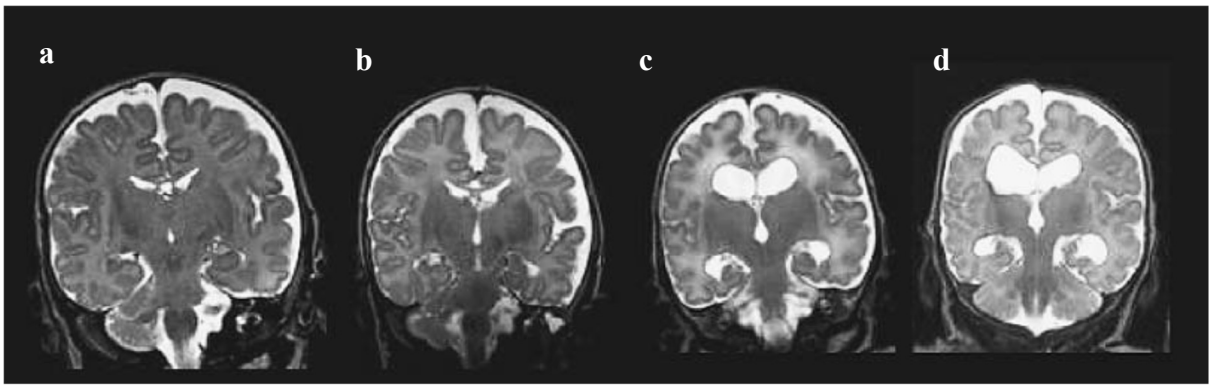

1.2.2.2 Diffusion Tensor Imaging

It is known that the quantitative measures of FA and MD are dynamic with increasing age and gestation (Huppi PS et al, 1998, Huppi PS & Dubois JS, 2006).

However, it has been shown that the underlying processes of development (myelination and white matter structural maturation) can be disrupted in preterm white matter injury. The effects of these injurious processes can be seen on structural MRI and can also be quantified using DTI. A study of serial MRI scans over 2-6 weeks after birth and again at term corrected age, showed that MD does not decrease and FA does not increase with increasing age in preterm infants with moderate white matter disease compared to those without (Miller SP et al, 2002). In addition, the appearance of white matter injury visible as DEHSI (diffuse excessive high intensity) on structural MRI is associated both with increases in MD compared to preterm infants without (Counsell S et al, 2006) and a reduction in relative anisotropy at the site of primary injury and within other distant white matter structures such as the PLIC (Huppi PS et al, 2001).

With regards to neurodevelopment, there is a large body of evidence linking alterations in DTI measurements and outcome in preterm infants. Table 1.1 summarises the findings from groups which have investigated the relationship between quantitative DTI measurements in major white matter structures (as outlined in 1.1.3) and neurodevelopmental outcome in the at risk neonatal population. These studies show that in specific white matter regions, a reduction in FA and increase in MD is associated with poorer outcomes in areas that include motor function, cognition and neurosensory development.

Therefore, we can describe DTI measurements as quantitative biomarkers of preterm brain injury which are predictive of neurodevelopmental outcome after preterm birth.

Table 1.1 The effect of prematurity on neurodevelopmental outcome as assessed by DTI – a summary of evidence in the literature

Group	Number	Birthweight or GA of preterm group	Age at MRI	Outcome Measures	Results	Method
Arzoumanian Y et al, 2003	137 preterm	Less than 1800 grams	TEA	Neurological Examination at 18-24 months	Lower FA in right PLIC is associated with CP	ROI
Bassi L et al, 2008	27 preterm	Less than 32 weeks	2 weeks CGA	Visual assessment	Lower FA in optic radiations is associated with poor visual function	TBSS
Boardman JP et al, 2010	80 preterm 20 term	Less than 34 weeks	TEA	Developmental Quotient (Griffiths Scale) at 2 years	Higher ADC in Centrum Semiovale is associated with lower DQ	ROI
Counsell SJ et al, 2008	33 preterm	Less than 32 weeks	2 years CGA	Developmental Quotient (Griffiths Scale) at 2 years	Lower FA in isthmus and body of CC is associated with lower DQ	TBSS
Krishnan ML et al, 2007	38 preterm	Less than 33 weeks	TEA	Developmental Quotient (Griffiths Scale) at 2 years	Higher ADC in Centrum Semiovale is associated with lower DQ	ROI
Rose J et al, 2007	24 preterm	Less than 1500 grams	TEA	Gross Motor Function Scale at 4 years	Lower FA in left and right PLIC is associated with CP and gait abnormalities	ROI
Thompson DK et al, 2011	106 preterm	Less than 30 weeks or less than 1250 grams	TEA	Bayley Scale of Infant Development	Higher ADC in splenium of CC is associated with impaired motor function	Tract
Kontis D et al, 2009	63 preterm 45 term	Less than 33 weeks	Early Adulthood	Performance IQ	Higher MD in genu of CC (in females) associated with lower IQ	Tract

Note: CC = corpus callosum, CP = cerebral palsy, DQ = developmental quotient, TEA = term equivalent age, ROI = Region of Interest Analysis, TBSS = Tract-Based Spatial Statistics, Tract = Tractography

1.3 Early Life Stress and the Role of Epigenetic Modification

1.3.1 The Developmental Origins of Health and Disease

The environment that the preterm infant experiences (Figure 1.9) is both physically stressful, with exposure to bright lights, high noise levels and noxious stimuli (Als H et al, 2004), and physiologically stressful due to hemodynamic instability and variable oxygen levels, temperature change, altered nutrition and susceptibility to infection. It is well documented that early life adversity is related to poor health outcomes. This was first described by Barker et al, who demonstrated that low birth weight was related to cardiovascular disease in later life (Barker DJ, 2007). Following on from this, several studies revealed that malnutrition in early life is linked to risk of later life health problems. For example, offspring from survivors of the Dutch Famine have alterations in their lipid profiles (Lumey LH et al, 2009) and differential rates of obesity (Ravelli GP et al, 1976) and paediatric survivors and offspring of survivors of the Chinese Famine have alterations in growth and rates of hypertension (Huang C et al, 2010). Additionally, within both these populations, early life adversity confers an increased risk of neuropsychiatric disease with increased rates of schizophrenia (Susser E et al 1992, St Clair D et al, 2005).

The molecular basis for the so called 'developmental origins of health and disease' include glucocorticoid excess and alterations to the hypothalamic–pituitary–adrenal axis (HPA), which in human and animal models of early life adversity are shown to be associated with hypertension, altered glycaemic control and behavioural changes (Drake AJ et al, 2007). These effects are transmissible throughout subsequent generations giving rise to the theory that epigenetic mechanisms are also involved (Drake AJ et al, 2004 and Drake AJ et al, 2005).

Figure 1.8 The neonatal intensive care environment

(Reproduced with permission from Simpson's Special Care babies www.sscb.org.uk)

1.3.2 Epigenetic Processes and DNA Methylation

The term epigenetics refers to a group of cellular mechanisms which alter gene expression, either transiently or permanently, without alteration to the underlying genome and in response to exogenous signals. They include DNA methylation, histone modifications (with acetylation, methylation, phosphorylation, ubiquitinyation and sumoylation) and non-coding RNAs (Nugent BM et al, 2015).

DNA methylation (DNAm) is the most commonly studied epigenetic mechanism and involves the addition of a methyl group to cytosine, most often at CpG dinucleotides, where cytosine is joined to guanine by a phosphate bond, to form 5-methylcytosine (5mC). Interestingly, the majority of CpG islands (areas of the genome which are rich in CpG regions) are usually not methylated, and the promoters of 'housekeeping genes' are often embedded in these areas. When CpG islands are methylated, this leads to transcriptional silencing or turning off of the gene by inhibition of transcription factor binding (Moore LD et al, 2013). DNA methylation is dynamic, particularly during early development and therefore fundamental to such processes as embryogenesis, gene imprinting and X chromosome inactivation (Shi L et al, 2009). It is regulated by a group of highly conserved proteins, DNA methyl transferases (DNMTs) with DNMT3s establishing de novo methylation in early development and DNMT1 preserving DNAm throughout cell divisions (Hochberg Z et al, 2011).

1.3.3 DNA Methylation

1.3.3.1 In Relation to Stressful Life Events

Both animal and human studies have shown that early life experience and stress can cause alterations to DNA methylation.

In mice, the early social environment is determined by differences in maternal care and is associated with long term behavioural outcomes and tissue specific differences in DNA methylation (DNAm) at the glucocorticoid receptor (GR) gene promoter within the hippocampus (Weaver IC et al, 2004). Similarly, prenatal stress during the first week of gestation causes alterations in DNAm of the corticotrophin-releasing factor (CRF) and GR genes, with associated changes in expression and offspring behaviour (Mueller BR et al, 2008). Additionally, in rat pups that are exposed to caregivers with abusive behaviour, there is alteration in DNAm at the BDNF (brain derived neurotrophic factor) gene expression in the adult prefrontal cortex (Roth TL et al, 2009).

In human studies, epigenetic analysis of individuals prenatally exposed to famine in the Dutch cohort has revealed alterations in DNA methylation at the IGF2 gene (Heijmans BT et al, 2008) and other loci implicated in growth and metabolism (Tobi EW et al, 2009). Examination of post mortem hippocampal tissue from suicide victims who experienced childhood abuse showed significant differences in DNAm across a range of neuronal gene promoters (Labonte B et al, 2012) and epigenome wide interrogation of blood samples from children raised in institutions compared to those raised by their biological parents revealed global increases in DNAm (Naumova OY et al, 2012). Several studies have also demonstrated differences in DNAm at the GR as well as altered stress reactivity in adults with a history of childhood abuse or adversity (McGowan PO et al, 2009, Tyrka AR et al, 2012).

1.3.3.2 Role in Normal Brain Development and Neural Function

DNA methylation is critical for normal embryogenesis, demonstrated by DNMT1 KO models which results in a recessive lethal phenotype (Li E et al, 1992). In addition, there is a large body of evidence that DNAm is essential for neuronal development and neural function. Mammalian brains show widespread expression of the key enzymes which mediate DNAm, DNMT1, DNMT3a and DNMT3b, which along with levels of 5mC vary by brain region and stage of postnatal development (Simmons RK et al, 2013). Differential patterns of DNA methylation are also demonstrated by MethylC-Seq in various brain regions of both mice and human samples and also vary according to cell type and stage of development, with neuronal cells and adult brains showing more DNAm at non-CpG sites compared to oligodendrocytes, embryonic stem cells and fetal brains (Lister R et al, 2013).

Selective knockout (KO) of DNMT1 in mouse embryonic CNS precursor cells causes hypomethylation of neuronal cells, with postnatal cell death and respiratory failure from abnormal neural control in the mutant offspring (Fan G et al, 2001). Using this KO mechanism crossed with a mutation which allows the mice to survive in to adulthood, Hutnick et al produced a generation of mice with ~90% hypomethylation in the dorsal forebrain. These animals showed striking cortical and hippocampal degeneration characterised by neuronal cell loss and severe deficits in learning and memory (Hutnick LK et al, 2009).

At the synaptic level, in vitro studies have shown that addition of DNMT inhibitors at the Schaeffer collateral-CA1 pathway reduces the magnitude of long term potentiation (LTP), which serves as a cellular correlate of learning (Levenson JM et al, 2006). In accordance with this, mutant mice with selective forebrain neuron DNMT1 and DNMT3a knockouts show similar impairment of LTP in hippocampal CA1 regions along with deficits of learning and memory demonstrated in behavioural testing (Feng J et al, 2010).

In reference to the importance of oligodendrocyte (OL) integrity in preterm white matter injury, DNA methylation has been shown to be significantly involved in OL development. Overall levels of 5-mC increase in OLIG2+ cells during stages of embryonic and postnatal mouse development and DNMT1 levels increase during in vitro differentiation of OLs. Furthermore, ablation of DNMT1 causes severe hypomyelination of the brain stem and spinal cord with subsequent ataxia and reduced survival in the mutant mouse population (Moyon S et al, 2016).

In addition to the involvement of DNMTs, a group of proteins known as MBDs or methyl binding domain proteins have been implicated in neurological processes and disease. These proteins bind to methylated regions of DNA and recruit histone deacetylase (HDAC) repressor complexes which inhibit transcription (Roloff TC et al, 2003). MBD1 KO mice display impaired spatial learning, reduced adult neurogenesis and a reduction in LTP in the hippocampus (Zhao X et al, 2003). This mutation is also associated with behavioural traits in mice similar to the pattern seen in autism, with anxiety, reduced social interaction and learning deficits (Allan AM et al, 2008).

1.3.3.3 Role in Neurological Disease

Of all the MBD proteins, MeCP2 is the most studied due to its involvement in Rett syndrome (RTT). RTT is characterised by neurological regression, mental retardation, autistic features and occurs exclusively in females, (Graff J & Mansuy IM, 2009) with imaging studies showing a reduction in both grey and white matter volumes (Naidu S et al, 2001). The majority of cases off RTT are caused by a mutation in the MeCP2 gene (Amir RE et al, 1999) and in mouse models this is associated with a reduction in levels of brain derived neurotropic factor, (BDNF) which is essential for neuronal survival (Chang Q et al, 2006).

With regards to other identifiable pathological neurological phenotypes, alterations in DNAm - both at specific gene loci and across the entire genome - have been implicated in the development of psychiatric disorders such as schizophrenia (Abdolmaleky HM et al, 2006, Huang HS et al, 2007, Iwamoto K et al, 2005), bipolar disorder (Fries GR et al, 2016) and depression (Khulan B et al, 2014, Tyrka AR et al, 2016, Poulter MO et al, 2008) and also behavioural disorders including autism (Loke YJ et al, 2015) and attention deficit (Walton E et al, 2016). As discussed earlier, infants that are born preterm have an increased risk of developing these behavioural and psychiatric problems.

1.3.3.4 In Relation to the Perinatal Environment

The perinatal risk factors for preterm birth include modifiable environmental conditions such as maternal diet and smoking as well as pathologies such as preeclampsia and chorioamnionitis, which may be treated but not necessarily prevented. Several studies have shown an association between these events and alterations in DNA methylation and therefore we may expect to see a significant difference in DNAm in preterm infants compared to those delivered at term.

The effect of malnutrition in pregnancy from famine cohort studies has already been discussed. However, further nutritional studies demonstrate that even an unbalanced maternal diet is associated with alterations in long term health outcomes in adult offspring including hypertension and raised cortisol levels and that these changes are associated with variation in DNA methylation at the glucocorticoid receptor in humans (Drake AJ et al, 2012). In addition, folic acid (an important methyl group donor) restriction antenatally is associated with global DNA hypomethylation in the intestine of mice offspring (McKay JA et al, 2011). In terms of postnatal nutrition, preterm infants have immature gastrointestinal tracts compared

to term infants and therefore their feeding must be carefully managed with the gradual introduction of enteral milk and support with TPN (total parenteral nutrition). The feeding and nutritional support of preterm infants is fraught with risk of intravenous catheter related infection and necrotizing enterocolitis, an inflammatory condition of the gut. Both are associated with poor neurodevelopmental outcome (Abott J et al, 2017) and therefore preterm cohorts have a very different experience with nutrition compared to term babies.

Maternal smoking during pregnancy is known to be associated with preterm birth and significantly reduced birth weight. DNA methylation and subsequent increased expression at CYP1A1, a gene encoding for an enzyme that catabolises carcinogenic polycyclic aromatic hydrocarbons to harmful DNA adducts, is reduced in the placentas of smokers compared to non-smokers (Suter M et al, 2010). Additionally, maternal smoking is associated with alterations in DNAm at the imprinted gene IGF2 and glucocorticoid receptor (GR/NR3C1) in fetal liver (Drake et al, 2015).

In the UK, socioeconomic class is strongly associated with low-quality diet (Roberts K et al, 2013), increased rates of maternal smoking during and after pregnancy (Dhalwani N et al, 2013) and increased rates of premature birth (Glinianaia SV et al, 2013) and therefore preterm infants may have additional risks compared to term infants.

Pathological states which may precipitate preterm birth include pregnancy induced hypertension and its progression to pre-eclampsia, infection such as chorioamnionitis and metabolic states including gestational diabetes. Pre-eclampsia, which involves placental insufficiency and high maternal blood pressure may also lead to intrauterine growth restriction and iatrogenic preterm delivery. Increased DNAm in specific gene loci including VEGF, FLT-1 and KDR (factors which are critical for angiogenesis) was found in the placentas

of women with preeclampsia compared to those without, with more significant changes present in cases of preeclampsia and preterm delivery (Sundrani DP et al, 2013).

Gestational Diabetes (GD) occurs in 3.5% of UK pregnancies and is characterised by impaired maternal glucose tolerance in the second trimester (Finer S et al, 2015). Offspring have higher rates of obesity than controls (Fetita LS et al, 2006). A genome wide analysis has shown GD is associated with differential DNA methylation not only in maternal placentas but also in cord blood samples compared to controls (Finer S et al, 2015).

Chorioamnionitis is characterised by inflammation of the foetal membranes on histological examination of the placenta. After preterm birth it is associated with increases in DNAm at the imprinted gene, PLAGL1. This gene is involved in tumour development and growth via IGF2 signalling, providing further evidence that early life environmental factors can affect later life disease susceptibility (Liu Y et al, 2013).

With regards to the effect of preterm birth as an independent variable, epigenome wide association studies (EWAS) have shown an association between gestational age and DNA methylation at specific gene loci with roles in haematopoiesis and the developmental of the brain and skeletal muscle (Lee H et al, 2012).

There are several recent candidate genome studies which have assessed DNAm in relation to neurobehavioural outcomes and cognitive development in term infants (Bromer C et al, 2013, Paquette AG et al, 2013 & Paquette AG et al 2014) yet there have been few studies examining the association of DNA methylation with preterm birth and long term outcome. In 2013, Cruickshank et al reported on levels of DNAm preterm infants (less than 31 weeks gestation) compared to term controls at birth and at 18 years of age. They showed differential methylation in 1,555 promoters (DMPs) at birth; for genes involved in GTPase signalling, transcription, cell growth and proliferation, neurological and haematological development.

These observed differences had resolved in the majority of DMPs by 18 years of age, but 10 CpG regions showed persistent changes (Cruickshank MN et al, 2013), thus providing evidence that preterm birth has a long term epigenetic legacy.

Therefore, in terms of early life experience, preterm infants may encounter a stressful intrauterine environment which is infected, has inadequate blood flow or altered metabolism in the case of gestational diabetes. They may have a mother who smokes or has a poor diet and post-natally they have a vastly different nutritional experience compared to term infants. These factors in combination with the multitude of difficult clinical scenarios preterm infants face compared to term infants such as sepsis, fluctuations in oxygen and altered temperature to name a few, all contribute to the risk of abnormal neurodevelopment, a risk which may leave its fingerprints by alterations in DNAm.

1.3.3.5 Variation Across Tissue Types

Patterns of DNA methylation are tissue specific, particularly during development (Song F et al, 2009) and as such serve as an important mechanism for the translation of the same genetic material to determine different cell type and function (Bird A, 2002). Therefore, ideally epigenetic studies should be conducted in the tissue of interest. With regards to neuroepigenetics, tissue specific studies are limited to translational animal models or post mortem cases. Nevertheless, it is important to consider that in post mortem studies the cause of death, mode of death and interval between death and collection of post-mortem material may affect DNA methylation (Rhein M et al, 2015).

If we wish to study DNAm in live human subjects, the selection of an accessible surrogate tissue is required. Recently, several studies have shown consistency between patterns of DNAm in the brain and peripheral tissue. For example, early life stress manifest by differential

rearing of Rhesus Macaques is associated with changes in DNAm in both the prefrontal cortex as well as peripheral T cells (Provencal N et al, 2012). Additionally, methylation of COMT in peripheral blood mononuclear cells (PBMCs) is associated with lifetime stress in humans, and that methylation patterns of COMT in the prefrontal cortex and PBMCs of rats are comparable (Ursini J et al, 2011). Other studies have also demonstrated similarities in DNA methylation at specific candidate genes between post mortem brain tissue of people with schizophrenia and saliva (Nohesara S et al, 2011 and Ghadirivasfi M et al, 2011).

In paediatric studies, the least invasive sampling of DNA material is preferable, and studies have shown that saliva samples even in small volumes produce good quality and quantity of DNA for genomic work (Nemoda Z et al, 2011). Genomic wide studies also show a positive correlation between patterns of DNA methylation in brain tissue, saliva and blood (Smith AK et al, 2015 and Wockner LF et al, 2014) with saliva showing better correspondence. This finding is further emphasised by comparison of DNA derived from blood and saliva with other tissues, revealing that buccal cells from saliva show significantly greater overlap with hypomethylated regions in other tissues (Lowe R et al, 2013). Therefore, the effect of DNAm on white matter integrity in preterm infants can be studied by non-invasive sampling of saliva.

1.4 Hypotheses and Aims

I hypothesised that preterm birth would have a significant effect on DTI parameters in white matter tracts at term equivalent age.

I hypothesised that there would be an associated effect from clinical risk and resilience factors on DTI parameters in white matter tracts of preterm infants at term equivalent age.

As DTI parameters can be assessed by region of interest and tract averaged techniques, I hypothesised that there would be good repeatability of ROI analysis but limited agreement between measurements of FA and MD generated by these methods.

I hypothesised that there would be a significant difference in DNA methylation between preterm infants sampled at term equivalent age and term control subjects and significant alteration in DNAm at gene loci which are associated with neurological function and/or neurological disease.

Finally, I also hypothesised that variance in DNAm is associated with dMRI parameters in major white matter tracts and clinical risk factors for adverse outcome in the preterm population.

Therefore, my aims were:

1. To examine the relationship between preterm birth and white matter integrity
2. To investigate the effect of neuroprotective treatments and deleterious clinical states on white matter integrity in preterm infants
3. To assess the best method of quantifying white matter integrity in a neonatal population by determining agreement between ROI and tract-based analysis
4. To investigate the effect of preterm birth on DNA methylation
5. To determine the clinical and imaging factors that contribute to the variance in DNA Methylation caused by preterm birth

Chapter 2: Materials and Methods

2.1 Patient Recruitment

2.1.1 Ethics

This thesis included patients from 2 separate ethics applications.

1. Ethical approval was granted from the National Research Ethics Service South East Scotland Ethics committee 2, reference number (REC) 11/SS/0061, (R&D) 2011/R/NE/04, principle investigator Professor James P Boardman.
2. Ethical approval was granted from the National Research Ethics Service South East Scotland Ethics committee 2, reference number (REC) 13/SS/0143, (R&D) 117024, principle investigator Professor James P Boardman.

The study was conducted in accordance with the recommendations for physicians involved in research on human subjects adopted by the 18th World Medical Assembly, Helsinki 1964 and later revisions.

2.1.2 Inclusion and Exclusion Criteria

INCLUSION CRITERIA

Group 1. Preterm infants born weighing less than 1500 grams at birth and/or being less than 32 weeks' gestation and cared for at The Simpson Centre for Reproductive Health.

Group 2. Term infants born at more than 37 weeks' gestation and weighing more than 1500 grams at The Simpson Centre for Reproductive Health.

All infants had to be fit for MR scanning at the CRIC (clinical research imaging centre) at term equivalent age (38 to 42 weeks corrected age).

EXCLUSION CRITERIA

- Any infant who did not pass the standard MR safety checklist including infants with an implanted medical device.
- Infants with congenital anomalies and chromosomal abnormalities
- Infants with overt parenchymal lesions including haemorrhagic parenchymal infarction (HPI) and cystic PVL visualised on cranial ultrasound.

WITHDRAWAL CRITERIA

If the person with parental responsibility for a participant withdrew consent he/she was able to do so without giving reason and with the assurance that the clinical care was not compromised.

2.1.3 Recruitment Pathway

Preterm participants from the Neonatal Intensive Care Unit and term participants from the postnatal wards at the Royal Infirmary of Edinburgh that met the inclusion and exclusion criteria were identified by a trained research fellow (Dr Sarah Sparrow, Dr Chinthika Piyasena, Dr Rozi Pataky and Dr E Telford).

A person with parental responsibility was then invited to enrol their child into the study. They were given verbal and written information about the study. They were given as much time as they desired to consider participation.

If the person with parental responsibility agreed to participation, a date and time for attendance at the Clinical Research Imaging Centre (CRIC) was given.

Infants of multiple gestation i.e. twins were consented as individual subjects. Therefore, the person with parental responsibility could consent, if they so wished, to include 1 twin but not

the other in to the study. It was also possible, that 1 or more infant(s) from a multiple gestation did not meet inclusion criteria/met exclusion criteria due to illness or mortality.

2.1.4 Consent

Informed written consent was obtained from a person with parental responsibility of the participating child. This included the option of withdrawal from the study at any stage of investigation.

2.1.5 Confidentiality

As part of the direct healthcare team the Principle Investigator and I had direct access to medical records. I adhered to the NHS code of practice for confidentiality and no unnecessary members of the research team had access to identifiable clinical information.

2.2 MRI Data Collection and Analysis

2.2.1 Pre-MRI Procedure

The infant was brought directly to the CRIC from home after the infant was discharged from the unit or postnatal ward. If the infant was still resident on the NICU or postnatal ward and deemed fit enough to visit the CRIC, he/she and the parents were taken over by the paediatric research nurse and the paediatric research fellow (Dr Sarah Sparrow, Dr Chinthika Piyasena, Dr Rozi Pataky and Dr E Telford).

At the reception area, a radiographer went through standard MR safety procedures.

The families were taken to the treatment room adjacent to the MR scanner, where the infants were examined, weight, OFC (occipital-frontal circumference of head) and temperature measured and findings documented. If the infant had clothing containing metal this was removed and replaced with metal free clothing.

MRI compatible monitoring was applied to measure vital signs (oxygen saturation and heart rate).

The infants were then given a feed (if considered timely) and wrapped in a blanket. Ear protection (Ear plugs and 'MiniMuffs') was applied to reduce disturbance from the noise of the MR scanner.

2.2.2 MR Imaging

Once asleep, the infant was taken to the adjoining MRI scan room. The parents were asked to wait in the adjoining waiting room. The infant was placed on the movable scan table on a moulding suction mattress and monitoring leads connected to the monitor. The scan duration was between 30 and 60 minutes depending on how still the infant remained.

A Siemens Magnetom Verio 3 T MRI clinical scanner and 12-channel phased-array head coil were used to acquire: T1-weighted MPRAGE volume (1 mm^3 resolution, TR = 1650 ms, TE = 2.43 ms, inversion time = 160 ms, flip angle = 9°, acquisition plane = sagittal, FOV = 256 mm, acquired matrix = 256 × 256, acquisition time = 7 min 49 sec and acceleration factor = 2), T2-weighted STIR (Short T1 inversion recovery, 0.9 mm^3 resolution), to allow fat suppression and allow better structural visualisation, T2-weighted FLAIR (Fluid-attenuated inversion recovery, 1 mm^3 resolution), to allow for CSF suppression and better identification of periventricular lesions, and diffusion MRI (11 T2- and 64 diffusion encoding direction (b=750 s mm^{-2}) single-shot spin-echo planar imaging volumes with 2 mm isotropic voxels using a prototype sequence, TR = 7300 ms, TE = 106 ms, FOV = 256 mm, acquired matrix = 128 × 128, 50 contiguous interleaved slices with 2 mm thickness, acquisition time = 9 min 29 s). To reduce eddy current induced artefacts and shimming errors to a minimum in the dMRI protocol, an optimized bipolar gradient pulse scheme was employed with a manually selected shim box covering a region extending from the top of the head to several centimetres below the chin. The infant's vital signs (saturation and heart rate) were monitored throughout with a

paediatric fellow and nurse in attendance. The MR examination was stopped if there were any signs of instability or distress.

The MRI protocol was optimised for neonatal subjects by Dr Mark Bastin, Dr Scott Semple and Dr Devasuda Anblagan before my involvement in this project began.

2.2.3 MRI Data Storage

Following acquisition MR images were immediately anonymised and stored offsite on a computer network in the King's Buildings, University of Edinburgh. The whole file system was backed up and the processed data were also backed up at regular intervals.

2.2.4 MRI Processing

This stage was conducted by Dr Devasuda Anblagan. After conversion from DICOM to NIfTI-1 format, diffusion MRI data were pre-processed using FSL tools (FMRIB, Oxford, UK; http://www.fmrib.ox.ac.uk). This included brain extraction and removal of bulk infant motion and eddy current induced artefacts by registering subsequent diffusion-weighted volumes to the first T2-weighted EPI volume for each subject. Using DTIFIT, MD and FA volumes were generated for every subject. Underlying connectivity data was provided by FSL's BedpostX/ProbTrackX algorithm run with its default parameters: 2-fiber model per voxel, 5000 probabilistic streamlines for each tract with a fixed separation distance of 0.5 mm between successive points (Behrens TE et al 2003 & Behrens TE et al 2007).

2.2.5 DTI Data Analysis

2.2.5.1 Region-Of-Interest Analysis

DTI images were visualized in the axial plane in 2mm slices using FSL viewer. Images were interpolated post-acquisition. The best slice for the corresponding ROI (genu corpus callosum, left or right PLIC, left or right anterior, middle and posterior centrum semiovale or cerebral white matter) was identified anatomically as described below, with the use of www.mrineonatalbrain.com as a reference guide. ROI placement is shown in figure 2.1.

Genu of Corpus Callosum: Axial view (figure 2.1a) shows anterior and posterior horns of both lateral ventricles, with genu being found between the superior margins of the ventricles, below the cerebral cortex in the midline.

Posterior Limb of Internal Capsule: Axial view (figure 2.1b) shows basal ganglia with PLIC visible as 2 diagonal bands of increased signal intensity. Voxels were placed inferior-lateral along this region with an attempt to standardise position between subjects. Voxel placement was as follows:

Right PLIC = 1 **Left PLIC** = 2

Centrum Semiovale (CSO): Axial view (figure 2.1c) shows cerebral cortex with cerebral white matter visible as confluent higher signal intensity without capture of superior margins of lateral ventricles. Voxel placement was as follows: **Anterior** = 1 and 4, **Central** = 2 and 5, **Posterior** = 3 and 6

Care was taken to avoid capture of cortical fold when placing voxels.

Diffusion values (MD and FA) were manually extracted from a $1mm^3$ ROI placed at the centre of each ROI and calculated using an in house MATLAB algorithm, designed with the help of Dr. Mark Bastin.

Figure 2.1 FA maps with ROI placement in the a. genu of corpus callosum, b. left and right PLIC, left and c. right anterior, central and posterior Centrum Semiovale.

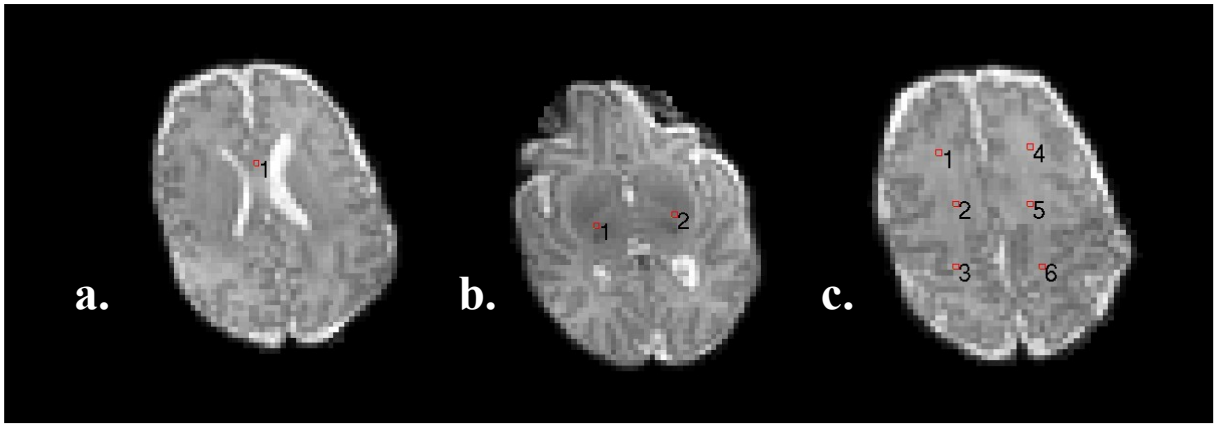

2.2.5.2 Tractography

Probabilistic neighbourhood tractography was performed by Dr. Devasuda Anblagan to provide whole tract averaged values of MD and FA for the Genu of the Corpus Callosum and left and right Corticospinal Tracts. The method used was first described by Clayden et al (Clayden JD et al, 2006 & Clayden JD et al, 2007) and developed for use with neonatal dMRI data by Anblagan et al (Anblagan D et al, 2015).

Candidate tracts were generated by seeding within a 7 x 7 x 7 neighbourhood of native space voxels, centred around a standard space seed point, defined using age specific T-2 weighted neonatal template, (Kuklisova-Murgasova M et al, 2011), located at the centre of a particular white matter structure-of-interest, and then transferred to the native space of each control. An experienced observer (Dr D Anblagan) selected the tracts from each control which best matched the anatomical shape of the white matter structure-of-interest. These 'best-matching' tracts were used to fit tract shape models to the tractography using maximum likelihood (Clayden JD et al, 2007), therefore capturing shape and length variation amongst the control's tracts. After creation of the reference tracts and shape models, PNT was re-run over a neighbourhood of 3 x 3 x 3 voxels, centred on the reference tract and transferred to the native space for all subjects; the seed point that produced the 'best matching' tract to the

reference tract was then determined. The computational analysis was implemented in TractoR (http://www.tractor-mri.org.uk). The tractography masks of the best match tracts were applied to each subjects' MD and FA maps, allowing tract-averaged values to be determined for each of the tract of interest.

2.3 DNA Collection

2.3.1 DNA Collection Procedure

A sample of saliva was obtained using the Oragene.DNA self-collection kit (http://www.dnagenotek.com). All preterm samples were recruited through the pathway as outlined in 2.1 and had imaged-linked data. Additional term DNA samples to ensure adequate numbers of sex-matched controls for the methylation array were provided by Dr Chinthika Piyasena from a parallel study which had informed consent and used the same collection procedure.

2.3.2 DNA Sample Storage

The Oragene DNA saliva samples are stable at room temperature for 5 years. After collection by the research nurse, each sample was assigned a study code number and taken to the secure, swipe-access, genomic laboratory, where they were stored in locked facilities. Only the neonatal research fellows and chief investigator have access to the identification code, which is stored in a secure office within the Neonatal Department in the Royal Infirmary of Edinburgh.

2.4 Molecular Procedures

2.4.1 DNA Extraction

Salivary DNA was collected from participating infants as detailed in 2.9.1.

The resulting Oragene DNA collection pots containing collection sponges and stabilisation fluid were mixed gently by inversion and incubated at 50 ºC for 2 hours. The free liquid was removed with sterile pipette tips and transferred to a conical centrifuge tube. The barrel of a disposable syringe was placed in the centrifuge tube and, using sterile forceps, the sponges transferred in to the syringe. This was then centrifuged at 1000rpm for 10 minutes at 20 ºC. The volume of solution was noted and a 25^{th} volume of PT-L2P was added and vortexed. The sample was incubated on ice for 10 minutes, then centrifuged at 3500rpm for 10 minutes at RT. The clear supernatant was transferred into a fresh centrifuge tube with a sterile pipette and 1.2 x volume of 100% ethanol (EtOH) was added. It was mixed by inversion and sat at RT for 10 minutes. It was centrifuged at 3500rpm for 10 minutes at RT. The supernatant was removed & discarded, taking care to not disturb the DNA pellet. 1mL of 70% EtOH was added for 1 minute then removed. The DNA was rehydrated in 0.2mL of TE and vortexed for 30 seconds. It was incubated at RT on a rotating mixing wheel overnight. The supernatant was transferred to a 1.5mL microcentrifuge tube and stored at 4 ºC.

2.4.2 DNA Quantification

DNA samples were quantified using the Qubit™2.0 Fluorometer with dsDNA HS assay kit. The Qubit™ Working Solution was prepared by diluting the Qubit™ Reagent 1:200 in Qubit™ buffer. 190µL of working solution and 10 µL of standard solution was combined as a control. 198 µL of working solution and 2µL of rehydrated patient DNA sample were combined per participant. Tubes were vortex 3 seconds and incubated at RT for 2 minutes before insertion in to the Qubit™2.0 Fluorometer for measurement.

2.4.3 DNA Qualification

All DNA samples were visualised using gel electrophoresis. A 1% agarose gel was made as described in 2.4. 2 µL DNA samples were combined with 2 µL of Glycerol Orange. A 100Bp DNA Ladder combined with Glycerol Orange was used as reference. Samples were ran in TBE 0.5 at 100 volts for 50 minutes. The DNA was visualised using Gel-Doc at 260nm. A thick DNA band without RNA smearing was considered a good quality sample. This is demonstrated in figure 2.2.

Figure 2.2. Gel electrophoresis of DNA samples

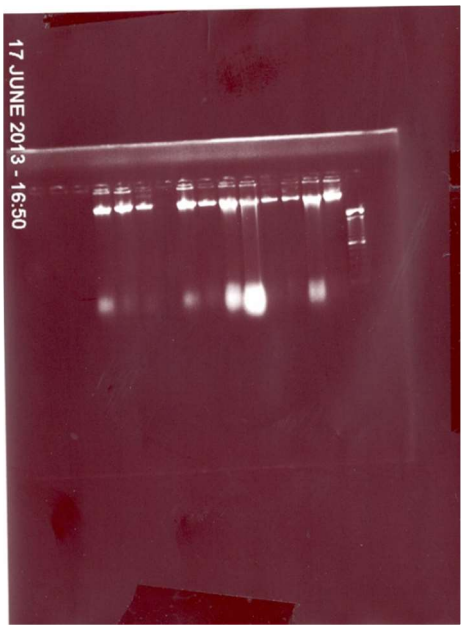

2.5 DNA Methylation

2.5.1 DNA Methylation Array

The extracted DNA from subjects was passed to a team at the Edinburgh Clinical Research Facility, Western General Hospital, to conduct an Illumina HumanMethylation 450 Beadchip array.

The process involves bisulphite conversion, DNA amplification, hybridization and single base extension and finally an immunohistochemical assay, which allowed DNA methylation to be expressed as a value from 0 to 1.

2.5.2 Bioinformatics Processing of DNA Methylation Array Data

The resulting data from the Methylation array was transferred to Dr Jon Manning, for bioinformatics processing with use of the RnBeads v0.99.17 package. The process involved pre-processing, normalisation and determination of differential methylation.

Pre-processing made use of the Chen annotation (Chen et al, Epigenetics 2013), which removes probes if their CpG loci overlapped with a known SNP identified in the 1000 Genomes Project (www.1000genomes.org), if a SNP occurred at a single-base extension site, if the probe was non-specific or unreliable.

Normalisation was completed using the method described by Teschendorff (Teschendorff AE et al, 2013) which considers distributions of Type I and Type II probes. A batch correction was applied using ComBat and then further probes removed if they occurred on sex chromosomes or in non CpG areas.

Differential methylation between the preterm and term infants was assessed using Limma in gene promotors (1.5 kb upstream to 0.5 kb downstream of the transcription start site) and gene bodies. A generalisation of Fisher's method with FDR correction (p value <0.05) generated genes with significantly differentially methylated regions (DMR), methods as per

Smyth GK, 2005. Gene function was established using the National Center for Biotechnology Information Gene database (http://www.ncbi.nlm.nih.gov/gene/about-generif).

2.6 Pyrosequencing

2.6.1 Bisulfite Conversion

All samples were bisulfite converted using the EZ DNA Methylation-Gold™ Kit. The concentration of DNA in ng/µl varied for any given sample. The CT conversion reagent and M-Wash Buffer were prepared according to Manufacturer's instructions. 130µl of the CT Conversion Reagent was added to 20µl of the DNA sample of interest in a PCR tube, then centrifuged briefly. The samples were placed in a thermal cycler with heating to 98°C for 10 minutes, 64°C for 2.5 hours and then cooling to 4°C overnight.

600µl of M-Binding Buffer was then added to a Zymo-Spin™ IC Column along with the full heat treated DNA sample, the column placed in a collection tube and the solutions mixed by inversion. It was then centrifuged at 10000rpm for 30 seconds. The follow through was discarded. 100µl of M-Wash Buffer was added to the column and centrifuged at full speed for 30 seconds. 200µl of M-Desulphonation Buffer was added to the column and incubated at RT for 20 minutes. The samples were then centrifuged at full speed for 30 seconds. The samples were washed twice with 200µl of M-Wash Buffer to the column followed by centrifugation at full speed for 30 seconds. The column was then removed and placed into a microcentrifuge tube. 10µl of M-Elution Buffer was added to the column and centrifuge for 30 seconds at full speed to elute the DNA. The samples were stored at -20°C.

2.6.2 PCR Amplification

Forward and reverse primers for each of the five genes of interest were designed by Dr Mandy Drake, using the Pyromark Assay Design 2.0 Software. Assays were purchased from Invitrogen, UK and are shown in table 2.1.

Primers were eluted in DNA free water according to the nmol concentration provided by the manufacturer to give a 100µM primer stock solution. For example, for a 20.91 nmol primer, 10X DNA free water (209µL) was added. Then, 4µL of forward and 4µL of reverse primers were combined with 192µL of DNA free water. For each sample a mix of 5µL Amplitaq Gold 360 Master Mix, 2µL of primer solution, 0.5µL of bisulfite converted DNA and 2.5µL of DNA free water was made up. A water control substituted the DNA for 0.5 µL of DNA free water.

A thermal cycle included initialisation at 95°C for 10 minutes, then 45 cycles of denaturation at 95°C for 20 seconds, annealing between 56-58°C for 20 seconds (according to primer's optimal annealing temperature) and extension at 72°C for 20 seconds. A final elongation was at 72°C for 7 minutes followed by cooling to 4°C for storage.

Optimal annealing temperature was determined for each primer by an optimisation PCR run using a gradient of 55-59°C and qualification by gel electrophoresis as described in 2.10.3. The water control was run at the same time to ensure no contamination and a 100Bp DNA ladder was used for comparison. Optimal annealing temperature was gauged by strength of DNA band, with sharp contrast between product and primer-dimer.

Table 2.1 Primer design for pyrosequencing validation of methylation array

Gene	Forward Primer	Reverse Primer (5' Biotinylated)	Sequencing Primer
NPBWR1	AGA GTT TTT TAT TAT TTT AGA TGG AGT GAG	Biotin- CCC CCA AAT TTA AAA AAT TCC TTT C	GAT GGA GTG AGG TTG
QPRT	TTG GGA GTT TTG GTT TTG AGT	Biotin - ACA AAA AAA ATA TCC CTT TAC CTT CA	AGA TAG TTG TAA GTT ATT ATG G
SLC1A2	GTT ATT TAG TTA GAA GGT GGT GAA GAA	Biotin - ACC AAA AAA ACC CAA ATC CCA ACA AA	GTG GTG AAG AAT TTA AGT TT
APOL-1	TTT GGT TAT GAG TTG TTG GGA AGT T	Biotin - ACA AAT CCT CCA ATC CCC AAA ATA TAC	GGG AAG TTG TGA TTT TTA
SLC7a5 (assay 1)	TGT GTG TTT TTT ATA GGG TAT GAG G	Biotin - AAA ACA CTC CTA TAT CCC CCT CT	TTT TTA TAG GGT ATG AGG T
SLC7a5 (assay 2)	GAG GAT GAT AGG TTG GGG AAG TTG	Biotin - ATA ACT ACC CTA ACC TCT ATC CAT	CTG TGT TGG GAT AGA ATT

2.6.3 Pyrosequencing

Pyrosequencing was completed using the PyroMark Q24 system with the assistance of Dr Jessy Cartier. The PyroMark processing file was prepared ahead of time using PyroMark Q24 software. An illustration of this is shown in figure 2.3 below. This allowed for calculation of appropriate enzyme, substrate and nucleotide volumes for loading of the Pyromark Cartridge, as shown in figure 2.4 below.

The appropriate buffers were allowed to warm to RT and the enzyme and substrate mixes were reconstituted from the Gold 24 Reagent Kit as per manufacturer's instructions. Sequencing primers for each gene of interest were prepared with 970 µL of annealing buffer and 30 µL of 10µM primer.

The PyroMark plate was loaded with DNA, random DNA and water control binding mixes. For DNA samples 2µL of sepharose beads, 40µL of binding buffer, 18µL of DNA free water and 20µL of PCR amplified product from 2.12.2 were combined and vortexed at RT for 10 minutes at 1400rpm. For DNA random controls, the PCR product was replaced with 20µL of a random primer and for water controls, 20 µL of DNA free water.

Figure 2.3 Organisation of the PyroMark processing file

	1	2	3	4	5	6
	APOL1 CpG 36649144 position 2 assay file	APOL1 CpG 36649144 position 2 assay file	APOL1 CpG 36649144 position 2 assay file	NPBWR CpG 1 assay file	NPBWR CpG 1 assay file	NPBWR CpG 1 assay file
A	DNA	WATER	SEQ	DNA	WATER	SEQ
	QPRT CpG 2 assay file	QPRT CpG 2 assay file	QPRT CpG 2 assay file	SLC1A2 CpG 35442225 (position 1) assay file	SLC1A2 CpG 35442225 (position 1) assay file	SLC1A2 CpG 35442225 (position 1) assay file
B	DNA	WATER	SEQ	DNA	WATER	SEQ

Figure 2.4 Illustration of the PyroMark Q24 cartridge

(Enzyme mixture (**E**), substrate (**S**), and nucleotides (**A, T, C, G**)

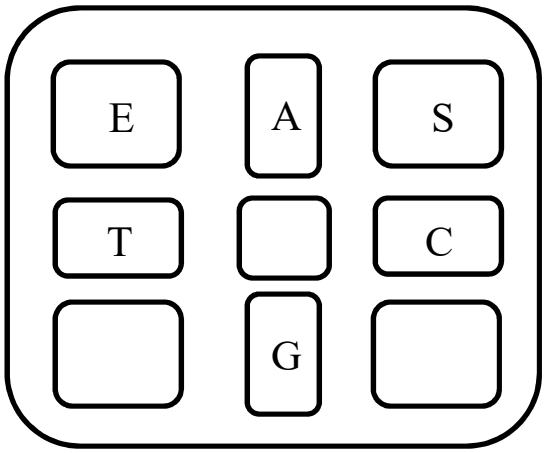

2.7 Laboratory Materials

2.7.1 General Chemicals

Agarose powder	Bioline, UK
Boric Acid	Sigma-Aldrich Ltd., UK
Ethanol	VWR International, UK
Ethylenediaminetetraacetic acid	Sigma-Aldrich Ltd., UK
GelRed Nucleic Acid Stain	Biotium, USA
Gycerol	Sigma-Aldrich Ltd., UK
Orange G	Sigma-Aldrich Ltd., UK
Potassium Hydroxide	Sigma-Aldrich Ltd., UK
Sodium Chloride	Sigma-Aldrich Ltd., UK
Trizma® base	Sigma-Aldrich Ltd., UK
Trizma® hydrochloride solution	Sigma-Aldrich Ltd., UK

2.7.2 Molecular Biology

Amplitaq Gold 360 Master Mix	Applied Biosystems, Life Technologies, UK
DNA 100Bp Ladder	Invitrogen, USA
EZ DNA Methylation Gold Kit including:	Zymo Research Corporation, USA
Zymo-Spin™ IC Column	
Collection tubes	
CT Conversion Reagent	
M-Dilution Buffer	
M- Dissolving Buffer	

M-Wash Buffer	
M-Binding Buffer	
M-Desulphonation Buffer	
M-Elution Buffer	
Gold 24 Reagent Kit Substrate Mix	Qiagen, UK
Gold 24 Reagent Kit Enzyme Mix	Qiagen, UK
PCR amplification Primers	Invitrogen, UK
PrepIT L2P solution	DNA Genotek, Canada
Pyromark Binding Buffer	Qiagen, UK
Pyromark Annealing Buffer	Qiagen, UK
Pyromark Wash Buffer	Qiagen, UK
Pyromark Denaturation Buffer	Qiagen, UK
Pyromark A, T, C, G nucleotides	Qiagen, UK
Qubit DNA High Sensitivity Assay Kit	Life Technologies, USA
Streptavidin Sepharose beads	GE Healthcare, Sweden
UltraPure™ DNase/RNase-Free Distilled Water	Life Technologies, USA

2.8 Laboratory Equipment

Bench Centrifuge 5424 & 5415R	Eppendorf, Germany
8 strip PCR tubes	Star Lab, UK
Falcon Conical centrifuge tubes	BD Biosciences, UK
G-Storm thermocycler	Labtech International, UK
Hybridisation Oven (Techne Hybridiser HB-1D)	Bibby Scientific Ltd, UK
IKA MS 3 Basic Shaker	IKA – Werke, Germany
Microcentrifuge tubes	Sigma-Aldrich Ltd., UK
Milli-Q integral water purification system	EMD Millipore, USA
Nanodrop ND-1000 Spectrophotometer	ThermoScientific, USA
Orbital Shaker	Voss Instruments, Maldon UK
Oragene OG-250 kits with saliva sponges CS-1	DNA Genotek, Canada
Pipettes p2, p20, p200, p1000	Gilson, UK
Pipette Tips	StarLab, UK
Power Pac 300	Biorad Laboratories Inc., UK
PyroMark Q24 system	Qiagen, UK
Pyrosequencing Technology	Biotage AB, Sweden
Qubit 2.0 Fluorimeter	Life Technologies, USA
Rotamixer Vortex	Hook and Tucker Instruments, UK
Sterile Disposable Forceps (Griprite Blue)	Rocialle, UK
Sterile Disposable syringe	BD Biosciences, UK
Sub-cell 96 electrophoresis tank	Biorad Laboratories Inc., UK
Transilluminator	UVitec, UK

2.9 Laboratory Software

ND-1000 v3.3	NanoDrop Technologies, Thermo Fisher Scientific, UK
SPSS Statistics 21	International Business Machines Corporation (IBM), USA
PyroMark Q24 Software 2.0 (assay design and analysis)	Qiagen, UK

2.10 Laboratory Solutions

Agarose gel 0.5g of 1% agarose powder was placed in 50mls TBE and heated to dissolve. 3µl of GelRed Nucleic Acid Stain was then added to the solution and it was set in a cool room.

0.5M EDTA pH 8.0 186.1g of EDTA (disodium ethylenediamine tetraacetate.$2H_2O$) was dissolved in 800mls of MilliQ water. The pH was then adjusted to 8.0 using 10M KOH and final volume made up to 1 litre with MilliQ water. The solution was autoclaved and stored at room temperature.

Orange G 30ml of glycerol and 0.25g of Orange G powder were combined and made up to 100ml with Polymerase Chain Reaction (PCR)-grade water.

10 x TBE 108g of tris base, 55g of boric acid and 40ml of 0.5M EDTA were combined, then made up to 1litre with MilliQ water to give Tris/Borate/EDTA (TBE). The solution was autoclaved and stored at room temperature.

0.5 x TBE 50ml of 10 X TBE was diluted in 950mls of MilliQ water. The solution was stored at room temperature.

TE 3.5ml of 1M Tris (pH 7.5) and 0.5ml of 0.5M EDTA was combined and made up to 250ml with MilliQ water to give Tris-EDTA. The solution was autoclaved and stored at room temperature.

2.11 MRI Equipment

MRI compatible ECG leads	
MRI compatible Neonatal Saturation Probe	
MRI compatible physiological monitoring	
Soft Foam Ear plugs	
MiniMuff Ear protection	Natus Medical, USA
Siemens MAGNETOM Verio 3T MRI clinical scanner	Siemens Healthcare Germany
12-channel phased-array head coil	Siemens Healthcare Germany

2.12 MRI Software

FSL (FMRIB Software Library v5.0)	Analysis Group, FMRIB, UK
MATLAB	Mathworks, USA
TractoR	http://www.tractor-mri.org.uk

Chapter 3: DTI Imaging of Preterm Infants: Risk and Resilience Factors

3.1 Introduction

3.1.1 Introduction

Preterm birth is associated with neurodevelopmental impairment including cerebral palsy, cognitive deficits, and behavioural problems including attention deficit, ASD and increased risk of later life psychiatric disease. 14% of very preterm infants (gestational age less than 32 weeks) have moderate to severe disability (Larroque B et al, 2008) and preterm infants have an increased risk of brain injury, with up to 50% of very low birth weight (less than 1500 grams) showing signs of diffuse white matter injury on MRI (Khwaja O & Volpe JJ, 2008). Clinically, as well as gestational age and birthweight there are factors which are deemed neuroprotective or neurotoxic with regards to long term neurodevelopmental outcome. Postnatal infection (Stoll BJ et al, 2004 & Mitha A et al, 2013), bronchopulmonary dysplasia (Majnemer A et al, 2000; Boardman JP et al, 2007; Ball G et al, 2010) and the presence of clinical or histological chorioamnionitis (HCA) (Shatrov JG et al, 2010; Soraisham AS et al 2013, Ylijoki M et al 2016, Anblagan D et al, 2016) have all been shown to have a negative effect on neurodevelopment. The antenatal administration of corticosteroids (Sotiriadis A et al, 2015) and magnesium sulphate (Doyle LW et al, 2009) have been shown to have a positive effect on neurodevelopment.

The pathogenesis of preterm white matter injury is multifactorial and involves mechanisms such as hypoxia, ischaemia, free radical damage and infection which ultimately lead to death or disruption of the pre-myelinating oligodendrocyte (Volpe JJ, 2011) and abnormalities in white matter micro and macro-architecture. Diffusion tensor imaging allows quantitative interrogation of the white matter microarchitecture by mapping the diffusion of water

through regions of interest or specific neuronal tracts. Three regions of white matter with significant roles in cognitive and motor function are the corpus callosum, the posterior limb of internal capsule and the centrum semiovale.

The outcome measures FA (fractional anisotropy) and MD (mean diffusivity) give an indication of white matter organisation, myelination and development (Huppi PS & Dubois JS, 2006). FA and MD are dynamic throughout neurodevelopment (Huppi et al, 1998) and decreased FA and increased MD at term equivalent age is associated with white matter injury (Counsell et al, 2006) and poorer neurodevelopmental outcome (Arzoumanian et al 2003, Boardman et al 2010, Krishnan et al 2007, Rose et al 2007, Bassi et al 2008, Counsell et al 2008, Kontis et al, 2009, Thompson et al, 2011). Therefore, DTI measurements can be described as quantitative biomarkers of preterm brain injury which are predictive of neurodevelopmental outcome after preterm birth and may be altered by clinical variables experienced by preterm infants.

3.1.2 Hypotheses and Aims

I hypothesised that would be a significant difference in FA and MD in brain white matter tracts in preterm infants at term equivalent age when compared to term controls. FA should be reduced in preterm infants compared to term controls and MD increased. Using precedence in the literature of preterm at TEA and term control imaging studies (Boardman JP et al, 2010) I aimed to collect DTI data on 80 preterm and 20 term control subjects.

I assessed this by performing DTI scans on preterm infants at term equivalent age and term control infants. Subsequent data were analysed using the ROI method within 5 regions-of-interest, the genu of the corpus callosum, the posterior limb or internal capsule and the anterior, central and posterior centrum semiovale (CSO).

I also hypothesised that there would be a beneficial effect, quantifiable at the microstructural level of white matter development in preterm infants, at term equivalent age, with the use of the antenatal neuroprotective agent - magnesium sulphate. I also expected to see a deleterious effect, associated with clinical states which are known to be associated with poorer neurodevelopmental outcome in preterm infants, including bronchopulmonary dysplasia, and chorioamnionitis (as defined by histological examination of the placenta). I chose not to investigate late onset sepsis due to the difficulty in defining its presence clearly, and antenatal corticosteroids due to the large discrepancy between preterm infants who were exposed versus not exposed in this population.

I aimed to investigate these independent factors by statistical analysis of the preterm cohort after DTI data capture and analysis.

3.2 Methods

3.2.1 Demographic Data Collection

With maternal consent, maternity notes were interrogated for maternal age and BMI (weight in kilograms/height in metres^2) at booking, preconception folic acid, use of artificial reproductive therapy (ART), maternal past medical history, multiple gestation, birthweight (kilograms) and gestational age of infants at birth, gender, IUGR (defined as birthweight less than 3rd centile for gestational age), mode of delivery, exposure to antenatal magnesium sulphate and corticosteroids (with a complete course defined as two doses of Betamethasone 12mg given 24hrs apart, before delivery). The presence of HCA was determined by maternal placental pathology report (not available for routine term delivery) which classifies the presence of HCA as an inflammatory response in the placental membranes of any grade or stage. With parental consent, infant notes were interrogated for bronchopulmonary dysplasia (BPD), defined as an oxygen requirement at 36 weeks corrected gestation, late-onset sepsis (LOS), defined as clinical instability requiring treatment with at least 5 days of antibiotics and a positive blood culture, and necrotising enterocolitis (NEC) if characterised as Bell Stage 2 or above. At time of scan, infants were weighed (kilograms) and had their occipital frontal circumference (OFC) of head measured, corrected gestational age (PMA) calculated and exposure to breast milk was determined.

3.2.2 MRI Scanning

All infants underwent the pre-MRI procedure as outlined in methods 2.2.1 and once asleep were taken to the MRI scanner and underwent the MRI scan protocol as detailed in methods 2.2.2. The scan was stopped if there was any sign of distress or clinical instability.

3.2.3 MRI Data Processing

Structural images were assessed offsite by Dr A G Wilkinson, a paediatric radiologist with experience in neonatal MR imaging. Results were reported to the families and made available in clinical notes. If there was unexpected cystic PVL or (haemorrhagic parenchymal infarction) HPI reported on structural imaging, the infants were excluded from the study. Data was stored and processed as per methods 2.2.3 and 2.2.4 with new study codes generated at this stage to allow blinding.

3.2.4 ROI Analysis

As described in methods 2.2.5.1 DTI images were visualized in the axial plane in 2mm slices using FSL viewer with best slice for each gCC, left and right PLIC and left and right anterior, central and posterior CSO identified. Images were interpolated post-acquisition. Diffusion values (MD and FA) were manually extracted from a $1mm^3$ ROI placed at the centre of each ROI and calculated using a MATLAB algorithm. Data were reviewed after analysis and significant outliers were reanalysed.

In order to avoid bias, I was blinded to the gestational age and clinical state of the infants at the ROI analysis stage.

3.2.5 Statistical Analysis

Data were analysed using SPSS Statistics version 21 (International Business Machines Corporation (IBM), USA). Data were checked for normality of distribution and homogeneity of variance. For analysis of demographic data and bivariate analysis of the effect of independent variables on FA and MD, and univariate analysis of the difference in independent variables between patient groups: independent t tests were used for continuous data and CHI

squared analysis for categorical data. For analysis of DTI parameters between left and right hemispheres, paired t testing was used. A multiple regression model was used to assess the effect of independent variables between patient groups after correction for GA at birth and PMA at time of scan. Type 1 error was controlled using false discovery rate (FDR) ($p < 0.05$).

3.3 Results

3.3.1 Patient Recruitment Pathway

A consort diagram from assessment of eligibility to individual subjects with available DTI data is shown in figure 3.2 below. There were 229 preterm infants with a birthweight of less than 1500 grams or a gestational age at birth of less than 32 weeks within the study period of January 2012 to April 2014. 61 infants (26.6%) did not meet inclusion criteria and a further 17 (7.4%) met exclusion criteria. Of the 151 preterm infants eligible for consent 151 (100%) were approached and 99 (65.6%) consented. Data were not collected on the number of term infants approached for consent, but 26 gave written consent during the study period.

After consent, DTI data were not captured on a subsequent 28 infants, with the main reasons being infants were too unwell to present for MRI scan (21.4%) or did not sleep throughout the scan (42.8%). Severe movement artefact, as demonstrated in figure 3.1, prevents the capture of diffusion data and therefore these infants were excluded post consent. However, for those infants who presented for MRI which included the DTI protocol (n= 109) the majority (n= 97, 89%) had DTI data captured of sufficient quality for analysis, with n= 12, 11% DTI scans lost due to lack of sleep/severe movement artefact or loss of data.

Figure 3.1 T1 weighted images showing a) moderate and b) severe movement artefact (anonymised images from Clinical Research Imaging Centre, Edinburgh UK)

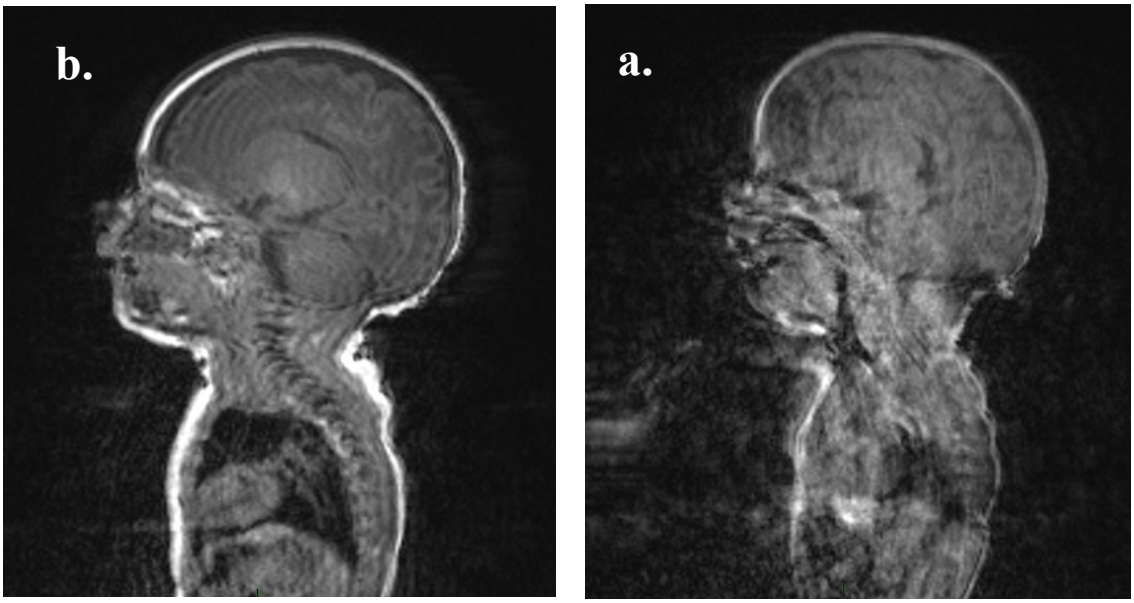

Figure 3.2 Consort diagram of infant recruitment

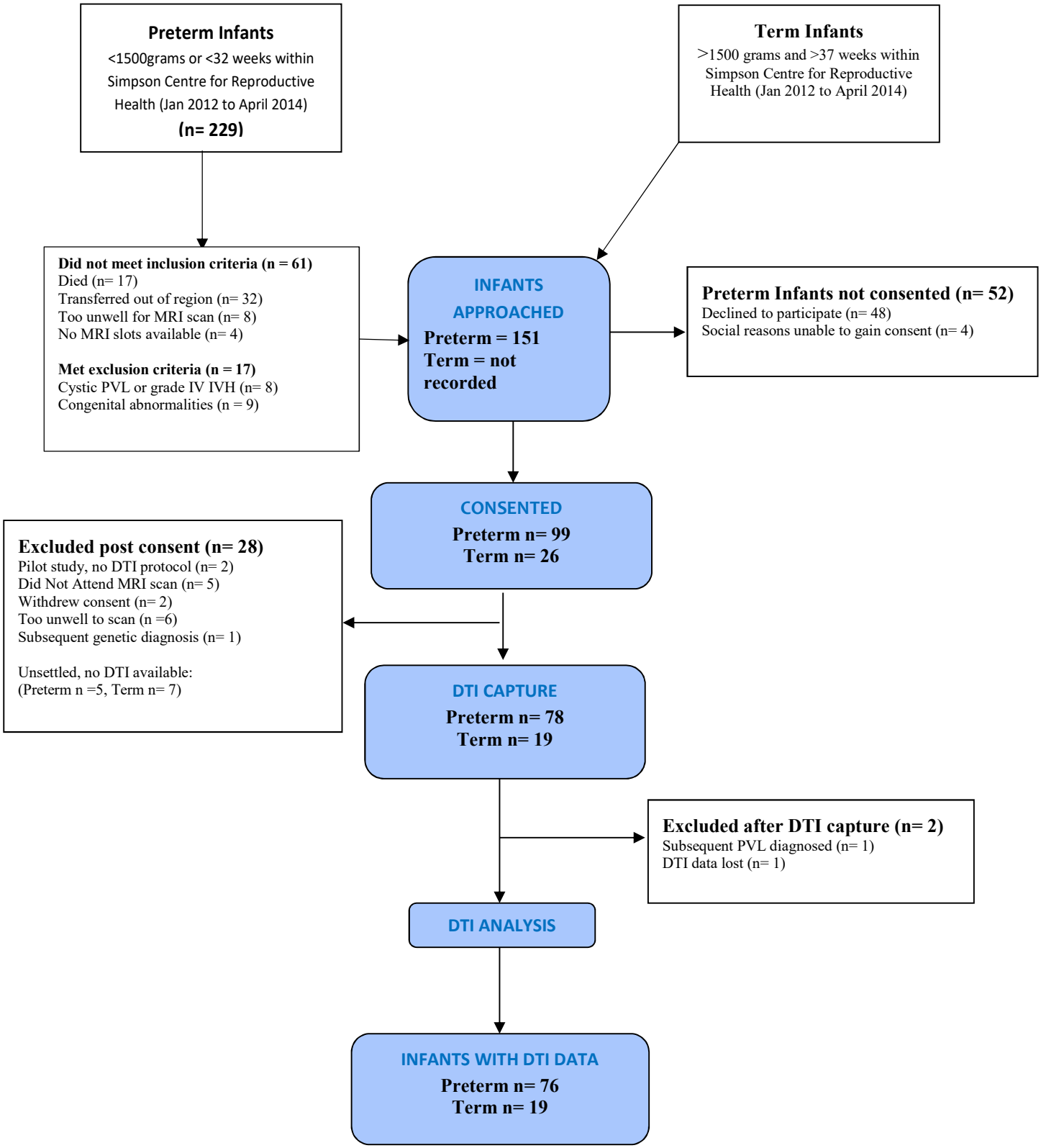

3.3.2 Demographics

The demographics of infants with available DTI data from MRI scanning (n= 95) are shown in the table 3.1. As expected, there is a significant difference between preterm and term infants with regards to birthweight (3.41Kg versus 1.16 Kg, $p < 0.001$) and gestational age (39.6 weeks versus 29.27 weeks, $p < 0.001$) at birth. There are also significant differences in growth of the preterm population at term corrected age, with preterm infants having significantly smaller OFC (36.2cm versus 34.6cm, $p < 0.001$) and weight (3.75Kg versus 2.85 Kg, $p < 0.001$). There was also a significant difference in corrected gestational age at time of scan between term and preterm infants (42.45 weeks versus 39.85 weeks, $p < 0.001$) and therefore subsequent analysis was corrected for PMA at time of scan.

Table 3.1. Demographics of Infants with ROI Analysed DTI Data

	Term Infants n = 19	**Preterm Infants n = 76**	**p value**
Birthweight (Kg)*	3.41 (2.87 to 4.26)	1.16 (0.55 to 1.635)	<0.001
Gestational Age at Birth (decimal weeks) *	39.6 (38.14 to 41.7)	29.27 (23.29 to 34.86)	<0.001
Corrected Gestational Age at Scan (decimal weeks) *	42.45 (39 to 47.14)	39.85 (37.28 to 42.71)	<0.001
Weight (Kg) at Sample*	3.75 (2.91 to 4.83)	2.85 (2.06 to 3.78)	<0.001
OFC (cm) at Sample*	36.2 (32.6 to 39.5)	34.6 (31.0 to 38.0)	<0.001
Female**	11 (57.8)	37 (48.6)	0.505
Maternal Age *	33 (19 to 45)	31 (17 to 44)	0.245
Maternal BMI*	25.1 (19.7 to 36.4)	25.7 (18 to 43)	0.662
Preconception Folic Acid**	10 (52.6)	33 (43.4)	0.5
Diabetes (Gestational or IDDM)**	0 (0)	7 (9.2)	0.166
Multiple Birth**	0 (0)	28 (36.8)	0.001
Severe IUGR**	0 (0)	6 (7.9)	0.206
ART**	1 (5.2)	15 (19.7)	0.338
Chorioamnionitis**	0 (0)	24 (31.6)	n/a
Exposure to Antenatal Steroids**	0 (0)	71 (93.4)	n/a
Exposure to Magnesium Sulphate**	0 (0)	36 (47.3)	n/a
Vaginal Delivery**	11 (57.8)	26 (34.2)	0.058
BPD **	0 (0)	20 (26.3)	n/a
NEC**	0 (0)	3 (3.9)	n/a
Late-onset sepsis**	0 (0)	17 (22.4)	n/a
Breast Milk**	16 (84.2)	56 (73.6)	0.338
Caucasian Origin	18 (94.7)	70 (92.1)	n/a
African Origin	0 (0)	2 (2.6)	n/a
Asian Origin	1 (5.3)	4 (5.3)	n/a

* Mean (range)

** Number (percentage)

ART = Artificial Reproductive Therapy

Severe IUGR = Birthweight below the 3rd centile for gestation

BPD = bronchopulmonary dysplasia defined as an oxygen requirement at 36 weeks corrected

NEC = necrotising enterocolitis, Bell Stage II or above

Late-onset sepsis = Clinical instability requiring antibiotics with a positive blood culture

Breast Milk = Exposure to Breast Milk at time of sample

3.3.3 Analysis of Left and Right Hemispheric Data

White matter regions of interest which included right and left sided data were analysed to assess significance between hemispheres. This data is presented in the tables 3.2 and 3.3.

There were no significant differences for FA or MD ($x10^{-3}mm^2/s$) between right and left hemispheric data within the frontal, central or posterior white matter and within the right and left PLIC.

Quantitative measurements were therefore combined and averaged in each individual to give regions of interest as Frontal CSO, Central CSO, Posterior CSO and PLIC.

Table 3.2: Analysis of Left and Right Hemispheric FA Measurements

	Mean	Std. Deviation	p value
Right Frontal CSO FA	0.126	0.052	0.555
Left Frontal CSO FA	0.123	0.056	
Right Middle CSO FA	0.142	0.053	0.059
Left Middle CSO FA	0.153	0.058	
Right Posterior CSO FA	0.186	0.058	0.088
Left Posterior CSO FA	0.175	0.063	
Right PLIC FA	0.422	0.052	0.987
Left PLIC FA	0.422	0.057	

Table 3.3: Analysis of Left and Right Hemispheric MD Measurements

	Mean ($x\ 10^{-3}\ mm^2/s$)	Std. Deviation ($x\ 10^{-3}\ mm^2/s$)	p value
Right Frontal CSO MD	1.636	0.177	0.832
Left Frontal CSO MD	1.633	0.182	
Right Middle CSO MD	1.564	0.191	0.686
Left Middle CSO MD	1.559	0.194	
Right Posterior CSO MD	1.537	0.203	0.283
Left Posterior CSO MD	1.523	0.184	
Right PLIC MD	1.034	0.06	0.213
Left PLIC MD	1.043	0.067	

3.3.4 The Effect of Prematurity on White Matter Microstructure

On bivariate analysis, there was a significant reduction in FA and significant increase in MD ($x10^{-3}mm^2/s$) in all white matter regions of interest in preterm infants at term equivalent age compared to term controls. These results are displayed in Figures 3.3 and 3.4.

After correction for PMA at scan, FA was reduced in preterm infants at term equivalent age compared with term controls in the genu (B 0.128 [95% CI 0.091 to 0.166], p <0.001), PLIC (B 0.029 [95% CI 0.006 to 0.052], p = 0.016) and frontal CSO (B 0.037 [95% CI 0.012 to 0.062], p = 0.04). Preterm birth did not determine FA in the central CSO (B 0.002 [95% CI -0.023 to 0.027], p = 0.894, whereas PMA at scan does (B 0.014 [95% CI 0.008 to 0.019], p <0.001) and the posterior CSO (B 0.028 [CI -0.001 to 0.057], p = 0.062), whereas PMA at scan does (B 0.007 [95% CI 0.001 to 0.013], p =0.031).

After correction for PMA at scan, MD ($x10^{-3}mm^2/s$) was increased in preterm infants at term equivalent age compared with term controls in the frontal CSO (B -0.171 [95% CI -0.257 to -0.084], p <0.001), central CSO (B -0.096 [95% CI -0.188 to -0.004], p =0.041) and the posterior CSO (B -0.134 [95% CI -0.237 to -0.30], p=0.012). Preterm birth did not determine MD ($x10^{-3}mm^2/s$) in the genu (B -0.046 [95% CI – 0.146 to 0.054], p = 0.359), whereas PMA at scan does (B -0.025 [95% CI -0.047 to -0.004], p = 0.020), or the PLIC (B -0.004 [95% CI -0.035 to 0.027], p = 0.814), whereas PMA at scan, does (B -0.011 [95% CI -0.017 to -0.004], p =0.002).

These results are summarised in Table 3.4.

Figure 3.3 The effect of prematurity on FA

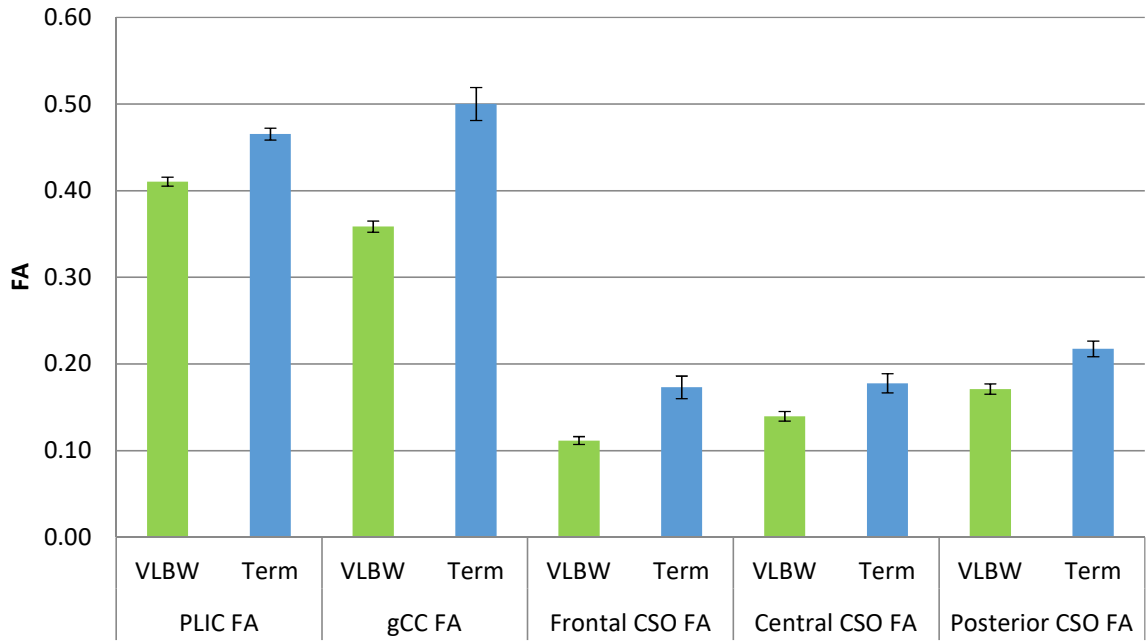

Figure 3.4 The effect of prematurity on MD

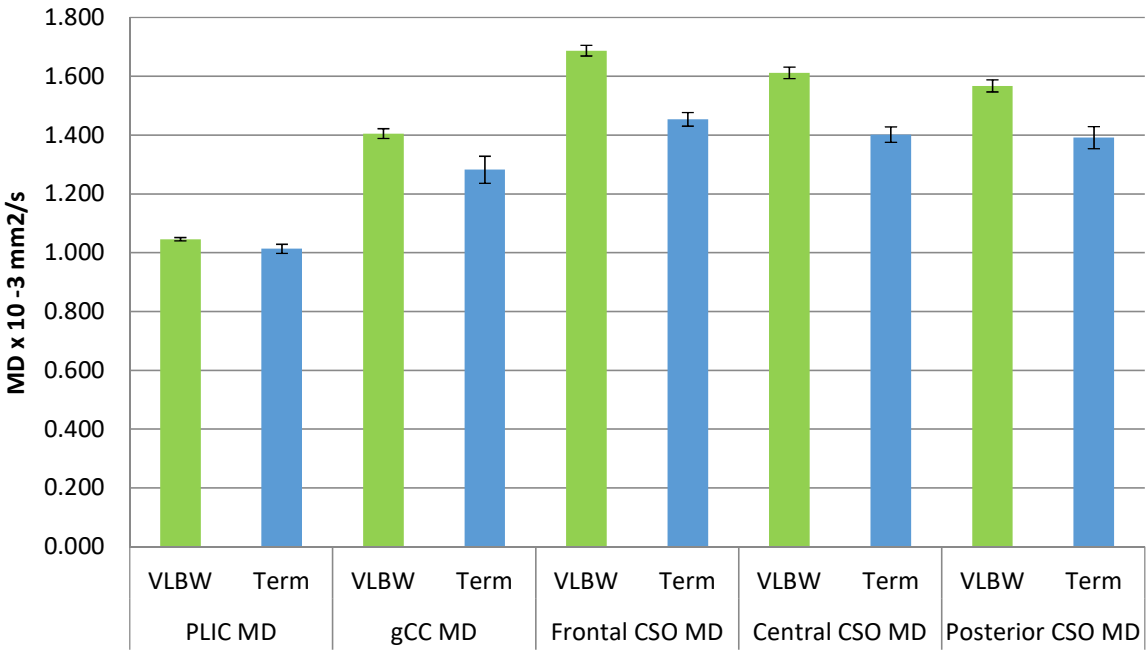

Note: FA – Fractional Anisotropy, MD – Mean Diffusivity, PLIC – Posterior Limb of Internal Capsule, gCC – Genu of Corpus Callosum, CSO – Centrum Semiovale

Table 3.4 Mean (SD) for mean diffusivity (MD) and fractional anisotropy (FA) in all regions-of-interest – effect of prematurity

	FA			
	Preterm (n=76)	**Control (n=19)**	**Unadjusted p-value**	**Adjusted p-value**
PLIC	0.41 (0.043)	0.465 (0.029)	<0.001	**0.016**
Genu	0.359 (0.054)	0.5 (0.083)	<0.001	**<0.001**
Frontal CSO	0.112 (0.039)	0.173 (0.057)	<0.001	**0.004**
Central CSO	0.139 (0.047)	0.178 (0.049)	0.002	0.894
Posterior CSO	0.171 (0.051)	0.217 (0.04)	<0.001	0.062
	Mean diffusivity MD (×10−3 mm2 /s)			
	Preterm (n=76)	**Control (n =19)**	**Unadjusted p-value**	**Adjusted p-value**
PLIC	1.046 (0.05)	1.013 (0.068)	**0.01**	0.814
Genu	1.405 (0.141)	1.282 (0.201)	**<0.001**	0.359
Frontal CSO	1.687 (0.154)	1.454 (0.1)	**<0.001**	**<0.001**
Central CSO	1.612 (0.17)	1.402 (0.115)	**<0.001**	**0.041**
Posterior CSO	1.567 (0.173)	1.391 (0.165)	**0.022**	**0.012**

Note:-

FA – Fractional Anisotropy, MD – Mean Diffusivity, PLIC – Posterior Limb of Internal Capsule, Genu – Genu of Corpus Callosum, CSO – Centrum Semiovale

3.3.5 The Effect of Antenatal Magnesium Sulphate Exposure on White Matter Microstructure in Preterm Infants

36 (47.3%) of the preterm group had been exposed to antenatal $MgSO_4$. On bivariate analysis, this was not associated with a significant difference in FA or MD ($x10^{-3}mm^2/s$) at term equivalent age, in any white matter region-of-interest. These data are presented in figures 3.5 and 3.6.

GA birth differed significantly (p =0.01) in infants who had been exposed to antenatal $MgSO_4$ [mean GA 28.6 ± 1.73 weeks] compared to those who had not [mean GA 29.9 ± 2.42 weeks].

After correction for GA at birth and PMA at time of scan, in multiple analysis, antenatal $MgSO_4$ was associated with a significant increase in FA in the genu (B -0.30, [95% CI -0.055 to -0.004], p = 0.023).

In all other areas analysed, after correction for GA at birth and PMA at time of scan, in multiple antenatal $MgSO_4$ was not associated with a significant difference in FA (PLIC: B -0.011, [95% CI -0.030 to 0.008], p = 0.239, Frontal CSO: B -0.006, [95% CI -0.025 to 0.012], p = 0.483, Central CSO: B 0.002, [95% CI -0.017 to 021], p = 0.82, Posterior CSO: B -0.008, [95% CI -0.032 to 0.017], p = 0.538) or MD x 10^{-3} mm^2/s (genu: B -0.057, [95% CI -0.016 to 0.130], p = 0.125, PLIC: B 0.011, [95% CI -0.01 to 0.032], p = 0.304, Frontal CSO: B -0.018, [95% CI -0.09 to 0.055, p = 0.63, Central CSO: B 0.012, [95% CI -0.062 to 0.087], p = 0.746, Posterior CSO: B 0.049, [95% CI -0.033 to 0.132], p = 0.237].

These results are summarised in table 3.5.

Figure 3.5 The effect of antenatal $MgSO_4$ on FA

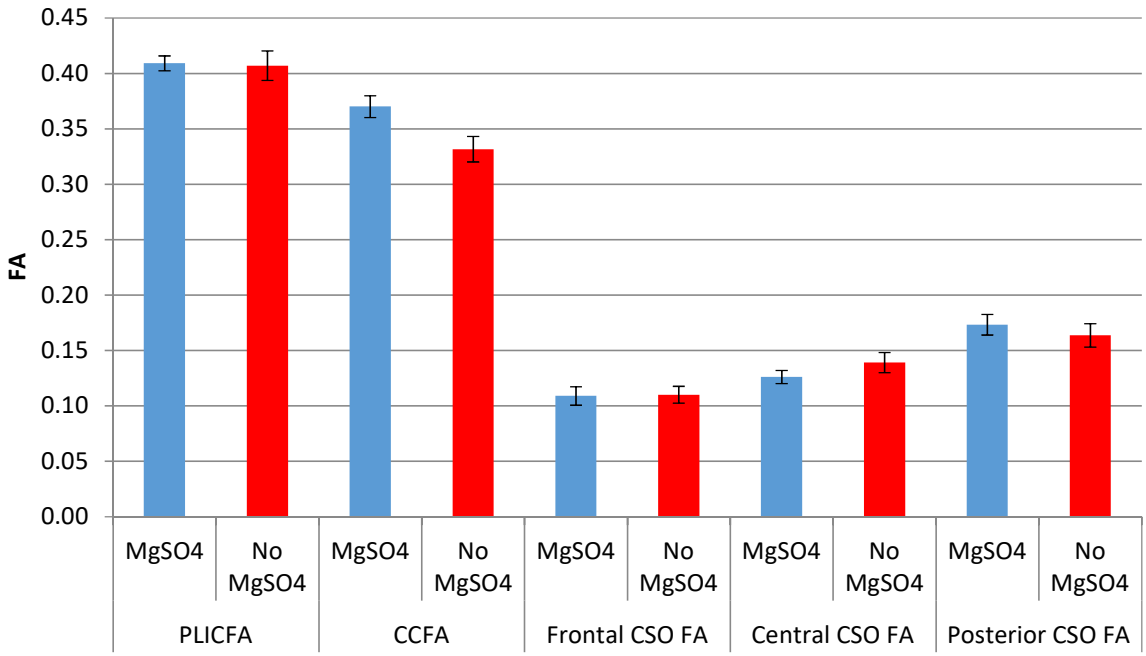

Figure 3.6 The effect of antenatal $MgSO_4$ on MD

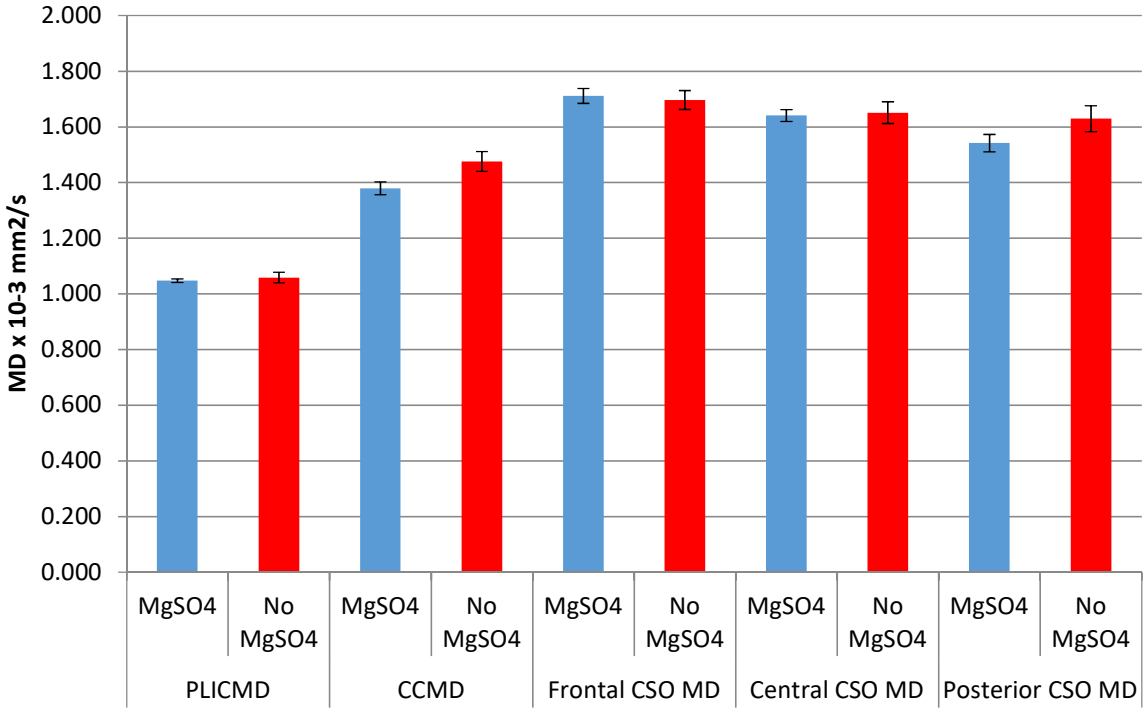

Note: FA – Fractional Anisotropy, MD – Mean Diffusivity, PLIC – Posterior Limb of Internal Capsule, gCC – Genu of Corpus Callosum, CSO – Centrum Semiovale

Table 3.5 Mean (SD) for mean diffusivity (MD) and fractional anisotropy (FA) in all regions-of-interest (Exposure to Antenatal $MgSO_4$)

	FA			
	$MgSO_4$ (n = 36)	**No $MgSO_4$ (n= 40)**	**Unadjusted p-value**	**Adjusted p-value**
PLIC	0.413 (0.040)	0.409 (0.046)	0.693	0.239
Genu	0.37 (0.055)	0.352 (0.055)	0.16	**0.023**
Frontal CSO	0.114 (0.047)	0.111 (0.031)	0.733	0.483
Central CSO	0.135 (0.048)	0.145 (0.043)	0.328	0.82
Posterior CSO	0.174 (0.049)	0.169 (0.053)	0.689	0.538
	Mean diffusivity MD ($\times 10^{-3}$ mm^2 /s)			
	$MgSO_4$ (n = 36)	**No $MgSO_4$ (n= 40)**	**Unadjusted p-value**	**Adjusted p-value**
PLIC	1.04 (0.04)	1.04 (0.06)	0.989	0.304
Genu	1.38 (0.13)	1.41 (0.18)	0.394	0.125
Frontal CSO	1.7 (0.16)	1.66 (0.15)	0.252	0.63
Central CSO	1.62 (0.15)	1.59 (0.19)	0.508	0.746
Posterior CSO	1.55 (0.17)	1.58 (0.18)	0.344	0.237

Note:-

FA – Fractional Anisotropy, MD – Mean Diffusivity, PLIC – Posterior Limb of Internal Capsule, Genu – Genu of Corpus Callosum, CSO – Centrum Semiovale, $MgSO_4$ – Magnesium Sulphate

3.3.6 The Effect of Bronchopulmonary Dysplasia on White Matter Microstructure in Preterm Infants

20 (26.3%) preterm infants had bronchopulmonary dysplasia (BPD) defined by the need for oxygen at 36 weeks corrected gestation. In bivariate analysis, this was associated with a significant decrease in FA (mean difference -0.16 [95% CI -0.031 to -0.001], p =0.036) and significant increase in MD ($x10^{-3}mm^2/s$) within the frontal CSO at term equivalent age (mean difference mean difference 0.091 [95% CI 0.023 to 0.16], p= 0.01). These results are displayed in figures 3.7 and 3.8.

There was no significant difference in PMA at time of scan (p = 0.407) between infants with BPD compared to those without. There was a significant difference in gestational age at birth (p =0.02) for infants with BPD (28.0 ± 2.16 weeks) compared to those without (29.7 ± 2.1 weeks).

After correction for GA at birth and PMA at time of scan, in multiple analysis BPD was not associated with significant changes in FA (genu: B -0.019, [95% CI -0.049 to 0.011], p = 0.207, PLIC: B -0.004, [95% CI -0.026 to 0.017], p = 0.706, Frontal CSO: B 0.17, [95% CI -0.004 to 0.038], p = 0.108, Central CSO: B 0.012, [95% CI -0.010 to 0.034], p = 0.271, Posterior CSO: B -0.007, [95% CI -0.035 to 0.021], p = 0.634) or MD $x10^{-3}$ mm^2/s (genu: B 0.043, [95% CI -0.042 to 0.128], p = 0.312, PLIC: B 0.01, [95% CI -0.023 to 0.026], p = 0.904, Frontal CSO: B -0.072, [95% CI -0.154 to 0.009], p = 0.08, Central CSO: B -0.051, [95% CI -0.136 to 0.033], p = 0.231, Posterior CSO: B 0.039, [95% CI -0.056 to 0.135], p = 0.416.

These results are summarised in table 3.6.

Figure 3.7: The effect of BPD on FA

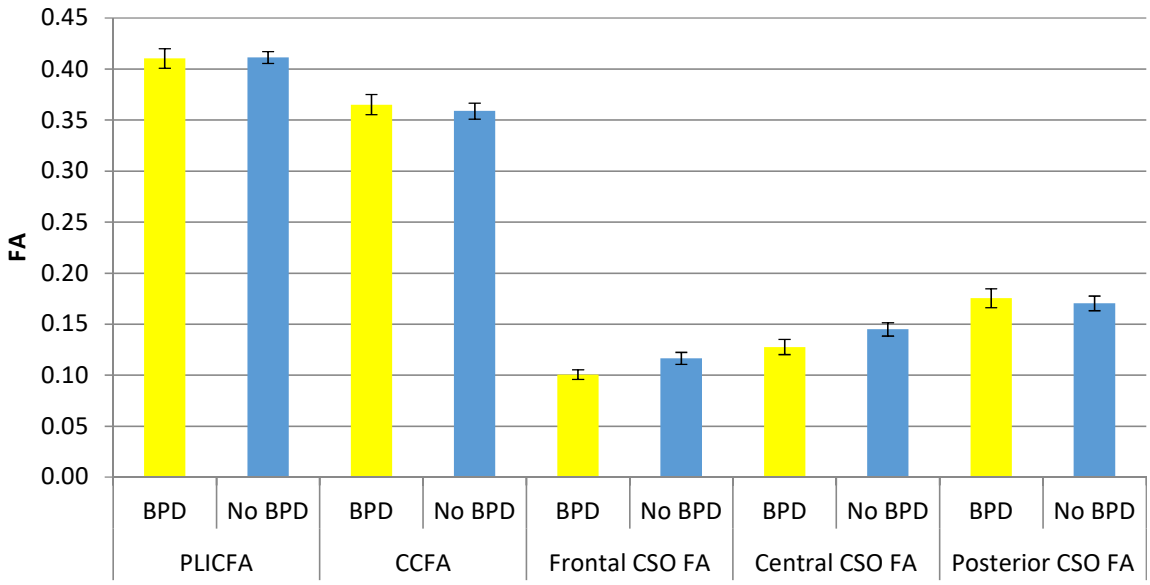

Figure 3.8: The effect of BPD on MD

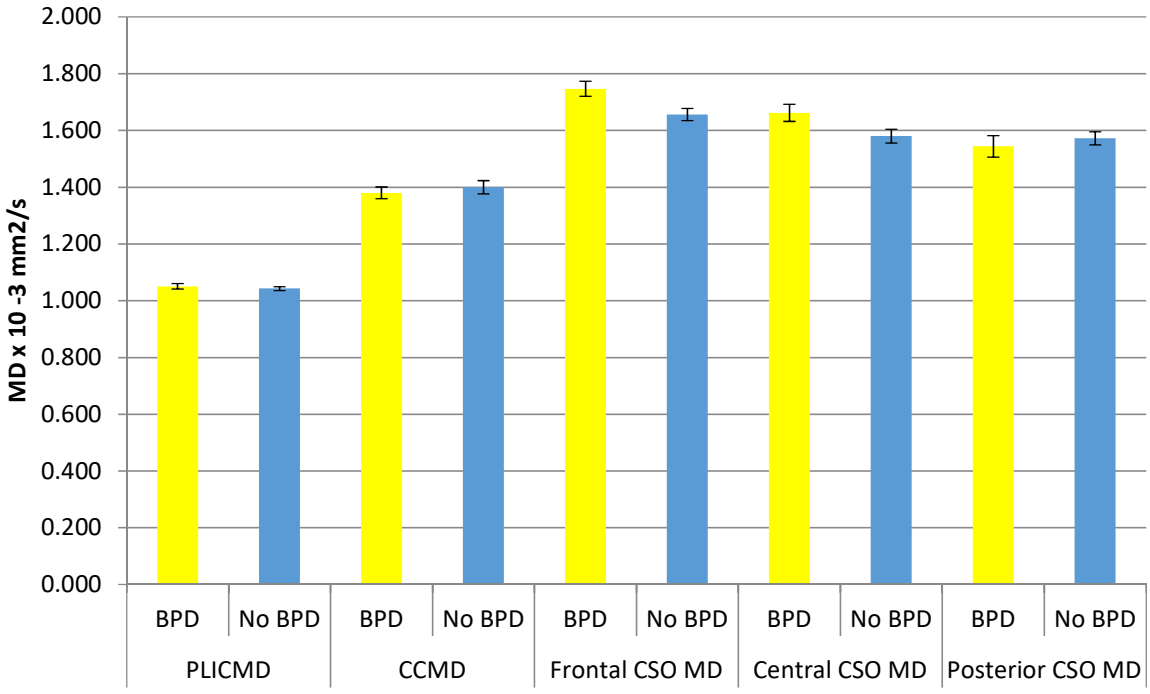

Note: FA – Fractional Anisotropy, MD – Mean Diffusivity, PLIC – Posterior Limb of Internal Capsule, gCC – Genu of Corpus Callosum, CSO – Centrum Semiovale

Table 3.6 Mean (SD) for mean diffusivity (MD) and fractional anisotropy (FA) in all regions-of-interest (Diagnosis of Bronchopulmonary Dysplasia)

	FA			
	BPD (n = 20)	**No BPD (n = 56)**	**Unadjusted p-value**	**Adjusted p-value**
PLIC	0.41 (0.043)	0.411 (0.043)	0.933	0.706
Genu	0.365 (0.044)	0.359 (0.059)	0.619	0.207
Frontal CSO	0.101 (0.021)	0.116 (0.044)	**0.036**	0.108
Central CSO	0.128 (0.033)	0.145 (0.049)	0.086	0.271
Posterior CSO	0.175 (0.041)	0.170 (0.054)	0.668	0.634
	Mean diffusivity MD ($\times 10^{-3}$ mm^2 /s)			
	BPD (n = 20)	**No BPD (n = 56)**	**Unadjusted p-value**	**Adjusted p-value**
PLIC	1.051 (0.042)	1.043 (0.051)	0.501	0.904
Genu	1.38 (0.091)	1.400 (0.177)	0.539	0.312
Frontal CSO	1.747 (0.118)	1.656 (0.159)	**0.01**	0.08
Central CSO	1.662 (0.135)	1.58 (0.179)	0.038	0.231
Posterior CSO	1.544 (0.169)	1.573 (0.173)	0.526	0.416

Note: FA – Fractional Anisotropy, MD – Mean Diffusivity, PLIC – Posterior Limb of Internal Capsule, genu – Genu of Corpus Callosum, CSO – Centrum Semiovale, BPD – Bronchopulmonary dysplasia

3.3.7 The Effect of Histological Chorioamnionitis on White Matter Microstructure in Preterm Infants

24 (31.6%) preterm infant had confirmed histological chorioamnionitis (HCA) on pathological examination of their placentas. On bivariate analysis, the presence of histological chorioamnionitis was associated with a significant reduction in FA in the Central CSO (mean difference -0.022 [95% CI -0.042 to -0.001], p = 0.037) and a significant increase in MD ($x10^{-3}mm^2/s$) in the Central CSO (mean difference 0.096 [95% CI 0.020 to 0.172], p= 0.013). These data are displayed in figures 3.9 and 3.10.

There was no significant difference in PMA at time of scan between infants with evidence of HCA compared to those without (p =0.076). There was a significant difference in gestational age at birth (p <0.001) between infants with HCA (27.9 ± 2.15 weeks) and those without (29.89 ± 1.97 weeks).

After correction for GA at birth and PMA at time of scan, in multiple analysis histological chorioamnionitis was not associated with changes in FA (Genu: B -0.003, [95% CI -0.033 to 0.027], p = 0.847, PLIC: B -0.004, [95% CI -0.025 to 0.017], p = 0.703, Frontal CSO: B 0.06, [95% CI -0.015 to 0.027], p = 0.56, Central CSO: B 0.012, [95% CI -0.010 to 0.033], p = 0.278, Posterior CSO: B -0.004, [95% CI -0.032 to 0.023], p = 0.766) or MD $x10^{-3}$ mm^2/s (Genu: B -0.18, [95% CI -0.102 to 0.066], p = 0.674, PLIC: B 0.002, [95% CI -0.022 to 0.026], p = 0.885, Frontal CSO: B -0.035, [95% CI -0.116 to 0.047], p = 0.4, Central CSO: B -0.051, [95% CI -0.134 to 0.033], p = 0.232, Posterior CSO: B -0.044, [95% CI -0.138 to 0.05], p = 0.357).

These results are summarised in table 3.7.

Figure 3.9 The effect of chorioamnionitis on FA

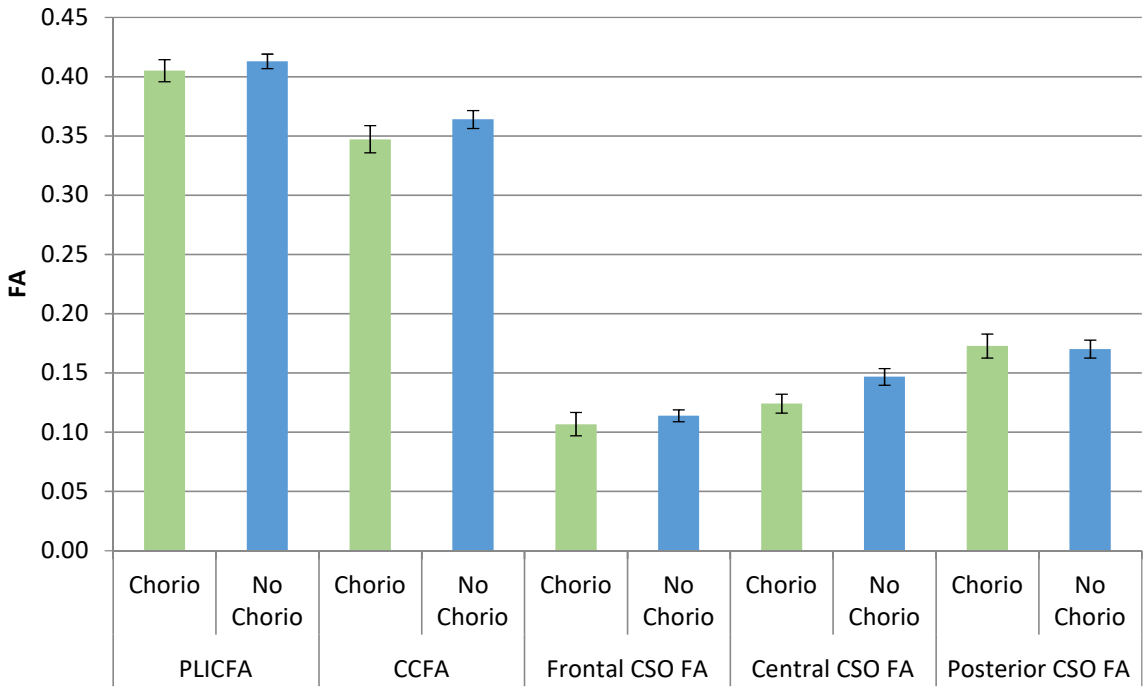

Figure 3.10 The effect of chorioamnionitis on MD

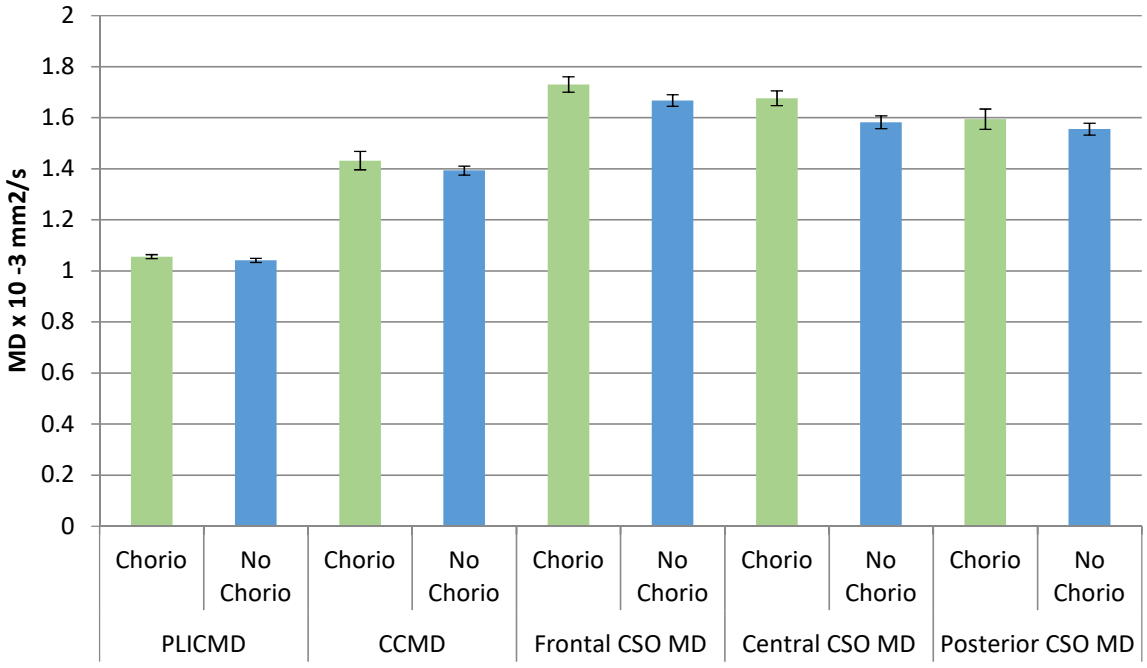

Note: FA – Fractional Anisotropy, MD – Mean Diffusivity, PLIC – Posterior Limb of Internal Capsule, gCC – Genu of Corpus Callosum, CSO – Centrum Semiovale

Table 3.7 Mean (SD) for mean diffusivity (MD) and fractional anisotropy (FA) in all regions-of-interest (Presence of Histological Chorioamnionitis)

	FA			
	HCA (n = 24)	**No HCA (n = 52)**	**Unadjusted p-value**	**Adjusted p-value**
PLIC	0.407 (0.045)	0.413 (0.042)	0.612	0.703
Genu	0.353 (0.061)	0.364 (0.053)	0.459	0.847
Frontal CSO	0.106 (0.046)	0.115 (0.036)	0.415	0.56
Central CSO	0.125 (0.038)	0.147 (0.048)	**0.037**	0.278
Posterior CSO	0.172 (0.048)	0.172 (0.052)	0.979	0.674
	Mean diffusivity MD (×10−3 mm2 /s)			
	HCA (n = 24)	**No HCA (n = 52)**	**Unadjusted p-value**	**Adjusted p-value**
PLIC	1.054 (0.037)	1.041 (0.053)	0.223	0.885
Genu	1.425 (0.712)	1.38 (0.152)	0.286	0.674
Frontal CSO	1.725 (0.144)	1.659 (0.156)	0.079	0.4
Central CSO	1.667 (0.140)	1.571 (0.178)	**0.013**	0.232
Posterior CSO	1.597 (0.188)	1.550 (0.163)	0.304	0.357

Note: FA – Fractional Anisotropy, MD – Mean Diffusivity, PLIC – Posterior Limb of Internal Capsule, gCC – Genu of Corpus Callosum, CSO – Centrum Semiovale, HCA – Histological Chorioamnionitis

3.4 Discussion

Within this chapter, in a population of 76 preterm and 19 term control infants, I have confirmed that preterm birth is associated with a reduction in FA and an increase in MD in specific white matter regions at term equivalent age.

Analyses of the preterm cohort, has shown that BPD, HCA and exposure to antenatal $MgSO_4$ may influence white matter microstructure at term equivalent age, however these results are altered by GA at birth and PMA at time of scan.

DTI measurements of FA and MD were significantly different in all regions of interest in preterm infants at term equivalent age compared to term controls in bivariate analysis. However, after adjustment for the significantly different PMA at time of scan, which was necessary as both FA and MD change rapidly during postnatal development (Huppi PS et al, 1998), only FA in the gCC, PLIC and frontal CSO and MD in the frontal, central and posterior CSO remained significantly different. These data are in agreement with previously published ROI studies (Counsell SJ et al, 2006, Rose J et al, 2007 & Skiöld B et al, 2010), which not only show significant differences between preterm infants at TEA and term controls in select white matter regions, but similar DTI values. This suggests this study population is representative.

DTI allows an objective measurement of white matter integrity and has been shown to be related to neurodevelopmental outcomes in the preterm population (Arzoumanian Y et al, 2003, Krishnan ML et al, 2007, Rose J et al, 2007, Boardman JP et al, 2010, & Thompson DK et al, 2011). As such, FA and MD in select white matter regions may be used as tools to aid prognosis and as biomarkers for the investigation of therapeutic interventions (O'Gorman RL et al, 2015).

Within the preterm population, I investigated the effect of the antenatal intervention, magnesium sulphate. $MgSO_4$ has biological plausibility as a neuroprotective agent due to its function as a NMDA receptor antagonist and its role in prevention of calcium related excitotoxic injury. It has also been linked to the reduction of inflammatory cytokines and free radicals following hypoxic-ischaemic reperfusion, all of which are linked to the pathogenesis of preterm white matter injury (Conde-Agudelo A et al, 2009). In addition, there is good evidence that it attenuates blood-brain-barrier permeability in models of eclampsia and sepsis (Esen F et al, 2005; Euser AG et al, 2008). A systematic review of 5 randomized controlled trials has shown that the administration of $MgSO_4$ reduces the incidence of cerebral palsy in infants born very preterm (Doyle LW et al, 2009), however long term cognitive data are contradictory (Doyle LW et al, 2014).

After correction for GA at birth and PMA at time of scan, I found a significant increase in FA within the gCC in preterm infants who had been exposed to antenatal $MgSO_4$ compared to those not exposed. However, as the genu of the corpus callosum connects the right and left frontal lobes which contain the prefrontal cortex and the motor cortex, it has a role in both motor and cognitive function (Fabri M et al, 2013). In support of this, Anblagan et al has shown that antenatal $MgSO_4$ exposure is associated with altered tract shape in the splenium of the corpus callosum (Anblagan et al, 2015). These data therefore suggest that $MgSO_4$ has a beneficial tissue effect which extends past motor function.

The other significant antenatal neuroprotective therapy delivered in expectant preterm birth is corticosteroids. The administration of antenatal corticosteroids is recommended by the RCOG for any woman at risk of preterm delivery (RCOG, 2010), with a complete course in this population defined as two doses of betamethasone 12mg, given 24 hours apart. It reduces the incidence of respiratory distress syndrome and therefore mortality in preterm infants, but

has also been shown to reduce the incidence of intraventricular haemorrhage and white matter lesions (Agarwal R et al, 2002) and improve neurodevelopmental outcome (Sotiriadis A et al, 2015). However, although repeated doses of corticosteroids do not show any benefit or risk to neurodevelopment (Crowther CA et al, 2007), in animal models there is an association with reduced myelination (Shields A et al, 2012). Although the mechanism by which corticosteroids may be of benefit to neurodevelopment is largely unknown, there is some evidence in animal models that they can reverse the effects of inflammatory cytokines such as INFγ and TNFα which block the differentiation of oligodendrocyte precursors (Mann SA et al, 2008). Within this population, I chose not to analyse the administration of corticosteroids as the number of infants without exposure was small (n = 5). A larger study population may allow analysis of the effect of this agent in the perinatal period at the microstructural level.

Within the preterm population, I also investigated the effect of histological chorioamnionitis and BPD on white matter microstructure at term equivalent age.

A meta-analysis has demonstrated that both clinical and HCA is associated with cerebral palsy, intraventricular haemorrhage and PVL (Shatrov JG et al, 2010) and a further study has linked HCA with poorer cognitive outcome at 5 years of age (Ylijoki M et al, 2016). Within this population, I chose to measure rates of HCA rather than clinical cases as this is a more objective measure of intrauterine infection.

Although both HCA and BPD initially showed significant differences in defined white matter regions-of-interest on bivariate analysis, these results were not significant after correction for GA at birth and PMA at time of scan.

As demonstrated in the preterm versus term control group, GA at birth has a significant effect on white matter microstructure and both FA and MD are dependent on the PMA at time of

scan. Future work with groups which are more closely matched in terms of PMA at time of scan/GA at birth may allow further assessment of the effect of these clinical states.

The lack of effect of HCA on white matter integrity in this population may be further explained by the heterogeneity of HCA which includes a range of maternal and foetal inflammation and therefore may impact on the foetal inflammatory response. This may also explain data produced by other groups which have shown that HCA confers no adverse effect on neurodevelopmental outcome (Dexter SC et al, 2000; Andrews WW et al, 2008). In future work, it would be interesting to report the degree and site of HCA. Furthermore, as HCA is known to increase PVL and IVH (Shatrov JG et al, 2010), it may be interesting to include infants with HPI or cystic PVL as determined on cranial ultrasound provided these lesions did not significantly impact on the ability to perform DTI analysis.

The use of DTI analysis technique may have contributed to the lack of effect observed by not only HCA but also with respect to the presence of BPD. Region-of-interest analysis was chosen for its high sensitivity, ease of application, and the presence of a clear hypothesis (generated by previous studies) which demonstrate a significant effect of prematurity on FA and MD in well-defined white matter regions. In addition, many clinical software packages ROI is the only option (Hakulinen U et al, 2012). A geometrical 1mm voxel square ROI was used to minimise variation between subjects and data which had significant motion artefact present was discarded. However, the lack of a robust neonatal atlas at the time of image analysis meant that my ROI placement required a manual approach. Techniques which require users to identify anatomical structures and manually describe regions-of-interest are subject to intra and inter user variability and therefore may not be suitable for cross-sectional studies (Froeling M et al, 2016). Furthermore, ROIs may not represent a white matter tract in its entirety and other voxel-based or tractography techniques may be more informative.

With this in mind, a recent voxel-based (TBSS) study by Anblagan et al, has shown that HCA is associated with decreased FA in the genu, cingulum cingulate gyri, centrum semiovale, inferior longitudinal fasciculi, limbs of the internal capsule, external capsule and cerebellum (Anblagan et al, 2016). Additionally, Ball et al demonstrated a significant reduction in FA within the centrum semiovale, corpus callosum and inferior longitudinal fasciculus in infants with BPD by using TBSS (Ball G et al, 2010), and Boardman et al showed that infants with prolonged respiratory illness have small cerebral volumes as determined by volumetric analysis (Boardman et al, 2007). It is therefore important to evaluate which approach is most informative for ongoing work and a comparison of ROI and tractography based techniques would inform this.

Further considerations which may have impacted results include problems with data collection. A difficulty I faced with acquiring the DTI data was movement artefact from unsettled infants, with a dropout rate of 5% of consented preterm and 27% of term infants. I was granted ethical approval to scan infants during natural sleep, with swaddling and ear protection to aid their comfort. Other studies have used sedation (Counsell SJ et al, 2008 & Boardman JP et al, 2010) to aid natural sleep, and this could have improved my data capture, particularly in the term cohort.

In addition, our DTI protocol could be varied in future to include less DTI directions or smaller b-values (Dudink J et al, 2008) which would allow for a shorter scan time and therefore increase the amount of subjects with DTI data.

Another challenge was the logistical organisation of consenting and scanning term infants, within the desired 38-42-week time period. As a result, PMA at time of scan was significantly higher for term infants compared to preterm infants. The DTI data were therefore corrected for PMA at birth as both FA and MD change rapidly during perinatal brain development (Huppi

PS et al, 1998). Antenatal consent of term infants may have reduced the discrepancy between PMA in the infant cohorts. However, despite these challenges, I was able to meet 95% of my target subject numbers for both preterm and term infants.

This method of DTI analysis, used manual ROI placement and therefore may be subject to operator bias, despite being blinded to gestational age and clinical state. As demonstrated in the paper by Woodward et al, (Woodward LJ et al, 2006) there are structural changes associated with preterm delivery which may be identifiable on FA maps such as gyral maturation and size of the subarachnoid space. Therefore, other techniques, such as tractography, which provide an objective measure of FA and MD could be considered to analyse this data.

3.5 Conclusions

In conclusion, within this cohort of preterm infants at term and term controls, preterm birth is associated with significant alterations to white matter integrity as assessed using ROI analysis.

Within the limits of this work, in our preterm population, exposure to antenatal magnesium sulphate, histological chorioamnionitis and the development of bronchopulmonary dysplasia may be associated with alterations in white matter microstructure at term equivalent age.

This methodology which involves manual placement of ROIs may be subject to operator bias and therefore other techniques which are more objective (such as tractography) should be considered for data analysis.

Chapter 4: Comparison of DTI techniques in a Neonatal Population

4.1 Introduction

4.1.1 Introduction

As discussed in chapter 3, the quantitative measurements of DTI, namely FA and MD are predictive of neurodevelopmental outcome after preterm birth, with FA consistently decreased and MD increased in preterm infants at term equivalent age (Counsell et al 2006, Counsell et al 2008, van Kooij et al 2012, Plaisier et al 2013, Roze et al 2015).

The corpus callosum, corticospinal tracts and posterior limbs of the internal capsule have been a focus of research attention as potential biomarkers because their microstructural properties in the neonatal period have been associated with functional outcome in childhood (Stewart AL et al 1999, Arzoumanian Y et al 2003, Anjari M et al 2007, Dudink J et al 2007, van Koij BJ et al 2012, Duerden EG et al 2015). These tracts show dynamic changes in myelination and organisation of white matter tracts during the 3rd trimester (Counsell et al 2002, Braga RM et al 2015) and are therefore susceptible to damage by preterm birth and its associated clinical sequelae.

As well as the method known as region-of-interest analysis (ROI) which, I used in chapter 3, DTI measurements can be calculated by a voxel based approach called tractography. The more traditional ROI approach performs calculations on the original MRI slice which minimises the possibility of post processing errors. However, ROIs do not represent white matter tracts as a whole and results can vary according to operator as well as shape and size of the ROI (Partridge S et al 2005, Bonekamp D et al 2007, Bisdas S et al 2008, Hakulinen U et al 2012).

Probabilistic neighbourhood tractography was first described by Clayden et al (Clayden JD et al 2006, Clayden JD et al 2007) and recently has been refined for use in the neonatal brain (Anblagan D et al 2015). In contrast to ROI, it is an unbiased method which produces measurements of FA and MD as an average of the entire fibre bundle, however data can be affected by image artefact and other crossing neuronal tracts (Alexander AL et al 2007). If DTI is to be used to quantify white matter injury in preterm infants for prognostic or therapeutic studies, it is important to know the agreement of results obtained between various methods and to assess the repeatability of measurements of subjective approaches such as ROI.

4.1.2 Hypotheses and Aims

I hypothesised that there would be limited agreement between measurements of FA and MD generated by different methods of DTI analysis, namely region-of-interest and tractography methods. I aimed to investigate this by testing agreement between measurements of FA and MD within the genu of the corpus callosum and the right and left corticospinal tract pathways/PLIC because these are of most obvious clinical utility and can be segmented reliably using PNT.

I also hypothesised that there would be good repeatability of the region-of-interest (ROI) technique when used by the same individual. In this study, I aimed to assess this by comparing repeated ROI measurements of FA and MD within the genu of corpus callosum, right and left PLIC on DTI data gathered from preterm and term infants at term equivalent age.

4.2 Methods

4.2.1 Demographic Data Collection

As per methodology in 3.2.1, birthweight (kilograms), gestational age at birth (weeks) and infant gender were collected with consent from maternal notes. Corrected gestational age (weeks) at time of scan was calculated and infants were weighed (kilograms) and had their OFC (cm) measured.

4.2.2 DTI Data Collection

Infants were recruited as per methods 2.1 and underwent MRI scanning at term equivalent age, as described in methods 2.2 with post MRI data processing as per 2.2.4.

4.2.3 Measuring FA and MD by Different DTI Methods

Probabilistic neighbourhood tractography (PNT) analysis was performed for all infants with suitable data after processing (n= 81) using the method described in 2.2.5.2. These methods are visualized in Figure 4.1

ROI data was analysed as per methods as per 2.2.5.1 from 81 tractography matched infants and tabulated for statistical analysis.

Figure 4.1 Illustration of ROI and tractography mapping

a. Reference tract of genu of corpus callosum calculated from term controls displayed in green and overlaid on an age-specific standard space template b. illustration of segmentation of whole genu for an individual subject calculated using PNT c: ROI placement in genu of corpus callosum d: reference tract of right CST e. reference tract of left CST f. ROI placement in right and left posterior limb of internal capsule

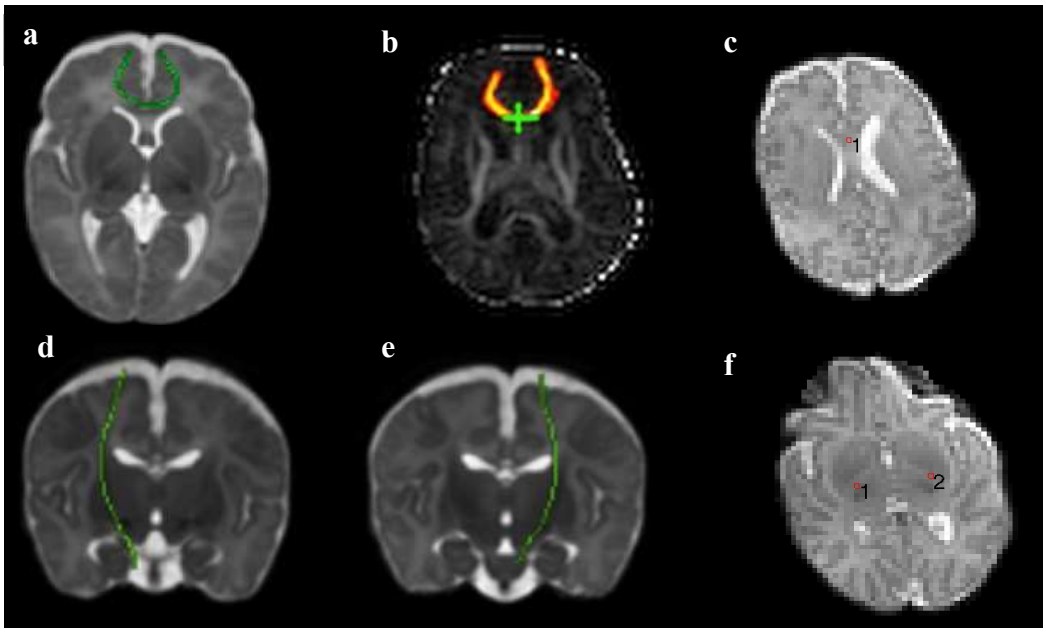

4.2.4 Repeatability of ROI Analysis

ROI analysis was repeated for 81 infants within the genu of the corpus callosum and the right and left PLIC, with subsequent FA and MD documented. These measurements were performed independent in time (on different dates) to previous ROI analysis and with blinding to previous results.

4.2.5 Statistical Analysis

Data were analysed using SPSS Statistics version 21 (International Business Machines Corporation (IBM), USA). Data were checked for normality of distribution and homogeneity of variance.

Pearson's correlation and Bland Altman plots were used to assess agreement between DTI parameters calculated from ROI and PNT for each tract. Scatter plots were utilised to further assess correlation between the 2 methods.

Intra-class correlation coefficient (ICC) and Bland Altman plots were used to assess intra-rater variability between ROI measurements.

95% limits of agreement were calculated rather than 95% confidence intervals for Bland-Altman as these were felt to provide more information on clinical utility of results.

A p value of <0.05 was considered significant.

4.3 Results

4.3.1 Patient Demographics

Matched tractography data was available for 81 patients of the original 95 infant DTI group. Data from preterm and term control infants were assessed as whole group because two technical approaches were being compared and gestational age of the infant would not confound that assessment. The demographics for this patient group are presented in table 4.1.

Table 4.1 Patient Demographics

	All Infants (n = 81)
Birthweight (Kg)*	1.58 (0.55 to 4.26)
Gestational Age at Birth (decimal weeks)*	31.28 (23.29 to 41.71)
Gestational Age at Sample (decimal weeks)*	40.3 (37.29 to 45.43)
Weight (Kg) at Sample*	2.99 (2.06 to 4.26)
OFC (cm) at Sample*	34.9 (31 to 38)
Female**	40 (49.4)

* Mean (range)
** Number (percentage)

4.3.2 Repeatability of Region-Of-Interest Analysis

The repeated ROI measurements of FA and MD ($\times 10^{-3}$ mm^2/s) in the genu of corpus callosum, right and left PLIC along with Intraclass Correlation Coefficients and Bland Altman plot values are shown in table 4.2.

There was a low magnitude of difference for both FA (0.005 to 0.004) and MD (0.003 to 0.005 $\times 10^{-3}$ mm^2/s) across the three white matter regions. Additionally, both FA and MD had 95% limits of agreement which included the possibility of no difference in the mean values between results.

ICC levels were high for FA in all 3 tracts (above 0.85). For MD, ICC was lower than FA with levels above 0.77 in the genu and right CST, falling to below 0.6 in the left CST.

This data are further represented by Bland Altman Plots (Figures 4.2a, b, c & 4.3a, b, c).

Table 4.2 Intra-rater agreement of FA and MD in 3 white matter regions-of-interest (ROI)

	gCC		Right PLIC		Left PLIC	
	FA	MD (x10-3 mm2/s)	FA	MD (x10-3 mm2/s)	FA	MD (x10-3 mm2/s)
ROI Measure 1*	0.38 (-0.08)	1.38 (-0.19)	0.423 (-0.06)	1.033 (-0.05)	0.43 (-0.05)	1.031 (-0.04)
ROI Measure 2*	0.39 (-0.09)	1.39 (-0.16)	0.421 (-0.06)	1.031 (-0.05)	0.42 (-0.05)	1.024 (-0.05)
Mean difference	-0.001	-0.005	-0.0005	0.003	0.004	0.002
95% Limits of agreement	-0.08 to 0.08	-0.30 to 0.29	0.08 to 0.08	-0.08 to 0.08	-0.06 to 0.07	-0.1 to 0.1
ICC	0.935	0.775	0.856	0.788	0.861	0.562
95% CI of ICC	0.90 to 0.96	0.65 to 0.86	0.78 to 0.91	0.67 to 0.86	0.78 to 0.91	0.32 to 0.72
p value of ICC	<0.001	<0.001	<0.001	<0.001	<0.001	<0.001

Note: - *Values are Mean (SD), ROI Measure 1 was first measurement obtained by assessor, ROI Measure 2 was second measurement obtained by assessor. Measurements were taken on different days with blinding to previous value.

95% limits of agreement - Mean difference between region of interest values ± 1.96 standard deviation of the difference

ICC – Intraclass correlation coefficient. <0.40—poor, 0.40 and 0.59 – fair, 0.60 and 0.74 – good, 0.75 and 1.00 - excellent.

p value of ICC - <0.05, is statistically significant

Figure 4.2a BA Plot: Agreement of FA values in right PLIC

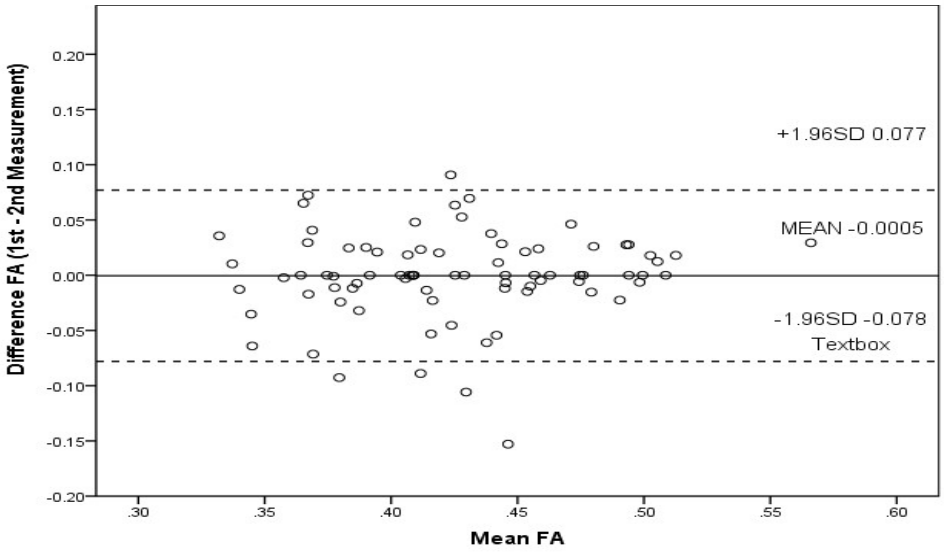

Figure 4.2b BA Plot: Agreement of FA values in left PLIC

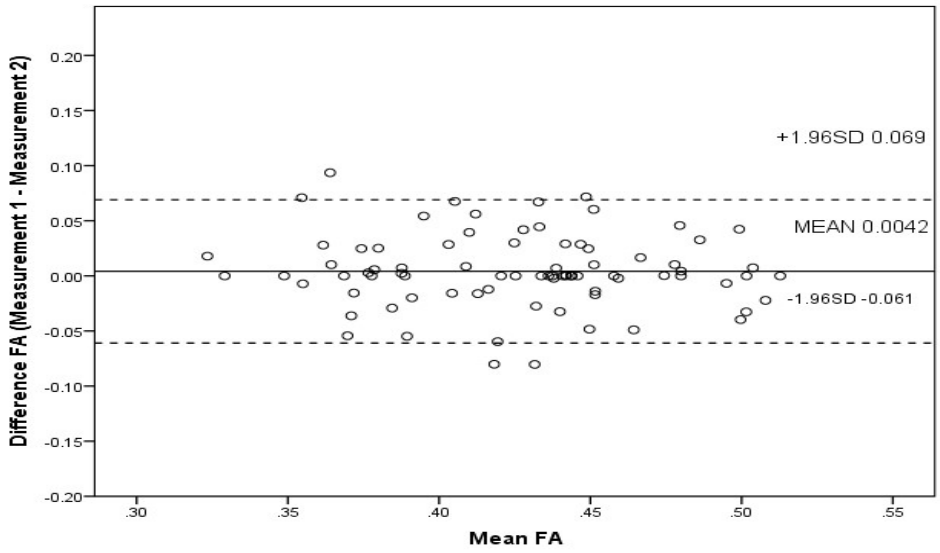

Figure 4.2c BA Plot: Agreement of FA values in gCC

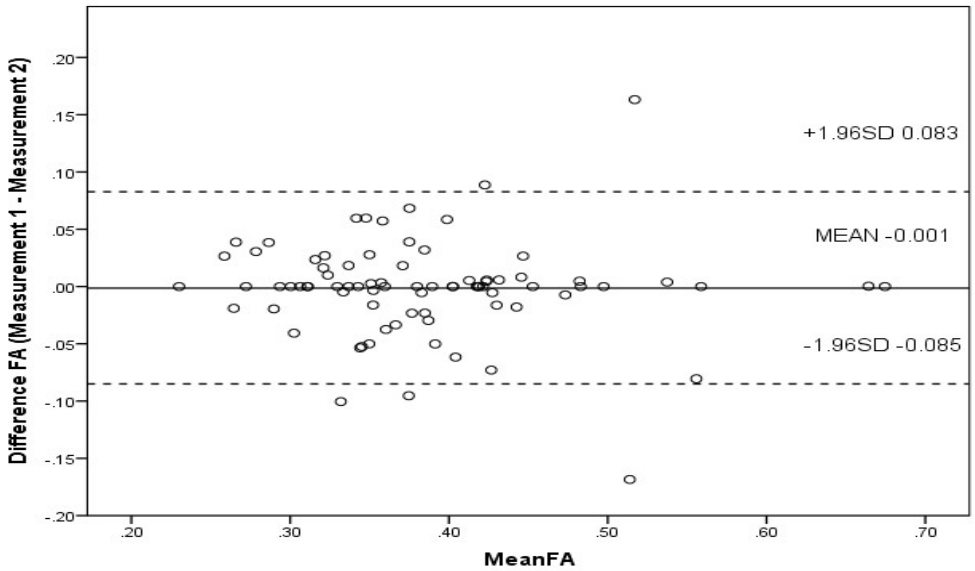

Figure 4.3a BA Plot: Agreement of MD values in right PLIC

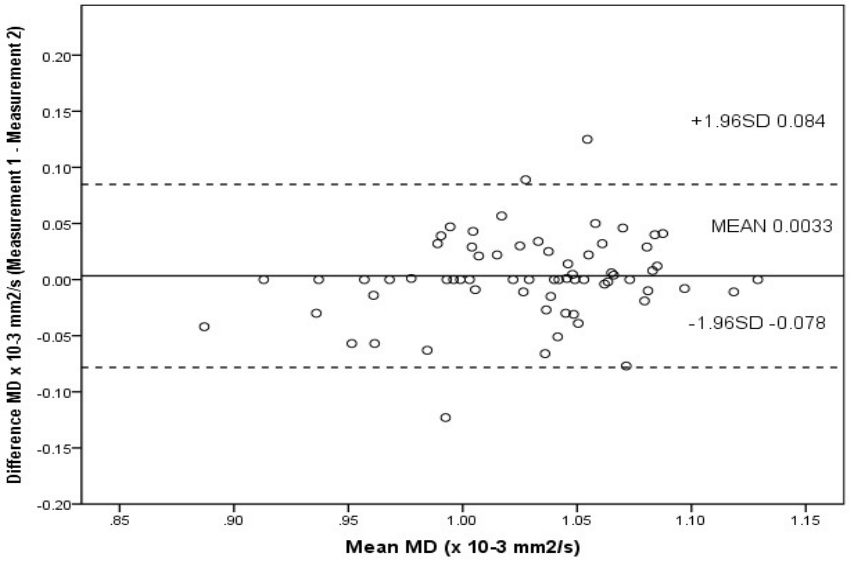

Figure 4.3b BA Plot: Agreement of MD values in left PLIC

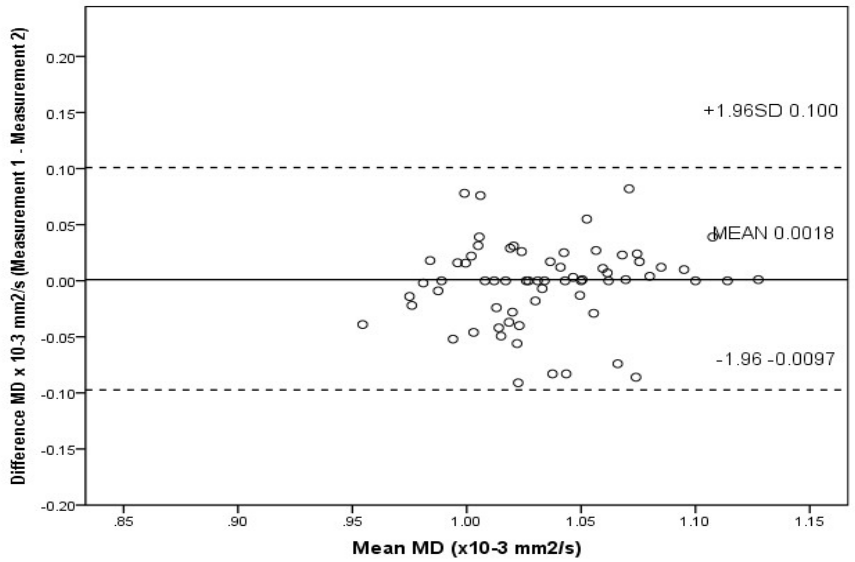

Figure 4.3c BA Plot: Agreement of MD values in gCC

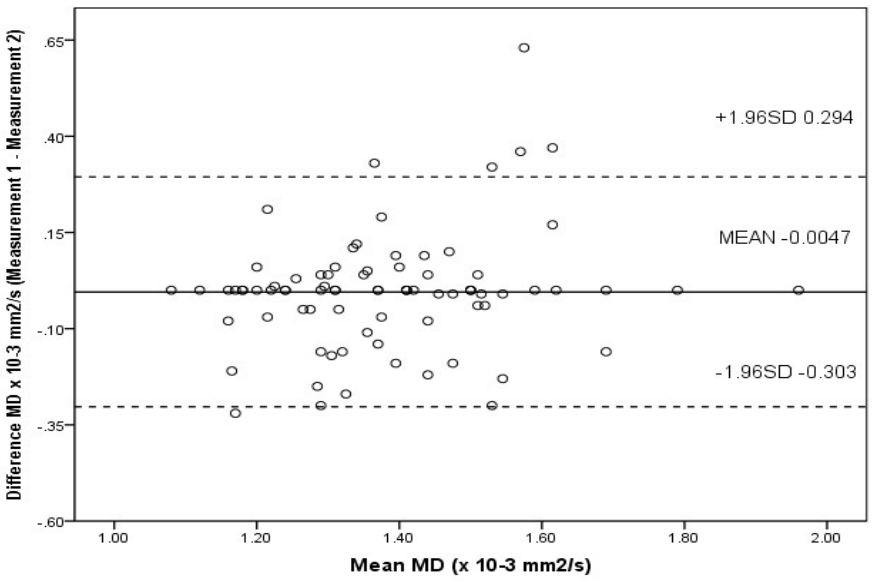

4.3.3 Agreement of Tract Averaged Versus Region-of-Interest Measured DTI Parameters

The Mean (SD) for FA and MD ($\times 10^{-3}$ mm^2/s) generated from PNT and ROI analysis within the genu of corpus callosum, left and right CST (PLIC) are displayed in table 4.3 along with Pearson correlation analysis and Bland Altman and Scatter Plot values.

In all three white matter regions, FA and MD showed significant correlation but poor agreement.

The mean difference in FA measured using PNT or ROI ranged between 0.13 and 0.17 for the three tracts. 95% limits of agreement for FA values did not include the possibility of no difference in the mean values generated by different techniques.

The mean difference in MD measured using PNT or ROI ranged between 0.101 and 0.184 $\times 10^{-3}$ mm^2/s for the three tracts. The 95% limits of agreement for MD values did include the possibility of no difference in the mean values within the genu of corpus callosum, when comparing results generated by PNT or ROI analysis.

Pearson's correlation in each region varied from high to low correlation, with lowest in FA of the genu (R = 0.24) to highest in FA of the right CST (R = 0.544).

This is further demonstrated by the Scatter Plot analysis which demonstrates positive correlation between the values.

This data are further represented by Bland Altman Plots (Figures 4.4a, b, c & 4.5a, b, c) and Scatter Plots (Figures 4.6 a, b, c & 4.7 a, b, c).

Table 4.3 Agreement of FA and MD in 3 white matter regions using PNT and ROI methods

	gCC		Right CST		Left CST	
	FA	**MD** (x10-3 mm2/s)	**FA**	**MD** (x10-3 mm2/s)	**FA**	**MD** (x10-3 mm2/s)
Bland Altman Analysis						
Tract averaged value*	0.22 (0.04)	1.473 (0.095)	0.27 (0.03)	1.167 (0.066)	0.29 (0.03)	1.216 (0.073)
Region of interest value*	0.38 (0.08)	1.371 (0.164)	0.42 (0.06)	1.032 (0.052)	0.43 (0.05)	1.031 (0.042)
Mean difference	-0.17	0.101	-0.15	0.136	-0.13	0.184
95% limits of agreement	-0.01 to -0.32	-0.212 to 0.415	-0.24 to -0.05	0.005 to 0.267	-0.22 to -0.05	0.062 to 0.307
Pearson correlation Analysis						
Pearson correlation (R)	0.24	0.335	0.544	0.38	0.467	0.529
p value of Pearson correlation	0.032	0.002	<0.001	<0.001	<0.001	<0.001
Scatter Plot Analysis						
Y intercept	0.28	0.52	0.18	0.68	0.24	0.67
Slope	0.46	0.58	0.89	0.3	0.64	0.3
R^2	0.057	0.112	0.296	0.144	0.218	0.279

Note: - *Values are Mean (SD)

95% limits of agreement - Average difference between tract averaged and region of interest values ± 1.96 standard deviation of the difference

Pearson correlation - high correlation: 0.5 to 1.0, medium correlation: 0.3 to 0.5, low correlation: 0.1 to 0.3

P value of Pearson correlation: <0.05, is statistically significant

Figure 4.4a BA Plot: Agreement of FA in right PLIC/CST (ROI

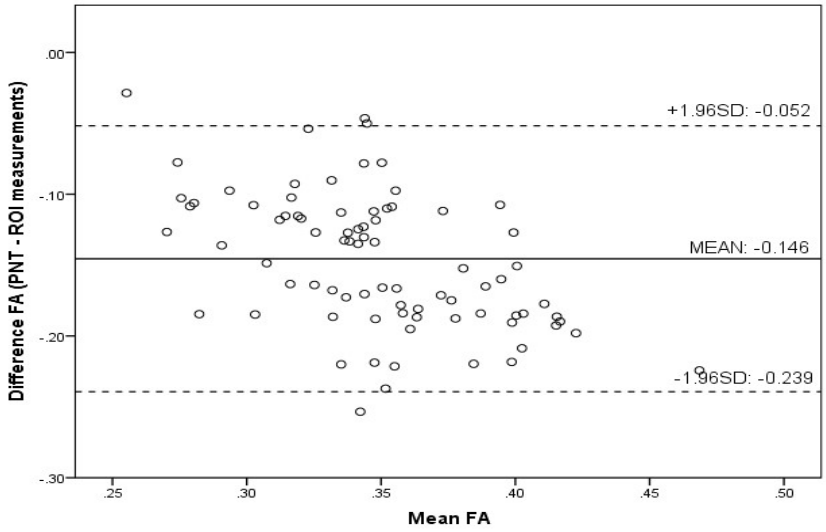

Figure 4.4b BA Plot: Agreement of FA in left PLIC/CST (ROI

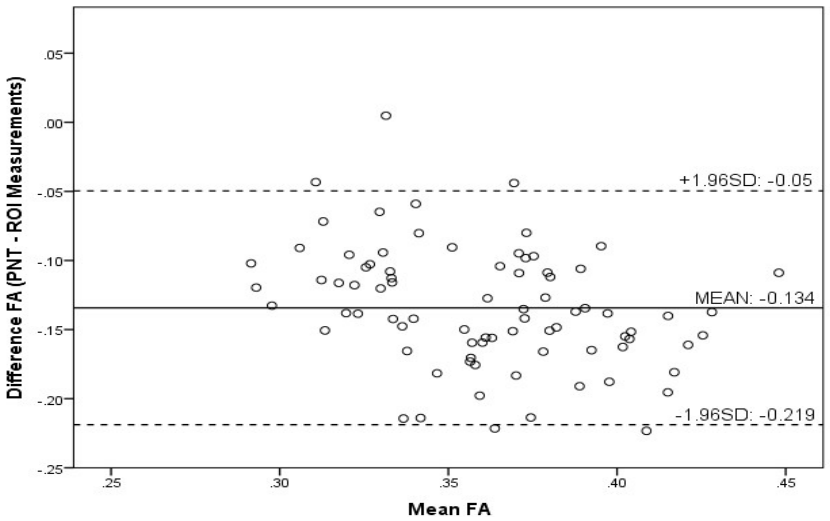

Figure 4.4c BA Plot: Agreement of FA in gCC (ROI versus PNT)

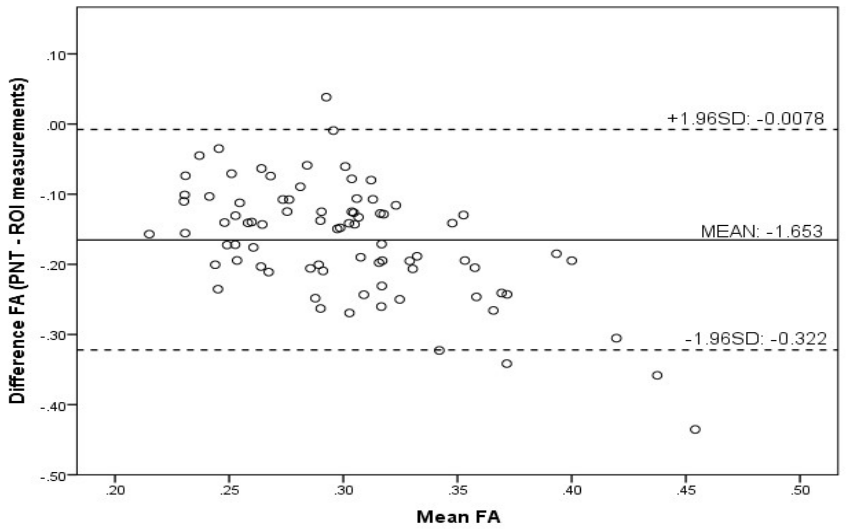

Figure 4.5a BA Plot: Agreement of MD in right PLIC/CST (ROI

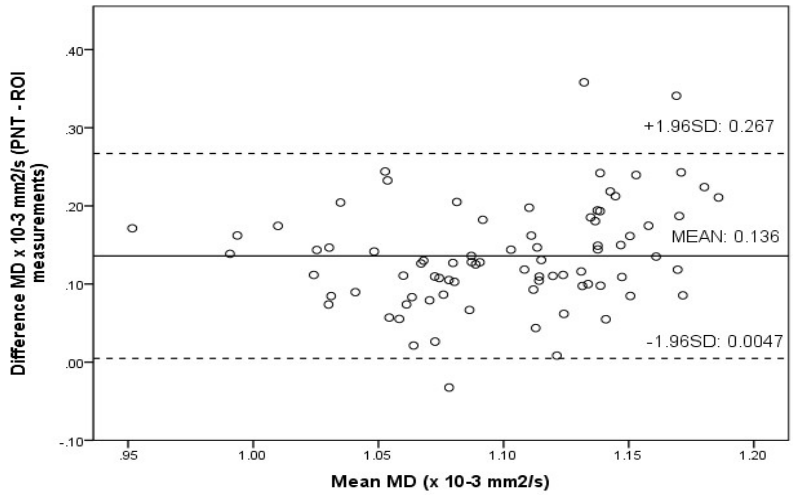

Figure 4.5b BA Plot: Agreement of MD in left PLIC/CST (ROI

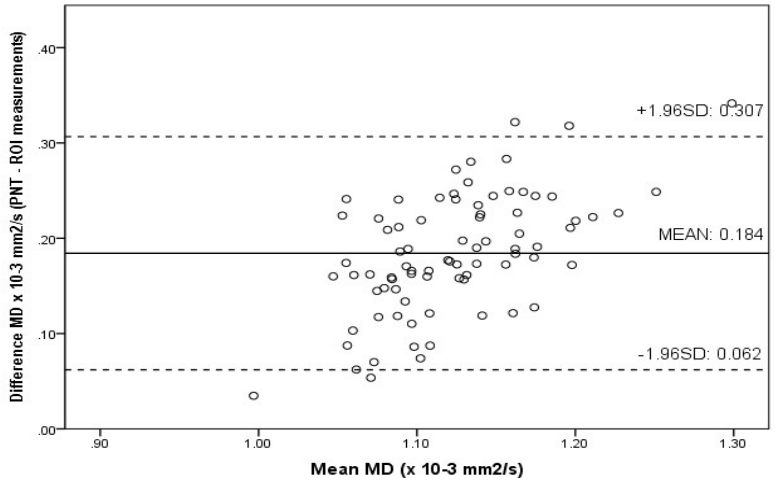

Figure 4.5c BA Plot: Agreement of MD in gCC (ROI versus PNT)

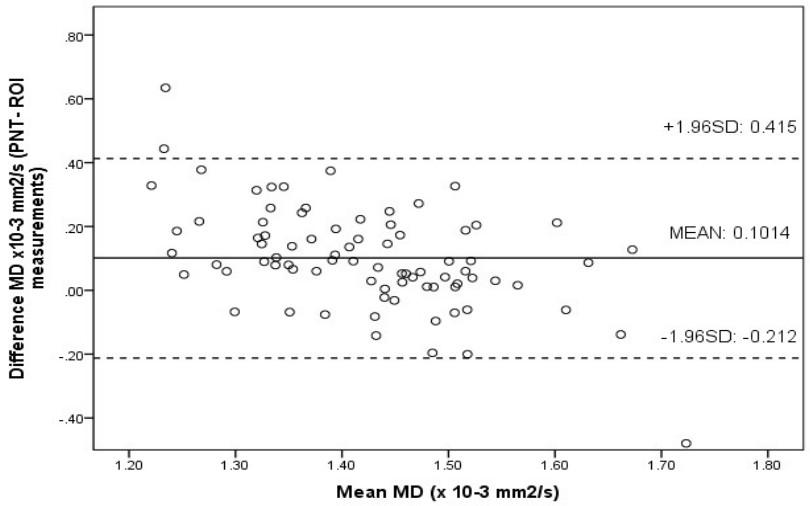

Figure 4.6a: Scatter Plot: Right PLIC versus Right CST

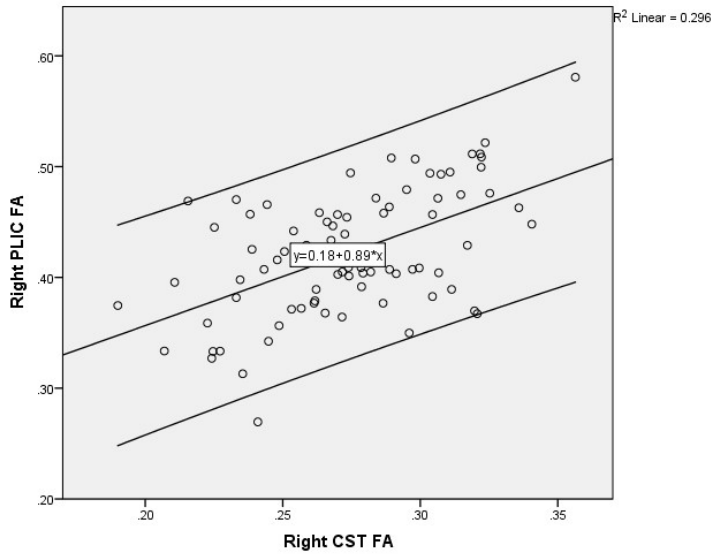

Figure 4.6b: Scatter Plot: FA Left PLIC versus Left CST

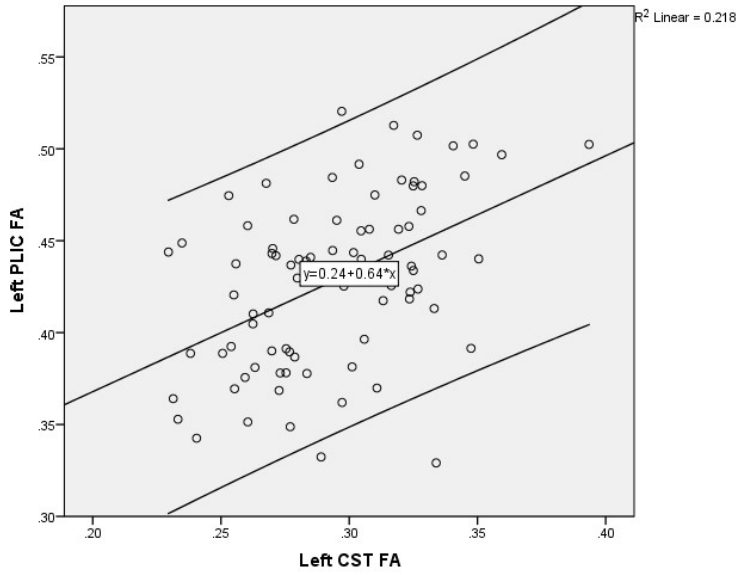

Figure 4.6c: Scatter Plot: FA gCC (ROI) versus gCC (PNT)

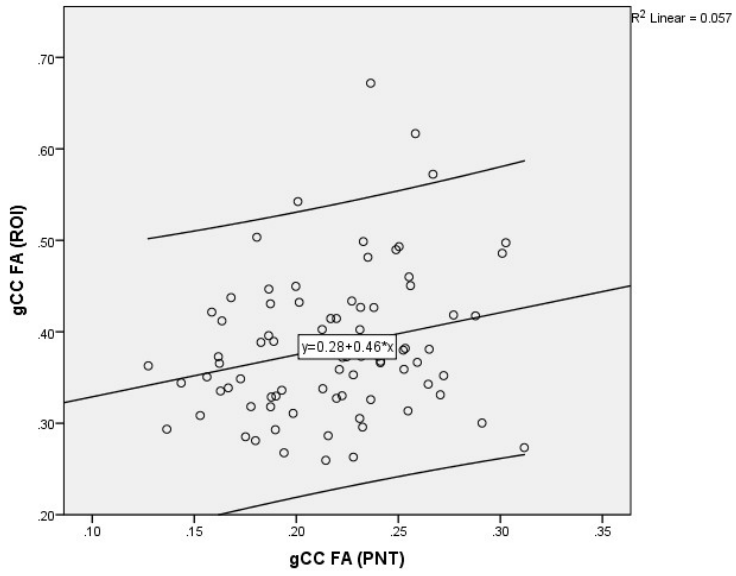

Figure 4.7a: Scatter Plot: MD Right PLIC versus Right CST

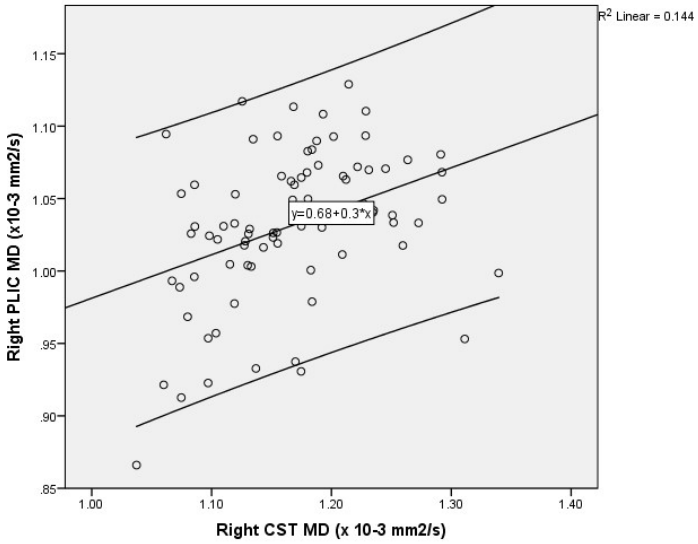

Figure 4.7b: Scatter Plot: MD Left PLIC versus CST

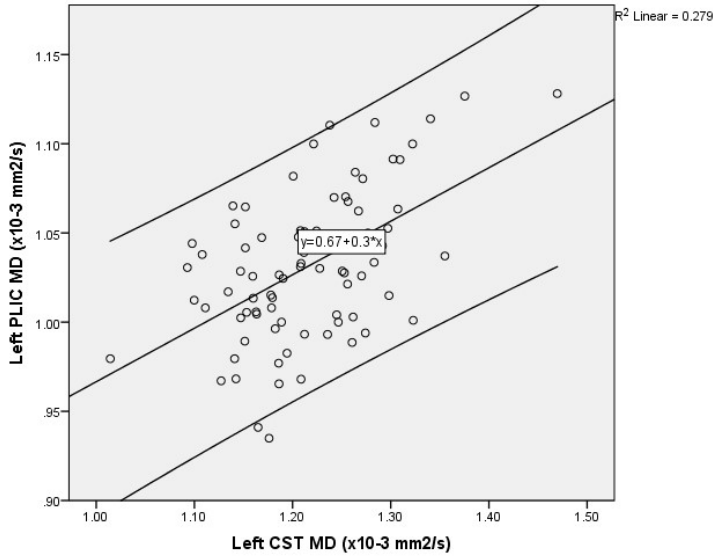

Figure 4.7c: Scatter Plot: MD gCC (ROI) versus gCC (PNT)

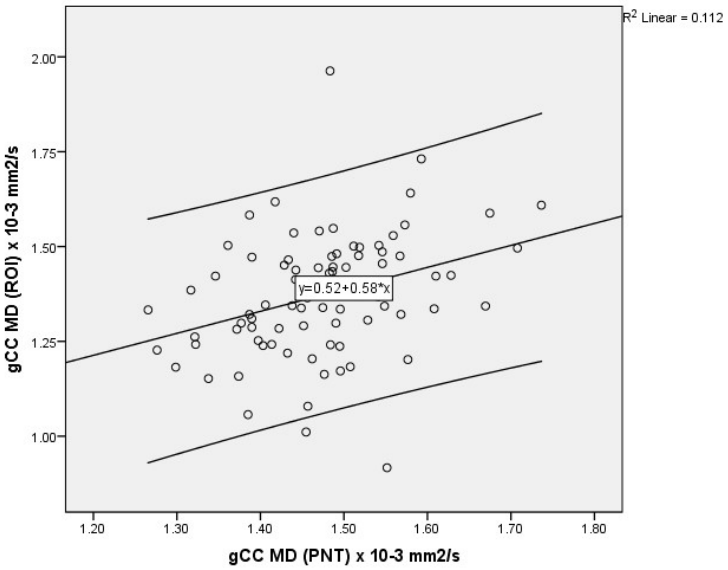

4.4 Discussion

Within this chapter, I have demonstrated that FA and MD values calculated with the corpus callosum (gCC) and corticospinal tract (CST) by region-of-interest (ROI) analysis show poor agreement with whole tract averaged values. The low level of variability found between repeated FA and MD values calculated by ROI analysis suggests that the variation seen between ROI and tract averages (PNT) techniques is not explained by operator bias.

As discussed in chapter 3, I observed similar values in the neonatal population compared to other ROI studies (Counsell et al, 2006, Arzoumanian et al, 2003, Rose et al, 2009) but also compared to other tractography studies (Liu et al, 2012) and therefore the data from this subject group can be considered representative.

Several studies have shown that relatively modest differences in FA and MD when measured in preterm infants at term equivalent age are associated with altered neurodevelopmental outcomes (Rose et al 2009, van Kooij et al, 2011, van Kooij et al 2012, Thompson et al, 2012). Therefore, the differences found between ROI and tract averaged DTI parameters may include clinically significant values.

The differences in values generated by ROI and PNT methods may be explained by patterns of myelination, tract growth and organisation which are observed in DTI studies of the developing neonate. The myelination of white matter proceeds in a staged fashion with the first phase involving proliferation and maturation of oligodendrocytes near axons and a reduction in brain water content. The second phase sees oligodendrocyte processes encapsulating the axons before full myelination occurs. Changes in anisotropy precede the macroscopic appearance of myelin (Wimberger et al, 1995, Zanin et al, 2011, Nossin-Manor et al, 2013, Dubois et al, 2014). Other maturational factors which can affect DTI

measurements include increasing axonal diameter and compactness of white matter fibres (Neil et al, 1998 & McGraw et al, 2002). These factors, along with the stages of myelination vary between and within white matter tracts and therefore the same tract can have differences in FA and MD along its length (Gilmore et al, 2007).

The corpus callosum undergoes linear volumetric growth during the third trimester, with dynamic increases in growth continuing in early childhood (Nishida et al, 2006 & Tanaka-Arakawa et al, 2015). Myelination of the corpus callosum proceeds caudo-cranially, and only reaches the genu (gCC) by 6 months' post term (Deoni et al, 2011). Therefore, the higher FA and lower MD values found with ROI analysis compared to PNT in the gCC must be explained by the maturational factors that precede myelination, such as axonal growth and reduced water content.

The corticospinal tract (CST) is partially myelinated by term equivalent age, with the posterior limb of the internal capsule showing increased signal on T1 weighted images by 38-40 weeks' gestation (Counsell et al, 2002, Gilles et al, 2012). However, myelination within the CST continues throughout the first 2 years of life with increases in FA and reductions in MD evident in sequential imaging studies (Mukherjee et al, 2001, Provenzale et al, 2007). The higher FA and lower MD values observed from ROI data in the PLIC compared to PNT in the CST can therefore be explained by differences in myelination across the tract.

The poor agreement of measurements observed demonstrates that DTI parameters produced by ROI methods do not represent the microstructural characteristics of a functional tract in its entirety. Therefore, when considering an ROI approach, it must be considered that the site of measurement within a particular tract can heavily influence the reliability of results.

In line with other ROI reliability studies, the intra-observer agreement of FA and MD values produced by manual ROI placement in the gCC and PLIC was high (Lepomaki et al, 2012). However, inter-observer precision is shown to be approximately 1/3rd of intra-observer (Muller et al, 2006 & Ciccarelli et al, 2003). These differences can be explained by the subjective nature of ROI analysis. It is reliant on slice choice and manual ROI placement, size and shape. Angulation between slices and the partial placement of ROIs in areas of CSF or grey matter may significantly alter FA and MD values (Bonekamp et al, 2007). Therefore, region-of-interest analysis requires an operator with experience in neonatal neuroanatomy and a consistent accurate placement of the ROI within specific white matter tracts before the resulting DTI parameters can be considered valid as biomarkers.

Further work with regards to understanding the variation between ROI and PNT methods could include the analysis of other white matter tracts/region of interest such as the anterior limb of the internal capsule and splenium of the corpus callosum. Additional imaging protocols such as myelin water fraction, a quantifiable measurement of T1 and T2 relaxation which is specific to myelin (Deoni et al, 2011 & Deoni et al, 2012) may also be informative in explaining the within tract variations I have observed. The reliability of ROI analysis was explored within this chapter, however the reliability of PNT was not, and future work to examine this would be of interest. In addition, it would be interesting to re-analyse the data within chapter 3 using the tractography approach, as this may provide results which are more representative of the effect of clinical parameters on white matter tracts.

4.5 Conclusions

In conclusion, FA and MD values obtained by ROI and tract-averaged approaches show limited agreement. ROI methodology is subjective and may not be representative of the

microstructural integrity of an entire white matter tract. Variability between measurements is an important factor to consider when using the ROI approach in cross-sectional and longitudinal studies, and a more objective method such as PNT may be preferable. ROI methods should be used with caution according to a rigid processing protocol and in the knowledge that they provide limited representation of the whole tract.

On the basis of these conclusions, the results obtained from PNT analysis will be used as the biomarkers of white matter development in the next chapter.

Chapter 5: The Epigenetics of Preterm Birth - From Methylome to Phenotype

5.1 Introduction

5.1.1 Introduction

The perinatal environment that the preterm infant experiences is both physically stressful; with exposure to bright lights, high noise levels and noxious stimuli (Als H et al, 2004) and physiologically stressful due to hemodynamic instability and variable oxygen levels, temperature change, altered nutrition and susceptibility to infection. Early life stress confers risk of later life metabolic and neuropsychiatric disease (Huang C et al 2010, Susser E et al 1992, St Clair D et al 2005) and these effects are transmissible through subsequent generations (Drake AJ et al, 2004 and Drake AJ et al, 2005).

DNA methylation is a stable form of epigenetic regulation which is heritable, at least through meiosis (Moore LD et al, 2013). There is evidence from both animal and human studies that DNA methylation is altered in association with early life stress (Weaver IC et al 2004, Mueller BR et al 2008, Roth TL et al 2009, Labonte B et al 2012, McGowan PO et al 2009, Tyrka AR et al 2012). DNA methylation is essential for normal neuronal development (Hutnick LK et al, 2009), myelination (Moyon S et al, 2016) and has a role in learning, memory and social cognition (Feng J et al 2010, Zhao X et al 2003, Allan AM et al 2008). In addition, disruption of normal DNA methylation patterns are implicated in neurodevelopmental and neuropsychiatric diseases including Rett Syndrome (Graff J et al, 2011), depression (Khulan B et al, 2014, Tyrka AR et al, 2016), bipolar disorder (Fries GR et al, 2016), schizophrenia (Abdolmaleky HM et al, 2006) and behavioural disorders such as autism (Loke YJ et al, 2015).

Preterm infants have an increased risk of developing autistic spectrum disorder (Johnson S et al, 2010a), attention deficit (Sucksdorff M et al, 2015) and depression or psychosis (Nosarti C et al, 2012) and there are studies showing altered DNA methylation in preterm infants (Bromer C et al, 2013, Paquette AG et al, 2013 & Paquette AG et al 2014, Cruickshank MN et al, 2013) which suggests a possible mechanism linking preterm birth, DNAm and neurodevelopmental disorders. In living human studies such as the preterm population, a surrogate tissue is required for neuroepigenetic investigation and DNAm from saliva has shown good correlation with patterns of DNAm in post-mortem brain tissue (Nohesara S et al 2011 and Ghadirivasfi M et al 2011). Therefore, it is possible to study the effect of prematurity on DNA methylation by non-invasive saliva sampling. Quantitative measurements generated by DTI can serve as a biomarker of preterm white matter injury and are predictive of neurodevelopmental outcome. Therefore, the relationship between DNAm and structural brain development can be investigated by diffusion MRI and evaluation of the methylome in preterm subjects.

5.1.2 Hypotheses and aims

I hypothesised that the stress of preterm birth will lead to alterations in the methylome that are apparent early in the newborn period. In particular, I hypothesised that there will be a significant alteration in DNAm at gene loci which are associated with neurological function and/or neurological disease.

I aimed to investigate this by collecting DNA from accessible tissue (saliva) from a sex-matched population of preterm infants at term corrected gestation and term control infants and performing a genome wide methylation array.

I also hypothesised that variance in DNAm is associated with DTI parameters in major white matter tracts and clinical risk factors for adverse outcome.

Chapter 4 concluded that PNT may provide more information about white matter integrity at the level of neural systems and therefore, I aimed to use whole tract-averaged data from 8 selected white matter tracts to compare DNAm with phenotypical changes in the preterm cohort.

5.2 Methods

5.2.1 Pilot Study

To assess feasibility, an initial pilot study was conducted using 5 term control infants and 7 preterm at term corrected age. The methodology for the collection of DNA, extraction, quantification, DNA methylation array and Bioinformatics processing were identical to those described below.

5.2.2 Patient Recruitment and Selection

I collected DNA from 72 infants (36 preterm and 36 term sex-matched controls) with DTI image linked data available for the entire preterm cohort. Inclusion and exclusion criteria and recruitment methods are outlined in 2.1.

5.2.3 Demographic Data Collection

As outlined in 3.2.1, with maternal consent, maternity notes were interrogated for maternal and perinatal demographics. With parental consent, infant notes were interrogated for relevant neonatal demographics. At time of sampling, infants were weighed (kilograms), corrected gestational age (PMA) calculated and exposure to breast milk was determined.

5.2.4 DNA Collection and Extraction

As described in 2.3 DNA was obtained by use of saliva collection swabs, anonymised with a study code and stored within a secure laboratory until time of analysis.

DNA was extracted from the samples, quantified and qualified as per methods 2.4.1 to 2.4.3 with a mean (range) DNA yield of 45.9 ng μl^{-1} (13.4 – 95.9) from preterm infant saliva samples

and 36.35 ng μl^{-1} (8.12 – 80) from term infant saliva samples. The extracted DNA was labelled with the appropriate anonymised study code and stored at 4ºC.

5.2.5 DNA Methylation Array

500 nanograms of DNA for 36 preterm and 36 term control subjects was passed to the Edinburgh Clinical Research Facility, for completion of a DNA methylation array using the Illumina HumanMethylation 450 Beadchip as described in 2.5.1 and provided results across approximately 485,000 probes.

The raw data is available to view at NCBI's Gene Expression Omnibus and is accessible through GEO Series accession number GSE72120 (http://www.ncbi.nlm.nih.gov/geo/query/acc.cgi?acc =GSE72120).

Raw data was then processed as per 2.5.2 with 112,818 probes were subsequently removed in steps that included:

Pre-filtering

1. Probes on SNPs (n = 66,877)
2. Non-specific probes (n = 26,505)
3. Sites with excess high detection P-values (n = 8,852)

Post-filtering

1. Non-CpG probes (n = 1130)
2. Probes on sex chromosomes (n = 9,454)

5.2.6 Assessment of Genes with Neurological Interest and Array Validation

I conducted a literature review of the protein coding genes which showed significantly differentially methylated regions between preterm and term infants. This allowed identification of genes which had evidence of involvement in neurological processes or the pathophysiology of neurological disease. This informed the choice of candidate genes used for pyrosequencing validation using methods described in 2.6.

5.2.6.a Literature review

The steps involved in this literature review were:

1. Identify from DNA methylation array, genes which are classified as protein coding
2. Gene codes were entered in to the National Center for Biotechnology Information
3. Gene codes aliases were tabulated i.e. SLC7a5 aka LAT1
4. A PubMed enquiry using the following search criteria was used for each gene alias, i.e. PubMed (GeneRIF) Links for Gene (Search slc7a5[gene] AND alive[prop] NOT newentry[gene])
5. Articles were interrogated for relevance to a defined human neurological disease or evidence for involvement in neural processes. If present, genes were classified as 'neural genes'
6. Information in relation to other genes was also collected and summarised

5.2.6.b Pyrosequencing

After bisulphite conversion, pyrosequencing PCR primers were optimised using a temperature gradient. The optimal annealing temperatures for each PCR product is displayed in table 5.1

with an illustration of the gel electrophoresis plate after temperature optimisation shown in figure 5.1.

Table 5.1 Optimal annealing temperature for pyrosequencing primers (°C)

	Optimal Annealing Temperature (°C)		
Gene symbol	**F and R Primer**	**Biotin Primer**	**Sequencing Primer**
SLC7a5	56.2	57.1	56.3
SLC1a2	55.7	57.1	56.3
NPBWR1	55.4	57.1	57.1
APOL1	55.4	57.1	57.1
QPRT	56.7	55.6	57.1

Figure 5.1 Qualification of optimal annealing temperature for F and R primers with gel electrophoresis

Image shows 100bp DNA Ladder in position 1 with subsequent positions displaying forward and reverse primers specific to a particular gene of interest with PCR amplification along a temperature gradient

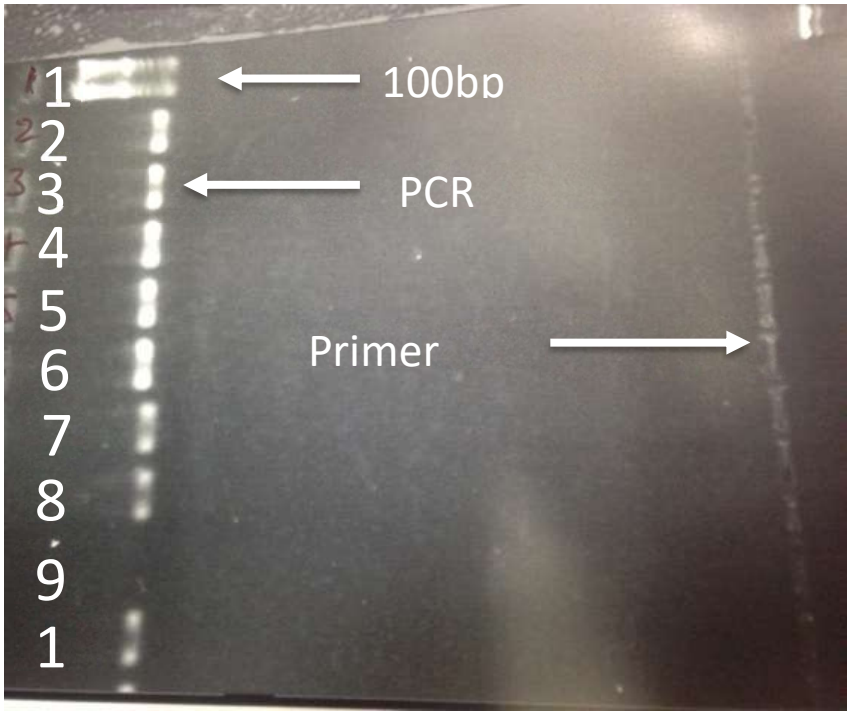

5.2.7 Quantification of White Matter Integrity

The preterm infants (n=36) had DTI parameters calculated by PNT analysis in eight major white matter fasciculi (genu and splenium of corpus callosum, left and right cingulum cingulate gyrus, left and right corticospinal tracts (CST), and left and right inferior longitudinal fasciculi) as per methods 2.2.5.2. In addition to the average FA and MD calculated for each tract of interest, a measurement of the absolute goodness-of fit of the segmented tract to the reference (*R*) was produced to quantify differences in tract shape between individual subjects.

5.2.8. Statistical Analysis

5.2.8.1 Bioinformatics

As described in methods, 2.5.2 Differential methylation between the preterm and term infants was assessed using Limma in i) gene promotors (1.5 kb upstream to 0.5 kb downstream of the transcription start site) and ii) gene bodies. A generalisation of Fisher's method with FDR correction (p value <0.05) generated genes with significantly differentially methylated regions (DMR) (Smyth GK, 2005).

5.2.8.2 Pyrosequencing

Pyrosequencing uses bisulphite treatment, which deaminates unmethylated cytosines to uracil, whilst methylated cytosines remain unaffected, to give a read out of % DNA methylation at individual CpGs within a population of cells. Mean methylation was compared using independent t-tests.

5.2.8.3 Demographics

Data were analysed using SPSS Statistics version 21 (International Business Machines Corporation (IBM), USA). Data were checked for normality of distribution and homogeneity of variance. Independent t-tests were used for continuous data and CHI squared analysis for categorical data.

5.2.8.4 Principle Components Analysis

Dimension reduction was performed using principal components analysis to assess which clinical variables and imaging features were related to signal in the methylation values within the preterm group. The clinical variables tested were: gender, PMA at birth, PMA at scan, chorioamnionitis, exposure to antenatal steroids, exposure to antenatal magnesium sulphate, number of days requiring parenteral nutrition and one/more episodes of late-onset sepsis. The image features tested were tract-averaged FA, tract-averaged MD, and R for the eight major fasciculi.

These clinical and image features along with co-ordinates of the principle components space were tested for association. For categorical data association, a 2-sided Fisher's exact test was used, for numerical data the correlation coefficient was calculated, and a p value estimated using permutation testing with 10,000 permutations. For comparison of numerical (A) and categorical data (B) associations then the p value was calculated by comparing the numerical values (A) in each category of (B), using a two-sided Wilcoxon rank sum test for 2 categories in (B) or a Kruskal-Wallis one-way analysis of variance if there were more than 2 categories. Due to the high number of variables, p-values were corrected using FDR and a p value of <0.05 was considered significant.

5.3 Results

5.3.1 Patient Demographics

Patient demographics in relation to epigenetic analysis are displayed in table 5.2.

Table 5.2 Patient demographics for infants selected for DNA methylation array

	Term Infants n=36	Preterm Infants n = 36	P value
Birthweight (Kg)*	3.57 (2.64 to 4.68)	1.047 (0.568 to 1.46)	
Gestational Age at Birth*	40 (38.14 to 42.0)	28.38 (23.29 to 32.71)	
Gestational Age at Sample*	41.24 (38.43 to 47.14)	39.76 (38.0 to 42.57)	0.001
Weight (Kg) at Sample*	3.717 (2.64 to 4.83)	2.83 (2.06 to 3.57)	<0.001
Female**	18 (50)	18 (50)	
Maternal Age *	34 (19 to 45)	31 (17 to 42)	0.071
Maternal BMI*	24.7 (19 to 36.4)	24.7 (18 to 37.6)	0.996
Preconception Folic Acid**	22 (61.1)	14 (38.9)	0.059
Diabetes (Gestational or IDDM)**	0 (0)	3 (8.3)	0.077
Multiple Birth**	0 (0)	17 (47.2)	<0.001
IUGR**	0 (0)	4 (11.1)	0.04
ART**	1 (2.8)	7 (19.4)	0.024
Chorioamnionitis**	n/a	11 (30.6)	n/a
Exposure to Antenatal Steroids**	0 (0)	35 (97.2)	n/a
Exposure to Magnesium Sulphate**	0 (0)	20 (55.6)	n/a
Vaginal Delivery**	12 (33.3)	11 (30.6)	0.465
BPD **	0 (0)	14 (38.9)	n/a
NEC**	0 (0)	2 (5.6)	n/a
Late onset sepsis**	0 (0)	10 (27.8)	n/a
Breast Milk**	31 (86.1)	23 (63.9)	0.029
TPN duration (days)*	0 (0)	11 (5-25)	n/a
Ethnicity: White British	34 (94.4)	31 (86.1)	n/a
Ethnicity: White Other	2 (5.6)	4 (11.1)	n/a
Ethnicity: African	0 (0)	1 (2.8)	n/a
Ethnicity: Asian	0 (0)	0 (0)	n/a

* Mean (range)
** Number (percentage)

ART = Artificial Reproductive Therapy
IUGR = Birthweight below the 3rd centile for gestation
BPD = Bronchopulmonary Dysplasia defined as an oxygen requirement at 36 weeks corrected gestation
NEC = Necrotising Enterocolitis, Bell Stage II or above
Late Onset Sepsis = Clinical instability requiring antibiotics with a positive blood culture
Breast Milk = Exposure to Breast Milk at time of sample

5.3.2 Methylation Array

There was significantly different methylation between term controls and preterm infants at term corrected age, within 87 gene bodies, of which 25 were classified as protein coding genes.

There was significantly different methylation within 138 promoter regions, of which 58 are known to be protein coding genes.

There were 34 genes which showed differential methylation in both gene body and promoter regions and of these, 11 were protein coding genes.

The data are available in supplementary tables 1 and 2 within the appendix.

5.3.3 Identification of Genes with Associated Neural Function/Neurodevelopment or Involvement in Neurological Pathology

I identified 10 protein coding genes which showed differential methylation between preterm infants at term and term controls and had good evidence for involvement in neural processes and/or neurological disease. These genes are summarised in tables 5.3a and 5.3b. The differential methylation patterns are displayed in figure 5.2.

The function of the other genes identified as significantly different by the methylation array is summarised in tables 5.4a and 5.4b.

Table 5.3a Differential methylation between preterm infants at term equivalent age and term control infants in protein-coding genes with neural functions and disease associations

Differentially Expressed Genes					
Gene Symbol	**Number CpG significant**	**Mean Methylation (Beta) Term**	**Mean Methylation (Beta) Preterm**	**P FDR**	**Direction of change in preterm infants compared to term**
SLC7a5	**26**	0.61	0.56	0.0019	Reduced
APOL1	**1**	0.086	0.061	0.052	Reduced
LRG1	**2**	0.69	0.62	0.018	Reduced
Differentially Expressed Promotors					
Gene Symbol	**Number CpG significant**	**Mean Methylation (Beta) Term**	**Mean Methylation (Beta) Preterm**	**P FDR**	**Direction of change in preterm infants compared to term**
SLC7a5	**1**	0.75	0.71	0.0053	Reduced
SLC1a2	**4**	0.19	0.17	0.0014	Reduced
NPBWR1	**1**	0.67	0.58	0.0084	Reduced
QPRT	**1**	0.14	0.18	0.00067	Increased
LRG1	**2**	0.58	0.48	0.00076	Reduced
PRPH	**1**	0.21	0.27	0.00034	Increased
GRIK5	**1**	0.18	0.22	0.0096	Increased
TREM2	**1**	0.76	0.73	0.029	Reduced
MCHR1	**1**	0.8	0.82	0.041	Increased

Table 5.3b Summary of protein-coding genes with neural functions and disease associations

Gene Symbol	Gene Name	Summary of Gene Function
SLC7a5	Solute carrier family 7 (amino acid transporter light chain, L system), member 5	Large amino acid transporter across the blood brain barrier
SLC1a2	Solute carrier family 1 (glial high affinity glutamate transporter), member 2	Clears excitotoxic neurotransmitter glutamate from extracellular space
QPRT	Quinolinate phosphoribosyltransferase	Catabolises quinolinate, an excitotoxic neurotransmitter
GRIK5	Glutamate receptor, ionotropic, kainate 5	Receptor to the excitotoxic neurotransmitter glutamate
APOL1	Apolipoprotein L, 1	Upregulated brains of schizophrenics, promotes autophagic cell death
LRG1	Leucine-rich alpha-2-glycoprotein 1	Increased in Alzheimer's disease & Parkinson's, may activate brain microglia
TREM2	Triggering receptor expressed on myeloid cells 2	Mutations associated with ALS, Alzheimer's, Parkinson's & dementia, regulates microglia
PRPH	Peripherin	Involved in neurite stability and development
NPBWR1	Neuropeptides B/W receptor 1	Receptor to neuropeptides B & W, K/O associated with altered social behavior
MCHR1	Melanin-concentrating hormone receptor 1	K/O associated with hyperactivity in mice

Table 5.4a Differential methylation between preterm infants at TEA and term controls in protein coding gene bodies (other genes)

Gene Body	Product	Summary of Biological Function	Literature
RTP4	chemosensory transporter 4	Golgi chaperone, regulates membrane targeting and functional activity of Mu opioid receptors	Decaillot FM et al, 2008
BAAT	bile acid CoA: amino acid N-acyltransferase	Mediates bile acid amidation, defects cause intrahepatic cholestasis	Hadžić N et al, 2012
ACKR4[2]	atypical chemokine receptor 4	Overexpression leads to inhibition of cancer cell proliferation, low expression - poor survival in breast cancer	Feng LY et al, 2009
XAF1[2]	XIAP associated factor 1	Inhibits tumour cell growth, increased methylation associated with oesophageal cancers	Chen XY et al, 2012
C5orf63	chromosome 5 open reading frame 63	*No data found on biological function*	*n/a*
TXNDC8	thioredoxin domain containing 8	Protein specific to spermatids and associated with golgi apparatus	Jiménez A et al, 2004
PF4V1[2]	platelet factor 4 variant 1	Angiostasis and anti-tumour effects in breast cancer and lymphatic cells	Van Raemdonck K et al, 2014
IFI35[1]	interferon-induced protein 35	Negatively regulates the antiviral interferon response to Vesicular stomatitis virus	Das A et al, 2014
AZU1[1]	azurocidin 1	Preprotoprotein which is proteolytically processed to a neutrophil lysosomal antimicrobial protein, multifunctional inflammatory mediator, upregulated in AD in pyramidal tracts, alterations associated with PPROM and ARDS	Kasus-Jacobi A et al, 2014 Dhaifalah I et al, 2013 Brock AJ et al, 2015 Lin Q et al, 2013
TRIM16L	tripartite motif containing 16-like	Belongs to B-box zinc finger protein family, upregulated by oestrogen	Liu et al, 1998
MSANTD3	Myb/SANT like DNA binding domain 3	*No data found on biological function*	*n/a*

Gene Body	Product	Summary of Biological Function	Literature
SLAMF9[1]	SLAM family member 9	Part of immunoglobulin subfamily, haematopoietic cell receptor - signal transduction of immune functions	Calpe S et al, 2008
GPR21	G protein linked receptor 21	Activates Gq signal pathway which mobilises calcium in response to extracellular stress	Bresnick JN et al, 2003
NXPH4	neurexophilin 4	Neuronal glycoprotein, may signal via alpha neurexin but limited data in literature	Missler M et al, 1998
CDKN2B[2]	cyclin-dependent kinase inhibitor 2B	Cell growth regulator, controls cell cycle G1 progression associated with melanoma and leukaemia	McNeal AS et al, 2015 Mai H et al 2016
ZC3H12A[1]	zinc finger CCCH-type containing 12A	Bifunctional enzyme, endoribonuclease and deubiquitinase activity. Involved in immune homeostasis, adipogenesis, angiogenesis and cardiomyocyte death	Zhou L et al, 2006
TMEM190	transmembrane protein 190	*No data found on biological function*	*n/a*
KRT32	keratin 32 type 1	Acidic protein which is essential for hair and nail growth	Langbein L et al 1999
PINLYP	phospholipase A2 inhibitor and LY6/PLAUR domain containing	*No data found on biological function*	*n/a*
C1orf65	chromosome 1 open reading frame 65	*No data found on biological function*	*n/a*
KRT76	keratin 76, type II	Produces keratin 76, essential for maintenance of skin 'tight junctions' absence causes inflammation, skin flaking, impaired wound healing and death < 3months age	DiTommaso T et al, 2014
C10orf62	chromosome 10 open reading frame 62	*No data found on biological function*	*n/a*

[1]Evidence for involvement in immune function

[2]Oncogenic potential

Table 5.4b Differential methylation between preterm infants at TEA and term controls in protein coding gene promoters (other genes)

Promoter Gene	Product	Summary of Biological Function	Literature
C5orf63	chromosome 5 open reading frame 63	*No data found on biological function*	*n/a*
RTP4	(chemosensory) transporter protein 4	Golgi chaperone, regulates membrane targeting and functional activity of Mu opioid receptors	Decaillot FM et al, 2008
SERPINA11	serpin peptidase inhibitor, clade A member 11	Extracellular serine protease inhibitor	Janciauskiene S, 2001
C15orf39	chromosome 15 open reading frame 39	*No data found on biological function*	*n/a*
KRT32	keratin 32	Acidic protein which is essential for hair and nail growth	Langbein L et al 1999
CYP3A4	cytochrome P450, family 3, subfamily A, polypeptide 4	Found in liver and small intestine, important role in drug metabolism	Thummel KE et al 1998
LIPN	lipase family N	Expressed in granular reticulocytes of epidermis, role in differentiation of keratinocytes	Toulza E et al, 2007
FAP[2]	fibroblast activation protein alpha	Membrane-bound serine protease, expression associated with carcinogenesis	Huber MA et al, 2003 & Liu F et al, 2015
INHBA	inhibin beta A	Forms subunit necessary for Inhibin and Activin, which have opposing effects on follicle stimulating hormone	de Kretser DM et al, 2002
FAM189A2	family with sequence similarity 189, member A2	*No data found on biological function*	*n/a*
TM4SF4	transmembrane 4 L six family member 4	Cell surface glycoprotein that regulates cell proliferation	Wice BM et al, 1995
CXCL10[1, 2]	chemokine (C-X-C motif) ligand 10	Chemokine - chemoattraction for T cells, inhibits angiogenesis and antitumour properties	Angiolillo AL et al, 1995 & Dufour JH et al, 2002
TXNDC8	thioredoxin domain containing 8	Protein specific to spermatids and associated with golgi apparatus	Jiménez A et al, 2004
GZMA[1]	granzyme A	Serine protease from NK cells cytotoxic granules, activates programmed cell death. Important in infection	Lieberman J, 2010
GPR116	G protein-coupled receptor 116	Regulates alveolar surfactant secretion	Bridges JP et al, 2013

S100a7a[2]	S100 calcium binding protein A7A	Shows enhanced expression in epithelial cell cancer and psoriasis	Wolf R, 2011
Promoter Gene	**Product**	**Summary of Biological Function**	**Literature**
PF4V1[2]	platelet factor 4 variant 1	Angiostasis and anti-tumour effects in melanoma, lymphatic cells	Van Raemdonck K et al 2014
GEMIN4	gem (nuclear organelle) associated protein 4	Involved in snRNP assembly and nuclear/cytoplasmic transportation	Lorson MA et al, 2008
NXF1	nuclear RNA export factor 1	Implicated in export of mRNA from nucleus	Herald A et al, 2000
SMAD3[1,2]	SMAD family member 3	Signal transducer, mediates TGF-beta signalling and has a role in regulation of carcinogenesis	Daly AC et al, 2010
GPR21	G protein linked receptor 21	Activates Gq signal pathway which mobilises calcium in response to extracellular stress	Bresnick JN et al, 2003
RPL22[2]	ribosomal protein L22	Protein which forms part of the ribosomal 60s unit, mutations associated with endometrial cancer	Novetsky AP et al, 2013
C16orf96	chromosome 16 open reading frame 96	*No data found on biological function*	*n/a*
LYN	LYN proto-oncogene, Src family tyrosine kinase	Extensively expressed on haematopoietic cells, involved in phosphatase dependent inhibitory signalling	Harder KW et al, 2001
ASB5	ankyrin repeat and SOCS box containing 5	May be involved in pathway protein ubiquitination	Andresen CA et al, 2014
IFNK[1]	interferon, kappa	Expressed in keratinocytes, confers cellular antiviral immunity	LaFleur DW et al, 2001
ARHGEF39[2]	Rho guanine nucleotide exchange factor 39	Upregulated in hepatocellular carcinoma	Wang H et al, 2012
ZDHHC11B	zinc finger, DHHC-type containing 11B	*No data found on biological function*	*n/a*
GSDMB[2]	gasdermin B	May be linked to hepatic and gastric secretory tumours	Carl-McGrath S et al, 2008
KPRP	keratinocyte proline-rich protein	Potential role in keratinocyte differentiation	Lee WH et al, 2005
PARP10	poly (ADP-ribose) polymerase family, member 10	Regulates gene transcription by altering chromatin structure, role in cell proliferation	Chou HY et al, 2006

IFI35[1]	interferon-induced protein 35	Negatively regulates the antiviral interferon response to Vesicular stomatitis virus	Das A et al, 2014
Promoter Gene	**Product**	**Summary of Biological Function**	**Literature**
ZBTB47	zinc finger and BTB domain containing 47	Role in regulation of gene expression	Kumar R et al, 2010
CD68[1]	CD68 molecule	Glycoprotein expressed by monocytes and macrophages, role in cell adhesion and antigen presentation and atherosclerosis	Ramprasad MP et al, 1996 & Kurushima H et al, 2000
NEIL1	nei endonuclease VIII-like 1	Involved in DNA repair pathway, primarily removal of oxidised pyrimidines	Odell ID et al, 2010
TFAP2E[2]	transcription factor AP-2 epsilon	Highly expressed in skin, DNA binding protein, may have role in cartilage development. Association with colorectal cancer	Niebler S et al, 2013 & Zhang ZM et al, 2014
GSG1	germ cell associated 1	*No data found on biological function*	*n/a*
PGLYRP3[1]	peptidoglycan recognition protein 3	Important role in innate immunity, recognises peptidoglycan - component of bacterial cell wall	Dziarski R et al, 2010
GLYCTK	glycerate kinase	Underactivity of this enzyme causes D-glyceric aciduria variable phenotype - normal development to encephalopathy	Sass JO et al, 2010
HRASLS2[2]	HRAS-like suppressor 2	Involved in cellular growth and differentiation, suppression of growth of cancer cells in vitro	Shyu RY et al, 2008
NAGS	N-acetylglutamate synthase	Catabolises NAG which activates CSPI, producing urea from ammonia. Deficiency leads to hyperammonemia	Morizono H et al, 2004
TNFRSF13C[1]	tumour necrosis factor receptor superfamily, member 13C	Regulation of peripheral B cell populations, overexpression may lead to autoimmune disease	Mackay F et al, 2009
PHLDB2	pleckstrin homology-like domain, family B member 2	Regulates cellular microtubule cytoskeleton and involved in delivery of AChR vesicles to NMJ	Lansbergen G et al, 2006 & Basu S et al, 2015
LY6G6D[1]	lymphocyte antigen 6 complex, locus G6D	Part of the major histocompatibility complex	Mallya M et al, 2002

DUSP13	dual specificity phosphatase 13	Tyrosine phosphatase enzyme role in spermatogenesis and skeletal muscle development	Katagiri C et al, 2011
LY6G6E[1]	lymphocyte antigen 6 complex, locus G6E	Part of the major histocompatibility complex	Mallya M et al, 2002
Promoter Gene	**Product**	**Summary of Biological Function**	**Literature**
C5orf45	chromosome 5 open reading frame 45	*No data found on biological function*	*n/a*
CCL20[1]	chemokine (C-C motif) ligand 20	Chemokine - chemoattraction for memory T cells and dendritic cells, inducible by LPS	Schutyser E et al, 2000
CTB-50L17.14	*uncharacterised protein*	*n/a*	*n/a*
Xxbac-BPG32J3.20	*uncharacterised protein*	*n/a*	*n/a*
RP11-20I23.1	*uncharacterised protein*	*n/a*	*n/a*

Figure 5.2 Differential Methylation between preterm infants at TEA and term controls at CpG sites in protein coding genes with neural function identified by Methylation Array

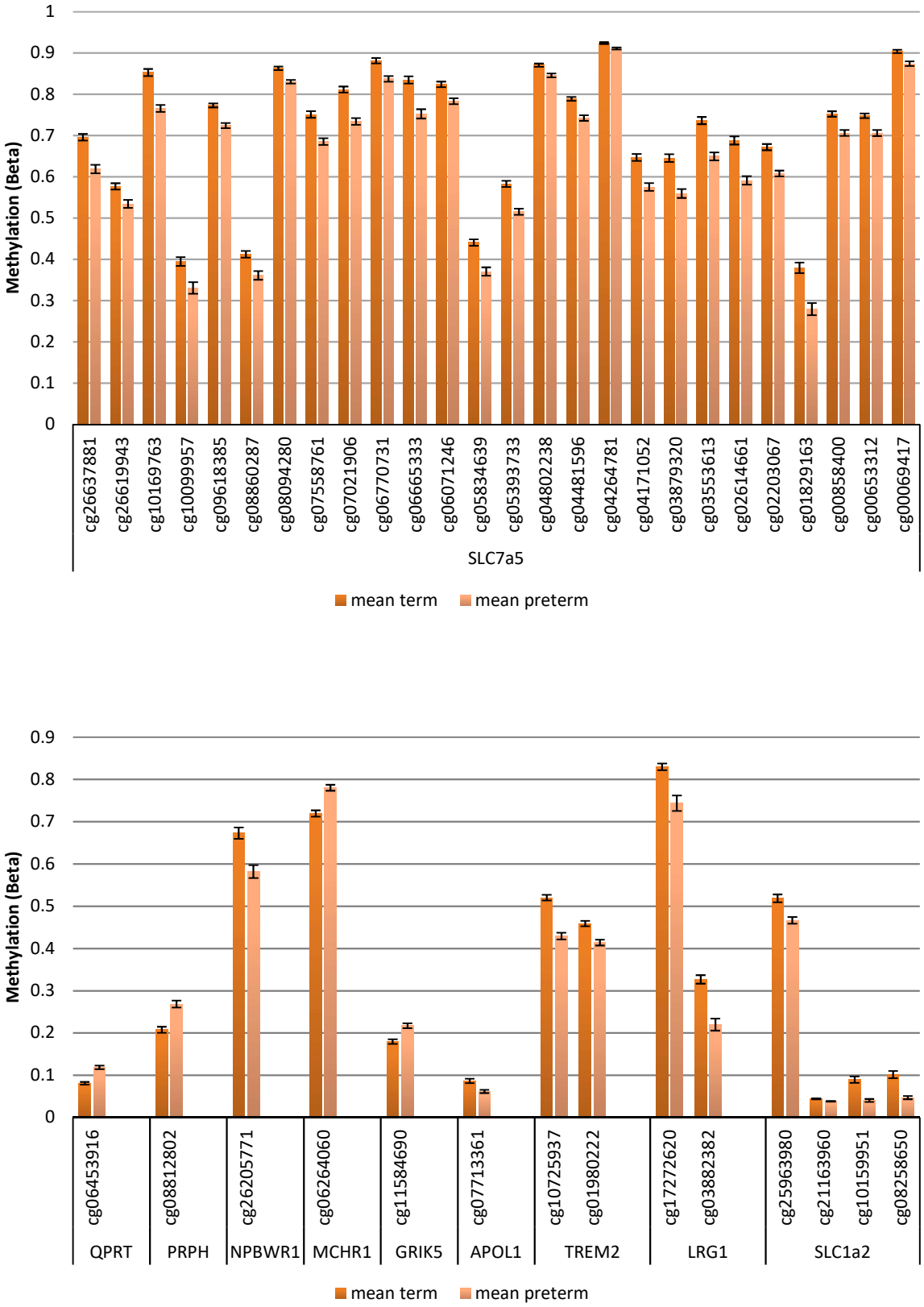

5.3.4 DNA Methylation Array Validation with Pyrosequencing

In addition to the annotated sites from the array, pyrosequencing assays covered additional neighbouring CpGs in SLC7a5 (3 additional upstream), APOL1 (1 additional downstream), SLC7a2 (1 additional downstream) and NPBWR1 (1 additional upstream and 1 additional downstream). All five genes showed significantly different methylation patterns on pyrosequencing at all CpG sites interrogated between preterm infants at term corrected age and term control infants. These methylation differences were of the same direction as the methylation array. The results are shown in table 5.5 and displayed in figure 5.3.

Table 5.5 Pyrosequencing results for 5 genes (13 CpG sites) selected for validation

Gene symbol	CpG site	Term mean % methylation (s.d.)	Preterm mean % methylation (s.d.)	% Difference (term–preterm)	P-value
SLC7a5	cg05834639	36.6 (7.2)	28.6 (8.6)	8.1	8.74E − 04
	minus 45	77.2 (7.4)	68.9 (8.8)	8.3	8.30E − 04
	minus 39	60.1 (8.2)	50.7 (8.9)	9.4	3.81E − 04
	minus 23	80.0 (5.9)	71.0 (10.9)	9.1	7.68E − 04
SLC1a2	cg25963980	31.2 (4.9)	25.7 (4.65)	5.5	5.94E − 06
	plus 10	41.2 (5.0)	34.4 (6.0)	6.8	2.43E − 06
NPBWR1	cg07629017	6.0 (2.8)	4.74 (1.3)	1.26	0.0195
	minus 5	64.5 (7.5)	56.5 (10.3)	8	4.11E − 04
	cg26205771	55.6 (7.1)	48.1 (8.1)	7.5	1.00E − 04
	plus 4	58.4 (8.6)	50.0 (10.4)	8.4	4.57E − 04
APOL1	cg36649144	29.5 (6.8)	24.3 (11.9)	5.2	0.0396
	plus 9	14.6 (3.6)	11.5 (5.8)	3.14	0.0159
QPRT	cg06453916	11.4 (1.1)	12.5 (1.5)	− 1.1	1.24E − 03

Figure 5.3 Pyrosequencing validation of selected neural genes: percentage methylation in preterm versus term control subjects

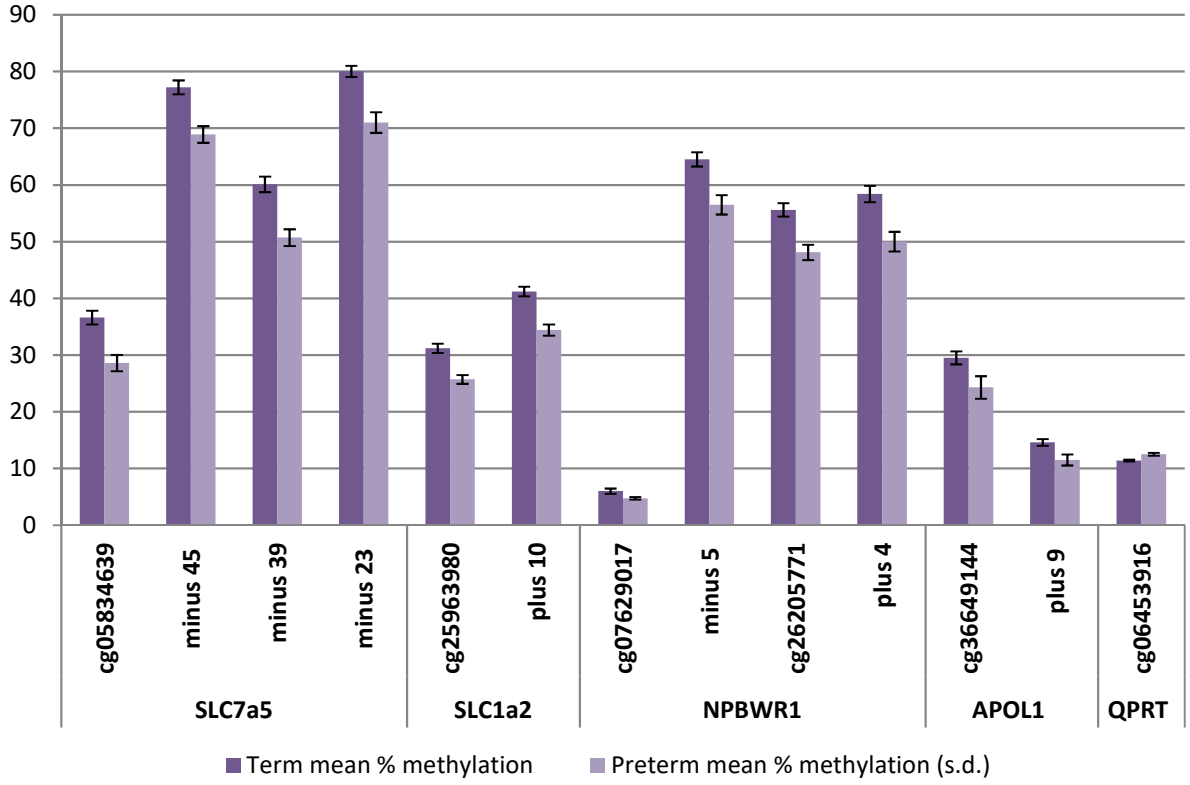

5.3.5 Diffusion MRI Analysis

DTI data were available for the entire preterm group (n=36). Figure 5.4 shows an illustration of the segmented white matter tracts for a representative subject. Table 5.6 shows descriptive statistics for FA, MD and R for the 8 eight major fasciculi identified from the DTI data in the preterm group using PNT.

Figure 5.4 Illustration of segmented tracts overlaid on FA maps.

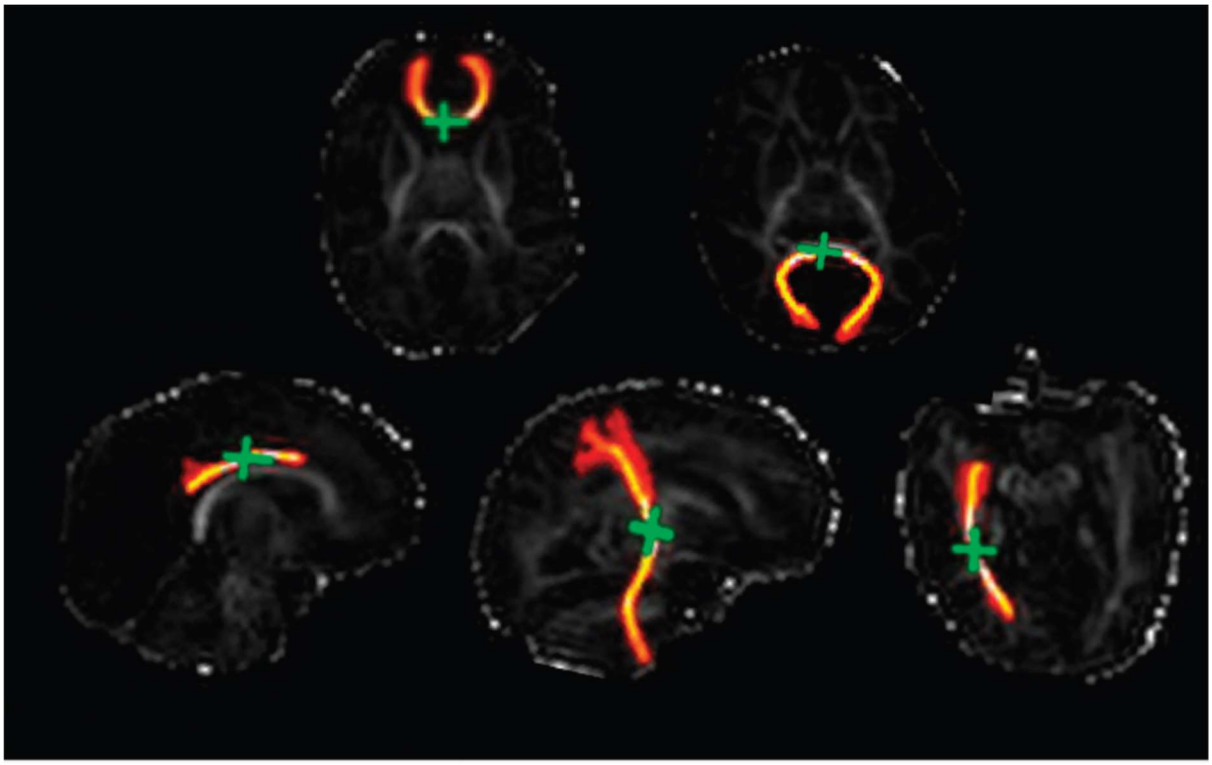

Top row: genu (left) and splenium (right) of corpus callosum. Bottom row (right to left): left CCG, right CST and right ILF. CCG = cingulum cingulate gyrus; CST =corticospinal tract; ILF = inferior longitudinal fasciculus.

Table 5.6 Mean DTI parameters for 8 major white matter fasciculi in the preterm cohort (n=36)

Mean (s.d) of tract-averaged FA and MD, and median (IQR/2) values of *R* for each major fasciculus								
	Genu	**Splenium**	**Right CST**	**Left CST**	**Right CCG**	**Left CCG**	**Right ILF**	**Left ILF**
FA	0.20 (0.04)	0.26 (0.04)	0.27 (0.03)	0.28 (0.04)	0.20 (0.03)	0.19 (0.03)	0.22 (0.03)	0.19 (0.03)
MD x 10-3 mm2/s	1.497 (0.075)	1.586 (0.162)	1.192 (0.077)	1.240 (0.065)	1.375 (0.186)	1.365 (0.067)	1.664 (0.207)	1.685 (0.210)
R (IQR/2)	-4.81 (2.27)	-7.73 (4.36)	-2.66 (1.41)	-3.30 (1.41)	-3.21 (2.44)	-2.78 (3.37)	-3.07 (2.67)	-0.97 (1.78)

Abbreviations: CCG, cingulum cingulate gyrus; CST, corticospinal tract;
FA, fractional anisotropy; ILF, inferior longitudinal fasciculus; IQR, interquartile range

5.3.6 From Methylome to Phenotype: Principle Component Analysis

95% of the variance in methylation within the preterm group was explained by 23 components. The most variance was explained by the first two principle components (31.8% and 20.1% respectively). These results are shown in table 5.7 with the corresponding heat map for association of the first 8 principle components being shown in figure 5.5.

In further exploratory analysis, gender was associated with the 1st principle component (PC) (variance 31.8%, p = 0.0071); FA in the genu of the corpus callosum was associated with the 5th PC (3.3% variance, p = 0.0061); R of the right corticospinal tract was associated with the 6th PC (2.9% variance, p = 0.0011) as was the presence of chorioamnionitis (2.9% variance, p = 0.0053). Both gender and duration of TPN were associated with the 7th PC (2.6% variance, p = 0.0016 and p = 0.0017 respectively).

After correction for multiple tests, there were three remaining associations. These were: R of the right corticospinal tract with the 6th PC (p =0.036); gender with the 7th PC (p = 0.028) and duration of TPN with the 7th PC (p =0.028).

No variable was significantly associated with any differentially methylated region when tested directly (adjusted p value = 0.05).

Table 5.7 Variance in differential methylation in the preterm cohort is explained by 23 principle components

Principle Component	Total Variance/%	Cumulative Variance/%
1	31.8	31.8
2	20.1	51.9
3	4.5	56.4
4	3.8	60.2
5	3.3	63.5
6	2.9	66.4
7	2.6	69
8	2.3	71.3
9	22	73.5
10	2.2	75.7
11	2	77.7
12	1.9	79.6
13	1.8	81.4
14	1.7	83.1
15	1.6	84.7
16	1.6	86.3
17	1.6	87.9
18	1.5	89.4
19	1.3	90.7
20	1.3	92
21	1.2	93.2
22	1.1	94.3
23	1	95.3

Figure 5.5 Heat map of p-values for association with each of the first 8 principle components

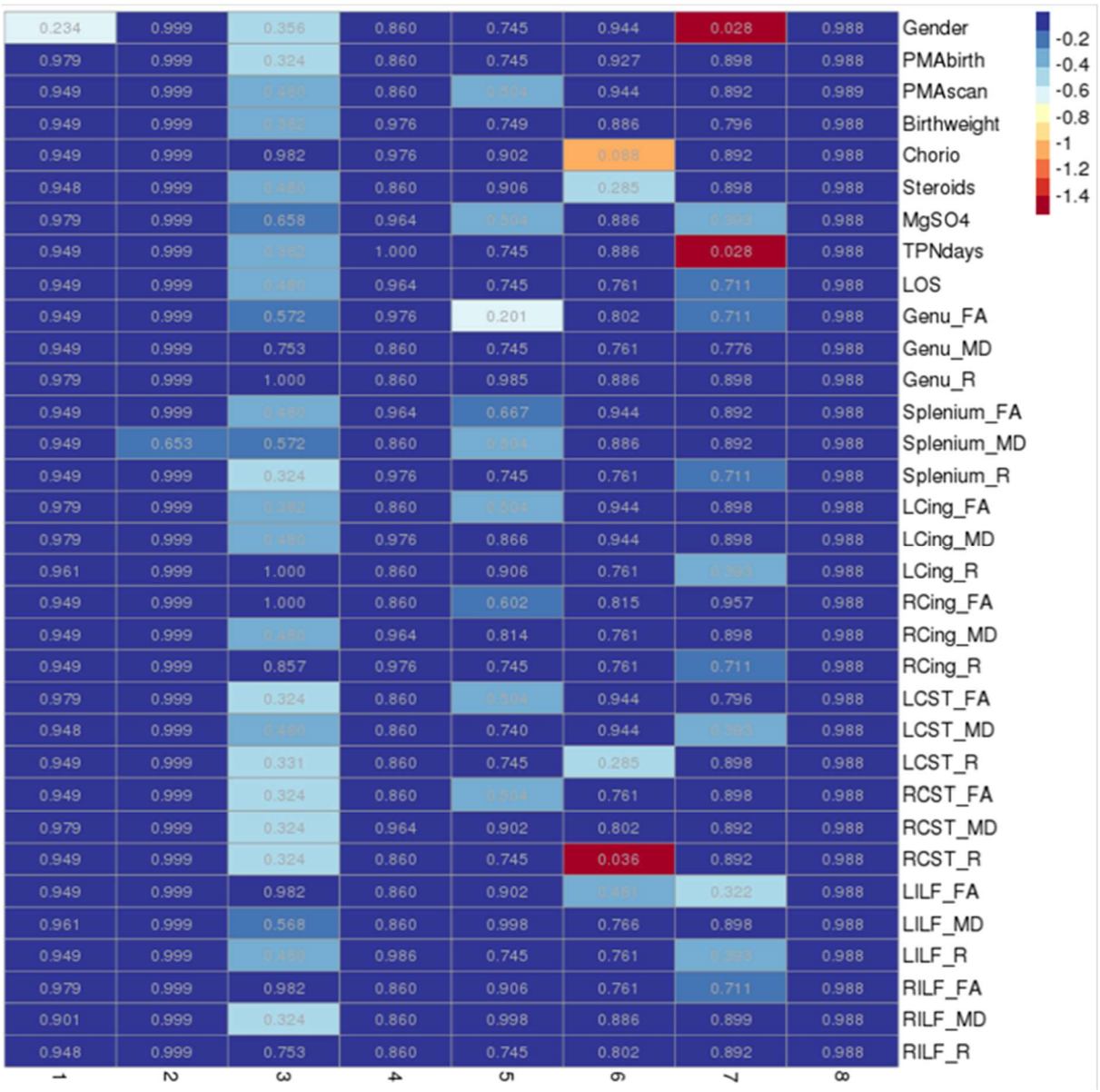

5.4 Discussion

Within this sample population of infants at term corrected gestation, preterm birth is associated with significant alteration of the methylome in 25 protein-coding genes and 58 protein-coding promoters. There are significantly different patterns of methylation in the regions of 10 protein-coding genes which have evidence of involvement in neural cell function and neurological disease. In addition, there are 15 protein-coding genes with an identified role in immune function and 13 protein-coding genes with oncogenic associations.

By using PCA analysis, I have demonstrated that the differential methylation seen in this preterm population is explained in part by clinical risk factors including: gender, exposure to chorioamnionitis and early nutrition i.e. the number of days of TPN required. Furthermore, the PCA analysis revealed that DNA methylation is associated with white matter integrity in the genu of corpus callosum and corticospinal tract, demonstrating a possible link between the methylome and preterm neurological phenotype.

Epigenome wide case control studies in schizophrenia (Aberg KA et al, 2014), autism (Ladd-Acosta C et al, 2014), victims of child abuse (Labonte B et al, 2012) and depression (Khulan B et al, 2014), and a recent ADHD cohort study (Walton E et al, 2016) have demonstrated differences in DNAm at genes important in neural function. However, few studies have investigated the effect of prematurity on DNAm using an EWAS approach. Other groups have shown a correlation between gestational age at birth and DNAm variation (Lee H et al, 2012 & Cruickshank MN et al, 2013) which may persist in to adulthood (Cruickshank MN et al, 2013). However, this study is the first to examine the variation in DNAm between preterm infants at term corrected age and term controls.

In accordance with Cruickshank et al, I found variation in DNAm between preterm and term infants in the neural genes PRPH and APOL1, the immune related genes SMAD3, ZC3H12A, LY6G6E and the oncogene TFAP2E.

The magnitude and direction of DNAm varied between and within genes, with multiple differentially methylated CpGs identified for most gene loci, supporting a biological role for these changes. In addition, pyrosequencing validation revealed additional neighbouring CpG sites with differential methylation for the genes studied, demonstrating a widespread effect of preterm birth at these loci. The majority of DNAm variation in protein-coding genes was identified in promoter regions (n=58) compared to the gene body (n=25) however, for some genes differential methylation also extended across both regions (n=11). In mammals, the majority of methylation occurs in a CpG context, with clusters of CpGs known as CpG islands often associated with transcriptional start sites (TSS) or gene promoter regions. Methylation at these regions is negatively correlated with gene expression (Moore LD et al, 2013 & Jones PA, 2012). In contrast, methylation of CpGs within the gene body, the region that extends past the first exon, can be associated with increased gene expression (Moore LD et al, 2013). Therefore, the significant difference I have observed in DNAm between preterm and term infants in identified neural gene loci may translate to differential gene expression and contribute to the preterm neurological phenotype.

This neurological phenotype as illustrated by pathological examination, structural MRI, diffusion MRI and volumetric studies includes a spectrum of change with disruption to myelination and white matter structural maturation, loss of grey and white matter volume, diffuse and cystic periventricular leukomalacia, neuronal loss and axonal degeneration (Back SA, 2014).

The functional profiles of the 10 neural genes include roles in neurological processes which may be involved in the pathogenesis of this preterm phenotype and in particular the pathogenesis of altered white matter integrity as summarised by Khwaja O and Volpe JJ, 2008. Their roles include the regulation of excitotoxic neurotransmitters, transport across the blood-brain-barrier, neuronal and glial signalling and involvement in memory, mood and social behaviour. Their candidacy is strengthened further by an association with neurological disease for the majority identified.

A large number of CpGs in 2 members of the solute carrier membrane transporter proteins, SLC7a5 and SLC1a2 were identified as differentially methylated in preterm infants. SLC7a5, also known as LAT1, is a large amino acid (including L-glutamine, methionine and tryptophan) transporter, which is expressed abundantly at the blood-brain barrier (O'Kane RL et al, 2003). L-glutamine is the main precursor for excitatory (L-glutamate) and inhibitory (GABA) neurotransmitters, and alterations in its levels are implicated in ischemic brain injury, epilepsy and huntington disease (Dolgodilina E et al, 2016). In addition, subunits of GABA receptors are differentially expressed during oligodendrocyte development, and use of the selective agonist baclofen increases proliferation of oligodendrocyte precursor cells (Luyt K et al, 2007) demonstrating its involvement in early neuronal development. Methionine is a key component of S-adeosylmethionine (SAM), the major methyl donor required by cellular methyltransferases for DNAm, therefore LAT1 has recently been implicated in regulation of the epigenome indirectly by this cellular delivery pathway (Dann SG et al, 2015). Tryptophan crosses the blood-brain barrier to participate in the synthesis of serotonin, which has a well-documented role in mood disorders such as Depression; stress responses and addiction behaviour (O'Mahony SM et al, 2015). Tryptophan is also metabolised via the kynurenine

pathway to quinolinic acid, a potent NMDA receptor which causes neuronal death and dysfunction (Rahman A et al, 2009). SLC7a5/ LAT-1 expression is affected by inflammation, with mRNA levels being reduced by the administration of LPS (Wittmann G et al, 2015), which implicates a possible pathway for inflammation/infection, excitoxicity and alteration to the white matter.

SLC1a2 (also known as EAAT2, GLT-1) is a sodium dependent glutamate transporter, which is expressed on astrocytes, oligodendrocytes, macrophages and neurons during both development and in the adult nervous system (Desilva et al, 2007). There is good evidence that EAAT2 serves to clear glutamate from the extracellular space therefore limiting its excitotoxic effect (Maragakis NJ, Rothstein JD 2004). Variation in its expression is associated with neurodegenerative diseases such as ALS (amyotrophic lateral sclerosis), Alzheimer's disease, Huntingdon disease and tuberous sclerosis (Sheldon AL et al, 2007) and neurological disorders including schizophrenia and bipolar bisorder (Shao L et al, 2008). However, EAAT2 appears to be developmentally regulated with increased expression observed between 24 to 32 weeks (the peak period for PVL) and upregulation in the astrocytes of infants with PVL compared to controls (Desilva TM et al, 2007 & 2008). A recent study investigating 2 SNPs (g.-200C>A and g.-181A>C) at EAAT2 has shown that the A allele at both loci is associated with increased risk of a low developmental score or cerebral palsy in preterm infants and alterations in EAAT2 promotor activity in vitro (Rajatileka S et al, 2017). In line with this, previous work revealed that replacement of the A allele to a C allele creates a binding site for GC binding factor 2 which represses EAAT2 expression and reduced glutamate uptake (Mallolas J et al, 2006) and infants with three C alleles have better outcomes than those with just one (Rajatileka S et al, 2017).

Whilst these findings initially seem conflicting in the context of preterm white matter injury, in vitro work with oligodendrocyte cultures demonstrate that ischaemia causes EAAT2 to operate in reverse with release of glutamate (Fern R & Möller T, 2000) and a EAAT2 knockout study has shown that although mutant mice have increased levels of glutamate in response to acute ischaemia, they have reduced levels in prolonged ischaemia (Mitani A, Tanaka K 2003). Therefore, the function of EAAT2 might change from a neuroprotective role to detrimental role in the face of ischaemia and the ability to down regulate EAAT2 expression in developing white matter may be beneficial.

Two other neural genes associated with excitotoxic processes showed differential DNAm between preterm and term populations, QPRT and GRIK5. QPRT or quinolinate phosphoribosyl transferase, catabolises quinolinate (quinolinic acid) which is, as discussed, a potent NMDA receptor agonist and considered neurotoxic (Rahman A et al, 2009). Elevated levels of quinolinate within brain tissue are associated with Alzheimer's disease (Rahman A et al, 2009) and epilepsy (Feldblum S et al, 1988); and elevated levels in the CSF occur with neuroinflammatory disorders such as meningitis (Heyes MP et al, 1992). GRIK5, Glutamate receptor, ionotropic, kainate 5, also known as KA2, is a receptor for the excitotoxic neurotransmitter glutamate, which shows specific regional distribution in human hippocampus, neocortex and cerebellum (Porter RH et al, 1997) and has evidence for developmental regulation in animal studies (Ripellinoa JA et al, 1997). Variation in its expression is associated with schizophrenia (Porter RH et al, 1997 and Meador-Woodruff JH et al, 2001).

APOL1, apolipoprotein L 1, is a secreted high-density lipoprotein with a role in lipid metabolism. It contains the Bcl-2 homology domain 3, a characteristic of proteins with a role

in cellular death, and accordingly overexpression and intracellular accumulation of APOL1 promotes autophagic cell death (AuCD) (Wan G et al, 2008). Its overexpression in the brains of schizophrenics (Mimmack ML et al, 2002) suggests it may also regulate AuCD in the central nervous system. Furthermore, it is inducible by the inflammatory cytokines IF-gamma and TNF-alpha (Zhaorigetu S et al, 2008), which like LAT1 suggests a pathway that links perinatal infection, inflammation and preterm brain injury.

The expression of LRG1, Leucine-rich alpha-2-glycoprotein 1, is also inducible by the inflammatory mediators IL-6, TNF alpha and IL-1 beta and administration of LPS (Shirai R et al, 2009). LRG1 is expressed in astrocytes and the cerebral cortex (Nakajima M et al, 2012) and increased levels in CSF are associated with ageing, Alzheimer's disease and Parkinson's disease dementia (Miyajima M et al, 2013). LRG1 has the same LRR structure as another member of the LRR super-family LRRK2, which has a role in brain microglial activation (Moehle MS et al, 2012) and therefore it is possible that LRG1 activation may mediate neurodegenerative effects via microglia, which have a well-documented role in periventricular leukomalacia (Volpe JJ, 2011).

Another of the neural genes which has a significant association with brain microglia is TREM2. Known in full as Triggering receptor expressed on myeloid cells 2, it is a member of the immunoglobulin superfamily which in the brain is mostly found within microglia, but expression on neurons and oligodendrocytes has also been reported (Lue LF et al, 2015). It is developmentally regulated, with decreasing levels in white matter structures found in postnatal mice brains (Chertoff M et al, 2013) but increasing expression observed with advancing age in human brain tissue (Forabosco P et al, 2013) with highest levels found in the white matter (Guerreiro R et al, 2013). Missense mutations at TREM2 have been associated

with Alzheimer's disease, ALS, Parkinson's disease and polycystic lipomembranous osteodysplasia with sclerosing leukoencephalopathy (PLOSL) a disease which causes severe bone cysts and pre-senile dementia (Klunemann HH et al, 2005 & Lue LF et al, 2015). From research characterising the role of TREM2 in these pathological processes, it has been shown that it TREM2 mediates the phagocytotic activity of microglia and regulates their pro-inflammatory responses to Toll-like receptor-mediated cytokines (Lue LF et al 2015 & Hickman SE et al, 2014).

The other identified neural genes (PRPH, NPBWR1 and MCHR1) do not currently have evidence in the literature in areas which may be linked directly to the pathogenesis of preterm white matter injury, however they do have significant roles in neuronal development and behaviours which can be related to the preterm population. PRPH encodes for peripherin, an intermediate filament protein that is mostly confined to the peripheral nervous system in adults, but has a variable pattern during embryonic development, with expression in a variety of neurons. It appears to have a role in neurite development and stability, with elevated levels found after neuronal injury (Zhao J et al, 2016) and variations in gene expression being associated with susceptibility to amyotrophic lateral sclerosis (Corrado L et al, 2011 and Gros-Louis F et al, 2004). There are 2 neural genes which have behavioural roles identified from knockout studies in mice, NPBWR1 and MCHR1. NPWR1 is a G protein linked receptor for neuropeptides W and R, and is also known as GPR7. There is good evidence for its involvement in regulation of anxiety, stress and emotional responses with discrete expression seen in the hypothalamus, hippocampus, ventral tegmental area (VTA), and amygdala (Sakurai T, 2013). NPBWR1-/- mice have altered social responses, with increased impulsive behaviour, contact and chase time when presented with an intruder mouse (Nagata-Kuroiwa R et al, 2011). In

addition, it has a role in energy homeostasis with GPR7-/- mice developing hyperphagia and obesity (Ishii M et al, 2003). MCHR1 (Melanin-concentrating hormone receptor 1) has similar roles in the regulation of body weight, energy expenditure and hyperactivity as demonstrated by the behaviour of MCHR1 -/- mice (Marsh DJ et al, 2002) and DNAm at MCHR1 is correlated with BMI (Stepanow S et al, 2011).

Principle component analysis was used to investigate the effect of diffusion MRI measures within 8 major white matter fasciculi and clinical neuroprotective and risk factors on DNA methylation within the preterm group. These parameters were chosen as there is good evidence in the literature that changes in FA, MD and *R* of the white matter is associated with preterm birth (Pandit AS et al, 2013 & Anblagan D et al, 2015) and the clinical risk and resilience factors were equally chosen for their well-documented effects on preterm clinical outcomes (Stoll BJ et al, 2002, Doyle LW et al, 2009, Schlapbach LJ et al, 2010, Ehrenkranz RA 2010, van Kooij BJ et al, 2011 & Sotiriadis A et al, 2015).

Initial analysis showed that the clinical factors of gender, exposure to chorioamnionitis and duration of TPN and the imaging parameters of FA in the corpus callosum and shape (*R*) of the right corticospinal tract contributed significantly to DNAm variation. After exclusion of CpG probes found on sex chromosomes, and a correction for multiple testing, three associations remained - shape (*R)* of the right corticospinal tract; and gender in combination with duration of TPN. However, when directly tested against the specific DMRs, none of these three variables showed a significant effect. This suggests that if there is an effect from these variables, it is subtle and distributed across many loci.

A summary of the functions of the immune related genes and promoters which have differential DNAm between preterm and control infants is given in tables 5.3a and 5.3b. The products of these genes include interferons, chemokines and other signalling molecules, proteins involved in both innate and adaptive immunity and inflammatory response regulators. The transfer of maternal antigen specific IgG is limited until after 32 weeks' gestation, therefore preterm infants are deficient in immunoglobulins. There is also a positive correlation between gestational age and levels of antimicrobial proteins and peptides (APPs) which are released from leukocytes, as well as reduced levels of complement proteins and granulocyte colony-stimulating factor (G-CSF) and granulocyte-macrophage colony-stimulating factor (GM-CSF) levels which lead to reduced circulating neutrophils and monocytes in preterm infants (Strunk T et al, 2011 & Melville JM et al, 2013). Relative to adults, all newborn infants have a reduced capacity for adaptive immunity (Melville JM et al, 2013), however preterm infants also have reduced levels of IFN-γ and TFN- α compared to term infants (Hartel C et al, 2005). This impairment to the innate and adaptive immune system in combination with clinical factors such the disruption of the skin barrier by invasive tests, indwelling catheters, the need for parenteral nutrition and mechanical ventilation leave the preterm infant exquisitely susceptible to infection. Around 20% of preterm infants will develop an episode of sepsis, and these infants have increased rates of mortality (Stoll BJ et al, 2002) and morbidity with increased risk of adverse neurodevelopmental outcomes including cerebral palsy (Stoll BJ et al, 2004). Although much of this immune function research is gestation specific, the results show that there are ongoing significant differences within key immune function genes at term equivalent age. In keeping with this, epidemiological studies have shown that preterm infants remain susceptible to infection after discharge from the

neonatal unit with increased ORs relating to respiratory infection and bacterial infections compared to infants born at term (Ray KN et al, 2013).

Genes with oncogenic associations which showed differential DNAm between the preterm and term population are also shown in tables 5.3.a and 5.3.b. With regards to perinatal risk factors, another study has shown that DNAm is altered in PLAGL1, a gene which is important for tumour development and growth, in infants exposed to chorioamnionitis (Liu Y et al, 2013) and a recent epigenome-wide study (Cruickshank MN et al, 2014) has shown that in keeping with my data, preterm birth is associated with differential DNAm in 18-year old individuals in SMAD3, which is involved in tumour cell proliferation (Daly AC et al, 2010) and TFAP2E, which confers risk for colorectal cancer (Zhang ZM et al, 2014). These findings show that preterm birth may have a lasting legacy, not only in terms of neurodevelopment but also by increasing the susceptibility to infections and later life diseases such as cancer, and that this may be mediated by alterations in the methylome.

The approaches I utilised in this study which may have impacted data include tissue type, the timing of sampling and the method of assessing DNAm. My approach used bisulphite conversion, which converts unmethylated 5-methylcytosines (5mC) to uracil, thus allowing thymine amplification during PCR and subsequent identification by the Illumina Methylation array. An inherent problem with this approach is that it does not differentiate between 5mC and 5-hydroxymethylcytosine (Jones PA, 2012), which may have different distributions and functions within the epigenome (Branco MR et al, 2012). The bioinformatics post-processing of the results, with removal of methylation at non-CpG sites helps to reduce some of this confounding data.

I chose to sample the population at term equivalent age, which allowed me to examine the allostatic load of preterm birth and its clinical sequelae. However, this approach may miss temporal cues for epigenetic modification throughout the perinatal period and indeed beyond. Two recent studies have demonstrated the dynamic nature of DNAm, with variations observed between preterm and term cohorts, which were significant at birth, or term corrected age, resolving by 1 year (Piyasena C et al, 2016) and 18 years of age (Cruickshank MN et al, 2014). Additionally, other studies have used other tissues types such as umbilical blood for analysis and this may account for the differences in loci I have identified compared to other groups (Fernando F et al, 2015). I used saliva samples for epigenetic tissue sampling due to its acceptable, non-invasive nature and the evidence that shows that DNAm from saliva shows better correlation with post-mortem brain tissue than blood (Smith AK et al, 2015). Therefore, in order to fully investigate the effect of preterm birth on the epigenome, a multiple sampling study which included maternal samples, placenta, cord blood and saliva from infants at birth and across their life-course would be required.

5.5 Conclusions

In conclusion, this chapter shows that the stress of preterm birth is associated with differential methylation in several protein-coding genes. These data include several promising neural candidate genes which could be involved in the pathogenesis of preterm white matter injury, neurodevelopmental and neuropsychiatric disorders. There are also a significant number of genes with involvement in immune function and oncogenic potential, demonstrating a mechanism for the link between early life stress and later life disease. The methylation array data was validated successfully using pyrosequencing.

By use of PNT to assess white matter integrity and principle component analysis, I was able to determine that there is an association between preterm neurological phenotype and the methylome which is modifiable by gender and early life nutritional factors. In this group, the association was subtle and therefore future work is required with more subjects. Future work should include a multiple sampling technique with assessment of the methylome at differential time points during pre and post-natal development.

Chapter 6: Discussion

6.1 Findings

I have demonstrated within this cohort of preterm infants at term, and with term controls, that preterm birth is associated with significant alterations to white matter integrity. Preterm infants with exposure to neuroprotective agents including antenatal steroids and magnesium sulphate have a quantifiable increase in white matter maturity in select regions, whilst those experiencing an episode of sepsis have a reduction.

The ROI approach used in this analysis was compared to a tract averaged technique and found to produce DTI parameters with limited agreement. The ROI approach may not be representative of the microstructural integrity of an entire white matter tract and can be subjective in nature. Therefore, a more objective method such as PNT may be preferable for assessing white matter integrity in an image linked epigenetic study.

From analysis of the entire methylome at term corrected age, I have shown that prematurity is associated with differential methylation in protein-coding genes with an identified role in neurological disease and neurodevelopment. In particular, there are several genes which can be linked to the pathogenic processes involved in white matter injury. There are also a significant number of genes with involvement in immune function and oncogenic potential, demonstrating a mechanism for the link between early life stress and later life disease. The methylation array data was validated successfully using pyrosequencing.

By use of PNT to assess white matter integrity and principle component analysis, I was able to determine that there is an association between preterm neurological phenotype and the methylome, which is modifiable by gender and early life nutritional factors.

6.2 Limitations

In chapter 3, 99 preterm and 26 term infants were recruited. However, 23 preterm and 7 term infants were lost post-consent for reasons that included a subsequent genetic diagnosis of Down Syndrome (n=1), and a further identification of PVL on structural MRI (n=1). Chromosomal abnormalities may lead to significant differences in DNA methylation as evidenced by recent investigation of the methylome in adults with Down syndrome, compared to control subjects (Jones MJ et al, 2013) and therefore this exclusion was important to ensure representative DNAm results. The loss of other subjects to illness (n =6) may have been prevented by seeking consent closer to term corrected age, thus identifying those who were unable to fulfil the inclusion criteria. Despite a protocol which included imaging infants in natural sleep with the aid of swaddling and suction molded head restraint, 12 infants were too unsettled for full DTI data capture (9.6%). Movement artefact also limited analysis in chapter 4 as 14 subjects (15%) from the 95 with DTI imaging were found to be unsuitable for PNT analysis due to difficulties in tract segmentation. As discussed, other groups have used sedation within their protocols (Counsell SJ et al, 2008 & Boardman JP et al, 2010) and this may have reduced post consent exclusion. A post-analysis correction was required between the preterm and term infants due to significant differences in PMA at time of scan and FA and MD have been shown to change rapidly during perinatal brain development (Huppi PS et al, 1998). Antenatal consent of term infants may have allowed the logistical organization of a cohort that was more closely matched in PMA at time of scan.

The exclusion of infants with haemorrhagic parenchymal infarction (HPI) and cystic PVL was considered valid, as these represent the minority of neonatal patients, which may have skewed

the results. Furthermore, in the case of severe injury, it may have been difficult to identify the correct regions for accurate placement of the ROI in DTI analysis. However, this subgroup is important, and indeed may benefit the most from research which includes protective strategies. Therefore, future work may include these patients, with a strategy that involves a separate subgroup analysis.

My results demonstrated alterations in white matter integrity after exposure to antenatal magnesium sulphate, corticosteroids and post-natal sepsis, however not all white matter regions were similarly affected and risk factors such as BPD, male gender and chorioamnionitis were not associated with any significant alteration. Power calculations were not possible for this study and therefore subject numbers were taken from precedent in the literature. I may have observed an effect with BPD, male gender or BPD in a larger cohort study. In addition, as concluded in chapter 3, ROI analysis may not offer the most complete representation of the preterm neurological phenotype and other methods such as TBSS, PNT or connectivity studies may offer additional information.

In chapter 4 I demonstrated that, in line with other ROI reliability studies (Lepomaki et al, 2012), the intra-observer agreement of FA and MD values produced by manual ROI placement in the gCC and PLIC was high. However, other groups have shown that inter-rater ROI analysis may be reduced to a 1/3rd of intra-user (Muller et al, 2006 & Ciccarelli et al, 2003). The evaluation of ROI methodology in this patient group could be improved by conducting inter-rater analysis and including other defined white matter areas such as the anterior limb of the internal capsule.

Our population of 36 preterm infants at TEA and 36 sex-matched term controls in chapter 5, were determined given patient numbers in other early life stress epigenome-wide human studies (Cruickshank MN et al, 2013; Labonte B et al, 2012; Khulan B et al, 2014). Due to time and logistical constraints, not all term infants had image-linked data available, which would be preferable for ongoing work.

The population studied in chapter 5, was predominantly of white British ethnic origin (94% term, 86% preterm). Recent studies have demonstrated that up to 75% of variation in DNA methylation between subgroups of subjects can be explained by genetic ancestry (Galanter JM et al, 2017). Therefore, although this is beneficial in that the differences observed in DNA methylation may not be significantly affected by ethnicity, it does mean that our results could vary significantly from patient groups found in other regions where there is more diversity.

Given the large quantity of data produced by the methylation array (>485,000 CpG probes), a bioinformatics expert was employed to process the data and run the statistical analysis. Analysis of this volume of data is subject to bias from sample processing and confounding experimental variables such as batch processing (Wright ML et al, 2016). Therefore, pre-processing and normalization stages were required to improve validity of the resulting data. Samples were filtered to ensure that they were of adequate quality using a control probe technique. A probe filtering step was used to remove unreliable or non-specific probes or those which overlapped with SNPs. The Illumina array has negative control probes, which allow for background intensity calculations. If a probe does not have a differential DNAm with p value of >0.01 compared to the negative control probes, it can be considered unreliable and therefore removed. SNPs are also removed as they can affect probe binding at the CpG site, lowering the signal artificially.

Normalisation of the data, allowed the true intensity signals to be analysed over any background artifact or 'noise'. It also allowed for harmonization of the differences in methylation discovered by the 2 probe types used in the assay (type I and type II probes). Finally, batch corrections were completed to account for any differences occurring from processing samples on different days, which was particularly relevant given that 12 samples were processed as part of an initial pilot study. From the 25 protein coding gene bodies and 58 protein coding gene promoters which showed differential DNAm in preterm infants compared to controls, 10 neural genes were identified using strict literature search criteria. This method is reliant on available literature and therefore future work may implicate other genes in neurological processes or disease. Principle component analysis enabled evaluation of the impact of clinical risk factors and the preterm neural phenotype (as determined by white matter integrity) on DNAm. However, after post-filtering and correction for multiple testing, only shape (*R)* of the right corticospinal tract and gender, in combination with duration of TPN, remained significantly associated with DNAm. Furthermore, no variable showed a significant effect when directly tested against the specific DMRs. This suggests that if there is an effect from these variables, it is subtle and distributed across many loci. As discussed in chapter 5, the choice of tissue type and time of sampling may alter results from both the methylation array and subsequent PCA analysis. In addition, increased patient numbers may reveal a more significant impact of clinical variables on DNAm.

6.3 Future Directions

This thesis has generated several questions for future investigation, including further evaluation of clinical risk factors such as inflammation, the effect of early-life stress on the epigenome and the impact of neuroprotective interventions on the preterm neurological phenotype.

Firstly, given my results which show that late-onset sepsis is associated with reduced white matter integrity in preterm infants at TEA, I would like to further investigate the impact of other inflammatory processes including chorioamnionitis, early-onset infection and late-onset-sepsis on the preterm neurological phenotype. I would complete DTI analysis using a tract-based technique (PNT) on preterm infants (<1500 grams or 32 weeks' gestation) at various developmental time-points including, within the first week of life, at term corrected age and at 2 years of age. I would include 8 major white matter fasciculi (genu and splenium of corpus callosum, left and right cingulum cingulate gyrus, left and right corticospinal tracts (CST) and left and right inferior longitudinal fasciculi). I would define infection as blood culture positive sepsis with signs of clinical instability and ensure chorioamnionitis was histologically defined. I would collect data on serum inflammatory markers including white blood cell count, platelets and CRP. I would also collect CSF in order to evaluate white cell count and presence of bacteria to identify meningitis or CNS infection. CSF could also be analysed for quinolinate which has been shown to be elevated in meningitis (Heyes MP et al, 1992) and in other neurological diseases such as Alzheimer's (Rahman A et al, 2009) and epilepsy (Feldblum S et al, 1988) as well as showing differential DNAm at QPRT (the enzyme which catabolises quinolinate) between preterm infants at TEA and term controls in my own work. As the collection of CSF is an invasive test, it may be limited to infants who are undergoing a lumbar puncture for suspected sepsis. Therefore, the

tissue specific effect of DNAm at QPRT and levels of quinolinate could be further investigated by employing an animal model of inflammation, by serum administration of LPS (lipopolysaccharide) (Silbereis JC et al, 2010). This temporal approach, as well as the investigation of a novel inflammatory marker such as quinolinate may allow early identification of those preterm infants at risk.

Secondly, as I have shown that preterm birth is associated with epigenetic changes at term equivalent age, I would like to investigate this in more detail with a candidate gene approach. Of particular interest is SLC1a2 (also known as EAAT2 or GLT-1). In my work, there is a reduction in DNAm at SLC1a2 (EAAT2) in preterm infants compared to term at TEA. Previous work has demonstrated that down-regulation of EAAT2 may be advantageous to neurodevelopment, particularly in the context of preterm white matter injury (Desilva TM et al, 2007 & 2008, Rajatileka S et al, 2017). In order to further investigate the effect of DNAm at SLC1a2 in relation to white matter injury, I would employ a multiple sampling approach with maternal samples, placenta, cord blood and saliva from preterm infants at birth, at TEA and 2 years of age. I would compare DNAm at SLC1a2 with white matter changes on DTI, using a tract based approach (PNT) in the 8 white matter regions mentioned above. I would include infants with PVL identified using cranial ultrasound screening. In order to investigate tissue specific DNAm of SLC1a2 and protein synthesis, an animal model of diffuse WMI (maternal sheep hypoxemia at 65% of gestation) could be utilized (Silbereis JC et al, 2010). This work would provide more information on the inheritance of DNAm at SLC1a2, its variation over time, how it relates to protein synthesis, its effect on the preterm neurological phenotype and its relation to PVL.

Finally, my work has demonstrated that antenatal administration of magnesium sulphate is associated with improved white matter integrity in select white matter regions in preterm infants at term equivalent age. Magnesium sulphate may partly exert a neuroprotective effect by effecting BBB permeability (Esen F et al, 2005; Euser AG et al, 2008), which renders the embryonic and newborn brain more vulnerable to circulating drugs and toxins than the adult brain (Saunders NR et al, 2012). Therefore, the effect of antenatal $MgSO_4$ treatment could be more thoroughly investigated by dynamic contrast enhanced MRI (DCE-MRI), a technique for studying BBB disruption in vivo (Heye AK et al, 2014). It involves introduction of a low molecular weight contrast agent, usually a Gadolinium (III)-based (Yan Y et al, 2017). Although these agents have been approved for clinical trials, they may not be acceptable for neonatal subjects. Therefore, an animal model of prematurity (Elovitz MA, 2004) could be used to assess BBB permeability in subjects who had been exposed to antenatal $MgSO_4$ compared to those who had not. It would also be interesting to replicate HCA or LOS as inflammation is also known to disrupt the BBB (Saunders NR et al, 2012) with the administration of LPS.

These future experiments, would allow a more comprehensive analysis of some of the risk and resilience factors associated with preterm white matter injury, and may lead to earlier identification of those at risk as well as the development of novel neuroprotective strategies.

References

- Abdolmaleky HM, Cheng KH, Faraone SV, et al. Hypomethylation of MB-COMT promoter is a major risk factor for schizophrenia and bipolar disorder. Hum Mol Genet 2006 15:3132–3145
- Aberg KA, McClay JL, Nerella S, et al. MBD-seq as a cost-effective approach for methylome-wide association studies: demonstration in 1500 case–control samples. Epigenomics. 2012;4(6):605–21.
- Aberg KA, McClay JL, Nerella S, et al. Methylome-Wide Association Study of Schizophrenia Identifying Blood Biomarker Signatures of Environmental Insults. JAMA Psychiatry. 2014;71(3):255-264.
- Agarwal R, Chiswick ML, Rimmer S et al. Antenatal steroids are associated with a reduction in the incidence of cerebral white matter lesions in very low birthweight infants. Arch Dis Child Fetal Neonatal Ed 2002;86: F96-F101.
- Alexander AL, Lee JE, Lazar M, et al. Field. Diffusion Tensor Imaging of the Brain. Neurotherapeutics. 2007; 4(3): 316–329
- Alexander JM, Gilstrap LC, Cox SM, et al. Clinical chorioamnionitis and the prognosis for very low birth weight infants. Obstet Gynecol. 1998; 91:725–729
- Allan AM, Liang X, Luo Y, et al. The loss of methyl-CpG binding protein 1 leads to autism-like behavioral deficits. Hum Mol Genet. 2008;17(13):2047-57.
- Als H, Duffy FH, McAnulty GB, et al. Early experience alters brain function and structure. Pediatrics. 2004;113(4):846-57.
- Amir RE, Van den Veyver IB, Wan M, et al. Rett syndrome is caused by mutations in X-linked MECP2, encoding methyl-CpG-binding protein 2. Nat Genet 1999, 23: 185–188,
- Anblagan D, Bastin ME, Sparrow S et al. Tract shape modeling detects changes associated with preterm birth and neuroprotective treatment effects. NeuroImage: Clinical 2015, DOI: 10.1016/j.nicl.2015.03.021
- Anblagan D, Pataky R, Evans MJ et al. Association between preterm brain injury and exposure to chorioamnionitis during fetal life. Sci. Rep (2016). 6, 37932
- Andresen CA, Smedegaard S, Sylvestersen KB, et al. Protein interaction screening for the ankyrin repeats and suppressor of cytokine signaling (SOCS) box (ASB) family identify Asb11 as a novel endoplasmic reticulum resident ubiquitin ligase. J Biol Chem. 2014;289(4):2043-54.
- Andrews WW, Cliver SP, Biasini F et al. Early preterm birth: association between in utero exposure to acute inflammation and severe neurodevelopmental disability at 6 years of age. Am J Obstet Gynecol. 2008;198(4): 466.e1-466.e11.
- Angiolillo AL, Sgadari C, Taub DD, et al. Human interferon-inducible protein 10 is a potent inhibitor of angiogenesis in vivo. J Exp Med. 1995;182(1):155-62.
- Anjari M, Srinivasan L, Allsop JM et al. Diffusion tensor imaging with tract-based spatial statistics reveals local white matter abnormalities in preterm infants NeuroImage 2007; 35: 1021–1027

- Arzoumanian Y, Mirmiran M, Barnes PD, et al. Diffusion tensor brain imaging findings at term-equivalent age may predict neurologic abnormalities in low birth weight preterm infants. AJNR Am J Neurorad 2003; 24: 1646–53.
- Back SA, Rosenberg PA. Pathophysiology of Glia in Perinatal White Matter Injury. Glia. 2014;62(11):1790-1815.
- Back SA, Miller SP. Brain injury in premature neonates: A primary cerebral dysmaturation disorder? Ann Neurol. 2014; 75(4):469-86.
- Back SA. Cerebral white and gray matter injury in newborns: New insights into pathophysiology and management. Clinics in perinatology. 2014;41(1):1-24.
- Badaruddin DH, Andrews GL, Bölte S, et al. Social and behavioral problems of children with agenesis of the corpus callosum. Child Psychiatry Hum Dev. 2007; 38:287–302.
- Ball G, Counsell SJ, Anjari M, et al. An optimised tract-based spatial statistics protocol for neonates: applications to prematurity and chronic lung disease. Neuroimage 2010 Oct 15; 53: 94e102. 14
- Barker DJ. The origins of the developmental origins theory. J Intern Med 2007;261(5):412–417.
- Bassi L, Ricci D, Volzone A, et al. Probabilistic diff usion tractography of the optic radiations and visual function in preterm infants at term equivalent age. Brain 2008; 131: 573–82.
- Basu S, Sladecek S, Martinez de la Peña y Valenzuela I, et al. CLASP2-dependent microtubule capture at the neuromuscular junction membrane requires LL5β and actin for focal delivery of acetylcholine receptor vesicles. Mol Biol Cell. 2015;26(5):938-51.
- Behrens TE, Berg HJ, Jbabdi S et al. Probabilistic diffusion tractography with multiple fibre orientations: what can we gain? Neuroimage 2007, 34 (1), 144– 155
- Behrens TE, Johansen-Berg H, Woolrich MW, et al. Non-invasive mapping of connections between human thalamus and cortex using diffusion imaging. Nat. Neurosci.2003, 6 (7), 750-57
- Billiards SS, Haynes RL, Folkerth RD, et al. Development of microglia in the cerebral white matter of the human fetus and infant. J Comp Neurol. 2006; 497:199–208.
- Bird A. DNA methylation patterns and epigenetic memory. Genes Dev. 2002; 16(1):6-21.
- Bisdas S, Bohning DE, Besenski N, et al. Reproducibility, interrater agreement and age-related changes of fractional anisotropy measures at 3 T in healthy subjects: effect of the applied b-value. Am J Neuroradiol. 2008, 29: 1128-1133. 10.3174/ajnr. A1044.
- Blencowe H, Cousens S, Oestergaard MZ, et al. National, regional, and worldwide estimates of preterm birth rates in the year 2010 with time trends since 1990 for selected countries: a systematic analysis and implications. Lancet. 2012; 379:2162–2172.
- Boardman JP, Counsell SJ, Rueckert D, et al. Early growth in brain volume is preserved in the majority of preterm infants. Ann Neurol 2007 Aug; 62: 185e92.
- Boardman JP, Craven C, Valappil S, et al. A common neonatal image phenotype predicts adverse neurodevelopmental outcome in children born preterm. Neuroimage 2010; 52:409-414.
- Bolisetty S, Dhawan A, Abdel-Latif M, et al. Intraventricular Hemorrhage and Neurodevelopmental Outcomes in Extreme Preterm Infants. Pediatrics 2014; 133:55–62

- Bonekamp D, Nagae LM, Degaonkar M, et al. Diffusion tensor imaging in children and adolescents: repeatability, hemispheric, and age-related differences. Neuroimage. 2007, 34: 733-742.
- Braga RM, Roze E, Ball G et al. Development of the Corticospinal and Callosal Tracts from Extremely Premature Birth up to 2 Years of Age. PLoS ONE 2015; 10(5): e0125681.
- Branco MR, Ficz G and Reik W. Uncovering the role of 5-hydroxymethylcytosine in the epigenome. Nature Reviews Genetics 2012, 13, 7-13
- Bresnick JN, Skynner HA, Chapman KL et al. Identification of signal transduction pathways used by orphan g protein-coupled receptors. Assay Drug Dev Technol. 2003 Apr;1(2):239-49.
- Bridges JP, Ludwig MG, Mueller M, et al. Orphan G protein-coupled receptor GPR116 regulates pulmonary surfactant pool size. Am J Respir Cell Mol Biol. 2013; 49(3):348-57.
- British Association of Perinatal Medicine. Fetal and Neonatal Brain Magnetic Resonance Imaging: Clinical Indications, Acquisitions and Reporting. A Framework for Practice July 2015
- Brock AJ, Kasus-Jacobi A, Lerner M, et al. The antimicrobial protein, CAP37, is upregulated in pyramidal neurons during Alzheimer's disease. Histochemistry and Cell Biology. 2015;144(4):293-308.
- Bromer C, Marsit CJ, Armstrong DA, et al. Genetic and Epigenetic Variation of the Glucocorticoid Receptor (NR3C1) in Placenta and Infant Neurobehavior. Developmental psychobiology. 2013;55(7):673-683.
- Calpe S, Wang N, Romero X, et al. The SLAM and SAP gene families control innate and adaptive immune responses. Adv Immunol. 2008; 97:177-250.
- Carl-McGrath S, Schneider-Stock R, Ebert M, et al. Differential expression and localisation of gasdermin-like (GSDML), a novel member of the cancer-associated GSDMDC protein family, in neoplastic and non-neoplastic gastric, hepatic, and colon tissues. Pathology. 2008;40(1):13-24.
- Chang Q, Khare G, Dani V, et al. The disease progression of Mecp2 mutant mice is affected by the level of BDNF expression. Neuron 2006, 49: 341–348.
- Chau V, Brant R, Poskitt KJ, et al. Postnatal infection is associated with widespread abnormalities of brain development in premature newborns. Pediatric research. 2012;71(3):274-279
- Chen XY, He QY, Guo MZ et al. XAF1 is frequently methylated in human esophageal cancer. World Journal of Gastroenterology: WJG. 2012;18(22):2844-2849.
- Chen YA, Lemire M, Choufani S, et al. Discovery of cross-reactive probes and polymorphic CpGs in the Illumina Infinium HumanMethylation450 microarray. Epigenetics 2013; 8: 203–209
- Chertoff M, Shrivastava K, Gonzalez B, et al. Differential modulation of TREM2 protein during postnatal brain development in mice. PLoS One 2013; 8: e72083
- Chou HY, Chou HT, Lee SC et al. CDK-dependent activation of poly(ADP-ribose) polymerase member 10 (PARP10). J Biol Chem. 2006;281(22):15201-7.
- Ciccarelli O, Parker GJ, Toosy AT, et al. From diffusion tractography to quantitative white matter tract measures: a reproducibility study. Neuroimage 2003; 18:348–59

- Clayden JD, Storkey AJ, Bastin ME. A Probabilistic Model-Based Approach to Consistent White Matter Tract Segmentation. IEEE Transactions on Medical Imaging. 2007; 26(11):1555-1561.
- Clayden, JD, Bastin, ME, Storkey, AJ. Improved segmentation reproducibility in group tractography using a quantitative tract similarity measure. Neuroimage. 2006; 33 (2) 482 – 492
- Conde-Agudelo A, Romero R. Antenatal magnesium sulfate for the prevention of cerebral palsy in preterm infants less than 34 weeks' gestation: a systematic review and metaanalysis. Am J Obstet Gynecol. 2009; 200:595–609
- Corrado L, Carlomagno Y, Falasco L, et al. A novel peripherin gene (PRPH) mutation identified in one sporadic amyotrophic lateral sclerosis patient. Neurobiol Aging. 2011;32(3): 552.e1-6.
- Costeloe K, et al. The EPICure Study: Outcomes to Discharge from Hospital for Infants Born at the Threshold of Viability. Pediatrics 2012; 106:4 659-671
- Counsell SJ, Edwards AD, Chew AT, et al. Specific relations between neurodevelopmental abilities and white matter microstructure in children born preterm. Brain 2008; 131:3201-3208.
- Counsell SJ, Maalouf EF, Fletcher AM et al. MR Imaging Assessment of Myelination in the Very Preterm Brain. AJNR Am J Neuroradiol. 2002; 23:872–881
- Counsell SJ, Shen Y, Boardman JP, et al. Axial and radial diffusivity in preterm infants who have diffuse white matter changes on magnetic resonance imaging at term-equivalent age. Pediatrics 2006; 117:376–86
- Crowther CA, Doyle LW, Haslam RR et al. Outcomes at 2 years of age after repeat doses of antenatal corticosteroids. N Engl J Med. 2007;357(12):1179-89.
- Cruickshank MN, Oshlack A, Theda C, et al. Analysis of epigenetic changes in survivors of preterm birth reveals the effect of gestational age and evidence for a long-term legacy. Genome Medicine. 2013;5(10):96. doi:10.1186/gm500.
- Dabney J, Meyer M. Length and GC-biases during sequencing library amplification: a comparison of various polymerase-buffer systems with ancient and modern DNA sequencing libraries. Biotechniques. 2012;52(2):87–94.
- Daly AC, Vizán P, Hill CS. Smad3 protein levels are modulated by Ras activity and during the cell cycle to dictate transforming growth factor-beta responses. J Biol Chem. 2010; 285(9):6489-97.
- Dann SG, Ryskin M, Barsotti AM, Golas J, Shi C, Miranda M et al. Reciprocal regulation of amino acid import and epigenetic state through Lat1 and EZH2. EMBO J 2015; 34: 1773–1785
- Das A, Dinh PX, Panda D, et al. Interferon-inducible protein IFI35 negatively regulates RIG-I antiviral signaling and supports vesicular stomatitis virus replication. J Virol. 2014;88(6):3103-13.
- de Kretser DM, Hedger MP, Loveland KL et al. Inhibins, activins and follistatin in reproduction. Hum Reprod Update. 2002;8(6):529-41.
- de Vries LS, Groenendaal F, van Haastert IC et al. Asymmetrical myelination of the posterior limb of the internal capsule in infants with periventricular haemorrhagic infarction; an early predictor of hemiplegia. Neuropediatrics 1999; 30, 314–319.

- de Vries LS, van H, I, Benders MJ, Groenendaal F. Myth: cerebral palsy cannot be predicted by neonatal brain imaging. Semin Fetal Neonatal Med 2011; 16:279-287.
- de Vries LS, van H, I, Rademaker KJ, et al. Ultrasound abnormalities preceding cerebral palsy in high-risk preterm infants. J Pediatr 2004; 144:815-820.
- Décaillot FM, Rozenfeld R, Gupta A, et al. Cell surface targeting of μ-δ opioid receptor heterodimers by RTP4. Proceedings of the National Academy of Sciences of the United States of America. 2008;105(41):16045-16050.
- Del Bigio MR. Cell proliferation in human ganglionic eminence and suppression after prematurity-associated haemorrhage. Brain. 2011;134(Pt 5):1344-61.
- Deoni SCL, Dean 3rd DC, O'Muircheartaigh J et al. Investigating white matter development in infancy and early childhood using myelin water faction and relaxation time mapping. Neuroimage 2012;63(3):1038–1053
- Deoni SCL, Mercure E, Blasi A et al. Mapping Infant Brain Myelination with Magnetic Resonance Imaging. The Journal of Neuroscience, 2011;31(2):784 –791
- Desilva TM, Billiards SS, Borenstein NS, et al. Glutamate transporter EAAT2 expression is up-regulated in reactive astrocytes in human periventricular leukomalacia. J Comp Neurol 2008; 508: 238–248.
- Desilva TM, Kinney HC, Borenstein NS, et al. The glutamate transporter EAAT2 is transiently expressed in developing human cerebral white matter. J Comp Neurol 2007; 501: 879–890.
- Dexter SC, Pinar H, Malee MP et al. Outcome of very low birth weight infants with histopathologic chorioamnionitis. Obstet Gynecol. 2000;96(2):172-7.
- Dhaifalah I, Andrys C, Drahosova M, et al. Azurocidin levels in maternal serum in the first trimester can predict preterm prelabor rupture of membranes. J Matern Fetal Neonatal Med. 2014;27(5):511-5.
- DiTommaso T, Cottle DL, Pearson HB, et al. Keratin 76 Is Required for Tight Junction Function and Maintenance of the Skin Barrier. PLoS Genet 2014. 10(10): e1004706.
- Dolgodilina E, Imobersteg S, Laczko E, et al. Brain interstitial fluid glutamine homeostasis is controlled by blood-brain barrier SLC7A5/LAT1 amino acid transporter. J Cereb Blood Flow Metab. 2016;36(11):1929-1941
- Dong Y, Speer CP. Late-onset neonatal sepsis: recent developments. Arch Dis Child Fetal Neonatal Ed. 2015;100(3): F257-63.
- Doyle LW, Anderson PJ, Haslam R et al. School-age outcomes of very preterm infants after antenatal treatment with magnesium sulfate vs placebo. JAMA, 312 (11) 2014:1105–1113
- Doyle LW, Crowther CA, Middleton P, et al. Magnesium sulphate for women at risk of preterm birth for neuroprotection of the fetus. Cochrane Database Syst Rev 2009;(1): CD004661.
- Drake AJ, McPherson RC, Godfrey KM, et al. An unbalanced maternal diet in pregnancy associates with offspring epigenetic changes in genes controlling glucocorticoid action and foetal growth. Clin Endocrinol (Oxf). 2012;77(6):808-15.
- Drake AJ, O'Shaughnessy PJ, Bhattacharya S et al. In utero exposure to cigarette chemicals induces sex-specific disruption of one-carbon metabolism and DNA methylation in the human fetal liver. BMC Medicine (2015) 13:18

- Drake AJ, Tang JI, Nyirenda MJ. Mechanisms underlying the role of glucocorticoids in the early life programming of adult disease. Clin Sci (Lond). 2007;113(5):219-32.
- Drake AJ, Walker BR and Seckl JR. Intergenerational consequences of fetal programming by in utero exposure to glucocorticoids in rats. Am. J.Physiol. Regul. Integr. Comp. Physiol. 2005; 288, R34–R38
- Drake AJ. and Walker BR. (2004) The intergenerational effects of fetal programming: non-genomic mechanisms for the inheritance of low birth weight and cardiovascular risk. J. Endocrinol. 180, 1–16
- Dubois J, Dehaene-Lambertz G, Kulikova S et al. The early development of brain white matter: a review of imaging studies in fetuses, newborns and infants. Neuroscience 2014;276:48-71
- Dudink J, Lequin M, van Pul C et al. Fractional anisotropy in white matter tracts of very-low-birth-weight infants. Pediatr Radiol. 2007; 37:1216–1223
- Dudink J, Larkman DJ, Kapellou O et al. High b-Value Diffusion Tensor Imaging of the Neonatal Brain at 3T. American Journal of Neuroradiology 2008, 29 (10) 1966-1972
- Duerden EG, Foong J, Chau V et al. Tract-Based Spatial Statistics in Preterm-Born Neonates Predicts Cognitive and Motor Outcomes at 18 Months. AJNR Am J Neuroradiol. 2015; 36(8):1565-71
- Dufour JH, Dziejman M, Liu MT, et al. IFN-gamma-inducible protein 10 (IP-10; CXCL10)-deficient mice reveal a role for IP-10 in effector T cell generation and trafficking. J Immunol. 2002;168(7):3195-204.
- Dziarski R, Gupta D. Review: Mammalian peptidoglycan recognition proteins (PGRPs) in innate immunity. Innate Immun. 2010;16(3):168-74.
- Ehrenkranz RA. Early nutritional support and outcomes in ELBW infants. Early Hum Dev. 2010;86 Suppl 1:21-5.
- Elovitz MA, Mrinalini C. Animal Models of Preterm Birth. Trends Endocrinol Metab. 2004; 15(10):479-87.
- Esen F, Erdem T, Aktan D, et al. Effect of magnesium sulfate administration on blood–brain barrier in a rat model of intraperitoneal sepsis: a randomized controlled experimental study. Critical Care. 2005;9(1): R18-R23.
- Euser AG, Bullinger L, Cipolla MJ. Magnesium sulphate treatment decreases blood-brain barrier permeability during acute hypertension in pregnant rats. Exp Physiol. 2008 Feb;93(2):254-61.
- Fabri M, Pierpaoli C, Barbaresi P, et al. Functional topography of the corpus callosum investigated by DTI and fMRI. World Journal of Radiology. 2014;6(12):895-906.
- Fan G, Beard C, Chen RZ, et al. DNA hypomethylation perturbs the function and survival of CNS neurons in postnatal animals. J Neurosci. 2001; 21:788-797
- Feldblum S, Rougier A, Loiseau H, et al. Quinolinic-phosphoribosyl transferase activity is decreased in epileptic human brain tissue. Epilepsia 1988; 29: 523–529
- Feng J, Zhou Y, Campbell SL, et al. Dnmt1 and Dnmt3a maintain DNA methylation and regulate synaptic function in adult forebrain neurons. Nat Neurosci. 2010; 13:423-430.
- Feng LY, Ou ZL, Wu FY, Shen ZZ, et al. Involvement of a novel chemokine decoy receptor CCX-CKR in breast cancer growth, metastasis and patient survival. Clin Cancer Res. 2009;15(9):2962-70.

- Fern R, Möller T. Rapid ischemic cell death in immature oligodendrocytes: a fatal glutamate release feedback loop. J Neurosci. 2000;20(1):34-42.
- Fernando F, Keijser R, Henneman P, et al. The idiopathic preterm delivery methylation profile in umbilical cord blood DNA. BMC Genomics 2015; 16: 736
- Fetita LS, Sobngwi E, Serradas P, et al, Consequences of fetal exposure to maternal diabetes in offspring. J. Clin. Endocrinol. Metab 2006; 91, 3718–3724
- Fields RD. A new mechanism of nervous system plasticity: activity-dependent myelination. Nature Reviews Neuroscience 2015; 16, 756–767
- Finer S, Mathews C, Lowe R, et al. Maternal gestational diabetes is associated with genome-wide DNA methylation variation in placenta and cord blood of exposed offspring. Hum Mol Genet. 2015;24(11):3021-9.
- Forabosco P, Ramasamy A, Trabzuni D, et al. Insights into TREM2 biology by network analysis of human brain gene expression data. Neurobiol Aging 2013; 34:2699–2714
- Fries GR, Li Q, McAlpin B et al. The role of DNA methylation in the pathophysiology and treatment of bipolar disorder. Neurosci Biobehav Rev. 2016; 68:474-488.
- Froeling M, Pullens P and Leemans A. DTI Analysis Methods: Region of Interest Analysis. Chapter in Diffusion Tensor Imaging. pp 175-182. Springer Link.
- Galanter JM, Gignoux CR, Oh SS, et al. Differential methylation between ethnic sub-groups reflects the effect of genetic ancestry and environmental exposures. Nordborg M, ed. eLife. 2017; 6:e20532.
- Gan C and Maingard J et al. The internal Capsule. Radiopedia. ttp://radiopaedia.org/articles/internal-capsule
- Garg V. Centrum Semiovale. Radiopedia. http://radiopaedia.org/articles/centrum-semiovale-1
- Ghadirivasfi M, Nohesara S, Ahmadkhaniha HR, et al. Hypomethylation of the serotonin receptor type-2A Gene (HTR2A) at T102C polymorphic site in DNA derived from the saliva of patients with schizophrenia and bipolar disorder. Am J Med Genet B Neuropsychiatr Genet. 2011;156B (5):536–45.
- Giedd JN et al. A quantitative MRI study of the corpus callosum in children and adolescents. Brain Research: Developmental Brain Research 1996; 91:274–80.
- Gilles FH and Nelson Jr. “Myelinated Tracts: growth patterns” pp 94-151 in The Developing Human Brain: Growth and adversities. Mac Keith Press 2012, London
- Gilmore JH, Lin W, Corouge I et al. Early Postnatal Development of Corpus Callosum and Corticospinal White Matter Assessed with Quantitative Tractography. AJNR Am J Neuroradiol 2007; 28:1789–95
- Glass HC, Shaw GM, Ma C, et al. Agenesis of the Corpus Callosum in California 1983−2003: A Population-Based Study. Am J Med Genet A. 2008; 146A (19): 2495–2500
- Graff J and Mansuy IM. Epigenetic dysregulation in cognitive disorders. Eur J Neurosci. 2009;30(1):1-8
- Graham DT, Cloke P and Vosper M. Principles of Radiological Physics 5th Edition. Churchill Livingstone Elsevier 2006
- Gros-Louis F, Larivière R, Gowing G. A frameshift deletion in peripherin gene associated with amyotrophic lateral sclerosis. J Biol Chem. 2004;279(44):45951-6.

- Guerreiro R, Bilgic B, Guven G, et al. Novel compound heterozygous mutation in TREM2 found in a Turkish frontotemporal dementia-like family. Neurobiol Aging 2013; 34: 2890–2895
- Guy A, Seaton SE, Boyle EM et al. Infants born late/moderately preterm are at increased risk for a positive autism screen at 2 years of age. J Pediatr. 2015;166(2):269-75. e3.
- Hadžić N, Bull LN, Clayton PT, et al. Diagnosis in bile acid-CoA: Amino acid N-acyltransferase deficiency. World Journal of Gastroenterology: WJG. 2012;18(25):3322-3326.
- Hakulinen U, Brander A, Ryymin P, et al. Repeatability and variation of region-of-interest methods using quantitative diffusion tensor MR imaging of the brain. BMC Medical Imaging 2012, 12:30
- Harder KW, Parsons LM, Armes J, et al. Gain- and loss-of-function Lyn mutant mice define a critical inhibitory role for Lyn in the myeloid lineage. Immunity. 2001;15(4):603-15.
- Hartel C, Adam N, Strunk T, et al. Cytokine responses correlate differentially with age in infancy and early childhood. Clin. Exp. Immunol 2005; 142:446–453
- Heijmans BT, Tobi EW, Stein AD, et al. Persistent epigenetic differences associated with prenatal exposure to famine in humans. Proc Natl Acad Sci USA 2008; 105:17046-9.
- Hendee WR and Ritenour ER. Medical Imaging Physics 4th Edition. Wiley-Liss 2002
- Herold A, Suyama M, Rodrigues JP, et al. TAP (NXF1) belongs to a multigene family of putative RNA export factors with a conserved modular architecture. Mol Cell Biol. 2000;20(23):8996-9008.
- Heuchan A, Evans N, Henderson S, et al. Perinatal risk factors for major intraventricular haemorrhage in the Australian and New Zealand Neonatal Network, 1995–97. Arch Dis Child Fetal Neonatal Ed. 2002; 86(2): F86–F90
- Heye AK, Culling RD, Valdés Hernández M del C, et al. Assessment of blood–brain barrier disruption using dynamic contrast-enhanced MRI. A systematic review. NeuroImage: Clinical. 2014; 6:262-274.
- Heyes MP, Saito K, Crowley JS, et al. Quinolinic acid and kynurenine pathway metabolism in inflammatory and non-inflammatory neurological disease. Brain. 1992;115 (Pt 5):1249-73.
- Hickman SE, El Khoury J. TREM2 and the neuroimmunology of Alzheimer's disease. Biochem Pharmacol. 2014;88(4):495-8.
- Hochberg Z, Feil R, Constancia M, et al. Child Health, Developmental Plasticity, and Epigenetic Programming. Endocrine Reviews. 2011;32(2):159-224.
- Huang C, Li Z, Wang M, et al. Early life exposure to the 1959-1961 Chinese famine has long-term health consequences. J Nutr 2010; 140:1874-8.
- Huang HS, Akbarian S. GAD1 mRNA expression and DNA methylation in prefrontal cortex of subjects with schizophrenia. PLoS ONE 2: e809, 2007.
- Huber MA, Kraut N, Park JE, et al. Fibroblast activation protein: differential expression and serine protease activity in reactive stromal fibroblasts of melanocytic skin tumors. J Invest Dermatol. 2003;120(2):182-8.
- Huppi PS and Dubois JS. Diffusion Tensor Imaging of Brain Development. Seminars in Fetal & Neonatal Medicine (2006) 11, 489e497

- Hüppi PS, Maier SE, Peled S, et al. Microstructural Development of Human Newborn Cerebral White Matter Assessed in Vivo by Diffusion Tensor Magnetic Resonance Imaging. Pediatric Research 1998; 44, 584–590
- Hüppi PS, Murphy B, Maier SE, et al. Microstructural brain development after perinatal cerebral white matter injury assessed by diffusion tensor magnetic resonance imaging. Pediatrics. 2001;107(3):455-60.
- Hutnick LK, Golshani P, Namihira M, et al. DNA hypomethylation restricted to the murine forebrain induces cortical degeneration and impairs postnatal neuronal maturation. Hum Mol Genet. 2009; 18:2875-2888.
- Inder TE, Wells SJ, Mogridge NB, et al. Defining the nature of the cerebral abnormalities in the premature infant: a qualitative magnetic resonance imaging study. Journal of Pediatrics 2003; 143(2):171-9
- Ishii M, Fei H, Friedman JM. Targeted disruption of GPR7, the endogenous receptor for neuropeptides B and W, leads to metabolic defects and adult-onset obesity. Proceedings of the National Academy of Sciences of the United States of America. 2003;100(18):10540-10545.
- Iwamoto K, Bundo M, Yamada K, et al. DNA methylation status of SOX10 correlates with its downregulation and oligodendrocyte dysfunction in schizophrenia. J Neurosci 2005; 25: 5376–5381
- Janciauskiene S. Conformational properties of serine proteinase inhibitors (serpins) confer multiple pathophysiological roles. Biochim Biophys Acta. 2001;1535(3):221-35.
- Jimenez C, Dang GT, Schultz PN et al. A novel point mutation of the RET protooncogene involving the second intracellular tyrosine kinase domain in a family with medullary thyroid carcinoma. J Clin Endocrinol Metab. 2004;89(7):3521-6.
- Johnson S (a), Hollis C, Kochhar P, et al. Autism spectrum disorders in extremely preterm children. J Pediatr. 2010;156(4):525-31. e2.
- Johnson S (b), Hollis C, Kochhar P, et al. Psychiatric disorders in extremely preterm children: longitudinal finding at age 11 years in the EPICure study. J Am Acad Child Adolesc Psychiatry. 2010;49(5):453-63. e1.
- Johnson S and Marlow N. Preterm Birth and Childhood Psychiatric Disorders. Pediatr Res. 2011;69(5 Pt 2):11R-8R
- Johnson S, Hennessy E, Smith R, et al. Academic attainment and special educational needs in extremely preterm children at 11 years of age: The EPICure study. Arch Dis Child Fetal Neonatal Ed. 2009;94(4): F283-9.
- Jones MJ, Farré P, McEwen LM, et al. Distinct DNA methylation patterns of cognitive impairment and trisomy 21 in down syndrome. BMC Medical Genomics. 2013; 6:58.
- Jones PA. Functions of DNA methylation: islands, start sites, gene bodies and beyond. Nature Reviews Genetics 2012; 13, 484-492
- Kasus-Jacobi A, Noor-Mohammadi S, Griffith GL, et al. A multifunctional peptide based on the neutrophil immune defense molecule, CAP37, has antibacterial and wound-healing properties. Journal of Leukocyte Biology. 2015;97(2):341-350.
- Katagiri C, Masuda K, Nomura M, et al. DUSP13B/TMDP inhibits stress-activated MAPKs and suppresses AP-1-dependent gene expression. Mol Cell Biochem. 2011;352(1-2):155-62.

- Keshavan M et al. Development of the corpus callosum in childhood, adolescence and early adulthood Life Sciences 70 2002; 1909–1922
- Khulan B, Manning, J, Dunbar, DR, et al. Epigenomic profiling of men exposed to early-life stress reveals DNA methylation differences in association with current mental state. Translational Psychiatry 2014, vol 4, pp. e448
- Khwaja O, Volpe JJ. Pathogenesis of cerebral white matter injury of prematurity. Archives of disease in childhood Fetal and neonatal edition. 2008;93(2): F153-F161.
- Klunemann HH, Ridha BH, Magy L, Wherrett JR, Hemelsoet DM, Keen RW et al. The genetic causes of basal ganglia calcification, dementia, and bone cysts: DAP12 and TREM2. Neurology 2005; 64: 1502–1507
- Kontis D, Catani M, Cuddy M, et al. Diffusion tensor MRI of the corpus callosum and cognitive function in adults born preterm. NeuroReport 2009; 20: 424–28.
- Krishnan ML, Dyet LE, Boardman JP, et al. Relationship between white matter apparent diff usion coefficients in preterm infants at term-equivalent age and developmental outcome at 2 years. Pediatrics 2007; 120: e604–09.
- Kuklisova-Murgasova M, Aljabar P, Srinivasan L, et al. A dynamic 4D probabilistic atlas of the developing brain. Neuroimage. 2011; 54(4):2750–2763
- Kumar R, Cheney KM, Neilsen PM, et al. CBFA2T3-ZNF651, like CBFA2T3-ZNF652, functions as a transcriptional corepressor complex. FEBS Lett. 2010;584(5):859-64.
- Kurushima H, Ramprasad M, Kondratenko N, et al. Surface expression and rapid internalization of macrosialin (mouse CD68) on elicited mouse peritoneal macrophages. J Leukoc Biol. 2000;67(1):104-8.
- Labonté B, Suderman M, Maussion G, et al. Genome-wide epigenetic regulation by early-life trauma. Arch Gen Psychiatry. 2012; 69:722–731
- Ladd-Acosta C, Hansen KD, Briem E, et al. Common DNA methylation alterations in multiple brain regions in autism. Mol Psychiatry 2014; 19: 862–871
- LaFleur DW, Nardelli B, Tsareva T, et al. Interferon-kappa, a novel type I interferon expressed in human keratinocytes. J Biol Chem. 2001;276(43):39765-71.
- Langbein L, Rogers MA, Winter H, et al. The catalog of human hair keratins. I. Expression of the nine type I members in the hair follicle. J. Biol. Chem 1999. 274: 19874-19884
- Lansbergen G, Grigoriev I, Mimori-Kiyosue Y, et al. CLASPs attach microtubule plus ends to the cell cortex through a complex with LL5beta. Dev Cell. 2006;11(1):21-32.
- Larroque B, Ancel PY, Marret S, et al. EPIPAGE Study group. Neurodevelopmental disabilities and special care of 5-year-old children born before 33 weeks of gestation (the EPIPAGE study): a longitudinal cohort study. Lancet. 2008;371(9615):813.
- Lee H, Jaffe AE, Feinberg JI, et al. DNA methylation shows genome-wide association of NFIX, RAPGEF2 and MSRB3 with gestational age at birth. International Journal of Epidemiology. 2012;41(1):188-199.
- Lee WH, Jang S, Lee JS, et al. Molecular cloning and expression of human keratinocyte proline-rich protein (hKPRP), an epidermal marker isolated from calcium-induced differentiating keratinocytes. J Invest Dermatol. 2005;125(5):995-1000.
- Lepomäki VK, Paavilainen TP, Hurme SA et al. Fractional anisotropy and mean diffusivity parameters of the brain white matter tracts in preterm infants: reproducibility of region-of-interest measurements. Pediatr Radiol 2012;42(2):175-82

- Levenson JM, Roth TL, Lubin FD, et al. Evidence that DNA (cytosine-5) methyltransferase regulates synaptic plasticity in the hippocampus. J Biol Chem. 2006; 281:15763-15773.
- Li E, Bestor TH, Jaenisch R. Targeted mutation of the DNA methyltransferase gene results in embryonic lethality. Cell. 1992; 69:915-926
- Lieberman J. Granzyme A activates another way to die. Immunol Rev. 2010 May;235(1):93-104.
- Lin Q, Shen J, Shen L, et al. Increased plasma levels of heparin-binding protein in patients with acute respiratory distress syndrome. Critical Care. 2013;17(4): R155.
- Linder N, Haskin O, Levit O, et al. Risk factors for intraventricular hemorrhage in very low birthweight premature infants: A retrospective case-control study. Pediatrics 2003;111: e590
- Linsell L, Malouf R, Morris J, et al. Prognostic Factors for Poor Cognitive Development in Children Born Very Preterm or With Very Low Birth Weight: A Systematic Review. JAMA Pediatr. 2015;169(12):1162-72.
- Lister R, Mukamel EA, Nery JR, et al. Global epigenomic reconfiguration during mammalian brain development. Science. 2013; 341:1237905.
- Liu F, Qi L, Liu B, et al. Fibroblast activation protein overexpression and clinical implications in solid tumors: a meta-analysis. PLoS One. 2015;10(3): e0116683.
- Liu HL, Golder-Novoselsky E, Seto MH, et al. The novel estrogen-responsive B-box protein (EBBP) gene is tamoxifen-regulated in cells expressing an estrogen receptor DNA-binding domain mutant. Mol Endocrinol. 1998; 12:1733–1748.
- Liu L, Johnson HL, Cousens S, et al. Global, regional, and national causes of child mortality: an updated systematic analysis for 2010 with time trends since 2000. Lancet. 2012; 379:2151–2161.
- Liu Y, Aeby A, Balériaux D, et al. White matter abnormalities are related to microstructural changes in preterm neonates at term-equivalent age: a diffusion tensor imaging and probabilistic tractography study. AJNR Am J Neuroradiol. 2012;33(5):839-45.
- Liu Y, Hoyo C, Murphy S, et al. DNA Methylation at Imprint Regulatory Regions in Preterm Birth and Infection. Am J Obstet Gynecol. 2013; 208(5)
- Loke YJ, Hannan AJ, Craig JM. The Role of Epigenetic Change in Autism Spectrum Disorders. Front Neurol. 2015; 6:107.
- Lorson MA, Dickson AM, Shaw DJ, et al. Identification and characterisation of a nuclear localisation signal in the SMN associated protein, Gemin4. Biochem Biophys Res Commun. 2008;375(1):33-7.
- Lowe R, Gemma C, Beyan H, et al. Buccals are likely to be a more informative surrogate tissue than blood for epigenome-wide association studies. Epigenetics 2013; 8: 445–454.
- Luders E, Thompson PM, Toga AW. The Development of the Corpus Callosum in the Healthy Human Brain. The Journal of Neuroscience, 2010: 30(33):10985–10990
- Lue LF, Schmitz C, Walker DG. What happens to microglial TREM2 in Alzheimer's disease: Immunoregulatory turned into immunopathogenic? Neuroscience 2015; 302:138–150
- Lumey LH, Stein AD, Kahn HS, et al. Lipid profiles in middle-aged men and women after famine exposure during gestation: the Dutch Hunger Winter Families Study. Am J Clin Nutr 2009; 89:1737-43.

- Luyt K, Slade TP, Dorward JJ et al. Developing oligodendrocytes express functional GABA(B) receptors that stimulate cell proliferation and migration. J Neurochem. 2007 Feb;100(3):822-40.
- Maalouf EF, Duggan PJ, Counsell SJ, et al. Comparison of findings on cranial ultrasound and magnetic resonance imaging in preterm infants. Pediatrics 2001; 107:719-727.
- MacKay DF, Smith GC, Dobbie R, et al. Gestational age at delivery and special educational need: retrospective cohort study of 407,503 schoolchildren. PLoS Med. 2010;7(6): e1000289.
- Mackay F, Schneider P. Cracking the BAFF code. Nat Rev Immunol. 2009;9(7):491-502.
- Mai H, Liu X, Chen Y et al. Hypermethylation of p15 gene associated with an inferior poor long-term outcome in childhood acute lymphoblastic leukemia. J Cancer Res Clin Oncol. 2016;142(2):497-504.
- Majnemer A, Riley P, Shevell M, et al. Severe bronchopulmonary dysplasia increases risk for later neurological and motor sequelae in preterm survivors. Dev Med Child Neurol. 2000;42(1):53-60.
- Malinger G, Zakut H, 1993. The corpus callosum: normal fetal development as shown by transvaginal sonography. AJR Am. J. Roentgenol. 161, 1041–1043.
- Mallolas J, Hurtado O, Castellanos M et al. A polymorphism in the EAAT2 promoter is associated with higher glutamate concentrations and higher frequency of progressing stroke. J Exp Med. 2006;203(3):711-7.
- Mallya M, Campbell RD, Aguado B. Transcriptional analysis of a novel cluster of LY-6 family members in the human and mouse major histocompatibility complex: five genes with many splice forms. Genomics. 2002;80(1):113-23.
- Mann SA, Versmold B, Marx R et al. Corticosteroids reverse cytokine-induced block of survival and differentiation of oligodendrocyte progenitor cells from rats. J Neuroinflammation. 2008; 5:39.
- Maragakis NJ, Rothstein JD. Glutamate transporters: animal models to neurologic disease. Neurobiol Dis. 2004;15(3):461-73.
- Marlow N, Wolke D, Bracewell MA and Samara M. Neurologic and developmental disability at six years of age after extremely preterm birth. N Engl J Med. 2005;352(1):9-19.
- Marsh DJ, Weingarth DT, Novi DE, et al. Melanin-concentrating hormone 1 receptor-deficient mice are lean, hyperactive, and hyperphagic and have altered metabolism. Proc Natl Acad Sci U S A. 2002;99(5):3240-5.
- McCrea HJ, Ment LR. The diagnosis, management, and postnatal prevention of intraventricular hemorrhage in the preterm neonate. Clin Perinatol. 2008;35(4):777-92, vii.
- McGowan PO, Sasaki A, D'Alessio AC, et al. Epigenetic regulation of the glucocorticoid receptor in human brain associates with childhood abuse. Nat Neurosci. 2009; 12:342–348.
- McGraw P, Liang L, Provenzale JM. Evaluation of normal age-related changes in anisotropy during infancy and childhood as shown by diffusion tensor imaging. Am J Roentgenol 2002; 179:1515–22

- McKay JA, Waltham KJ, Williams EA, et al. Folate depletion during pregnancy and lactation reduces genomic DNA methylation in murine adult offspring. Genes Nutr. 2011, 6,189–196.
- McNeal AS, Liu K, Nakhate V, et al. CDKN2B loss promotes progression from benign melanocytic nevus to melanoma. Cancer discovery. 2015;5(10):1072-1085.
- Meador-Woodruff JH, Davis KL, Haroutunian V et al. Abnormal kainate receptor expression in prefrontal cortex in schizophrenia. Neuropsychopharmacology. 2001;24(5):545-52.
- Melville JM, Moss TJM. The immune consequences of preterm birth. Frontiers in Neuroscience. 2013;7:79.
- Miller SP, Ferriero DM, Leonard C, et al. Early brain injury in premature newborns detected with magnetic resonance imaging is associated with adverse early neurodevelopmental outcome. J Pediatr. 2005; 147(5):609-16.
- Miller SP, Vigneron DB, Henry RG et al. Serial quantitative diffusion tensor MRI of the preterm brain: development in newborns with and without injury. J Magn Reson Imaging 2002; 16:621-32
- Mimmack ML, Ryan M, Baba H, et al. Gene expression analysis in schizophrenia: reproducible up-regulation of several members of the apolipoprotein L family located in a high-susceptibility locus for schizophrenia on chromosome 22. Proc Natl Acad Sci USA 2002; 99: 4680–4685
- Mirmiran M, Barnes PD, Keller K, et al. Neonatal Brain Magnetic Resonance Imaging Before Discharge Is Better Than Serial Cranial Ultrasound in Predicting Cerebral Palsy in Very Low Birth Weight Preterm Infants. Pediatrics 2004;114;992
- Missler M, Südhof TC. Neurexophilins form a conserved family of neuropeptide-like glycoproteins. J Neurosci. 1998;18(10):3630-8.
- Mitani A, Tanaka K. Functional changes of glial glutamate transporter GLT-1 during ischemia: an in vivo study in the hippocampal CA1 of normal mice and mutant mice lacking GLT-1. J Neurosci. 2003;23(18):7176-82.
- Mitha A, Foix-L'Hélias L, Arnaud C, et al. EPIPAGE Study Group. Neonatal infection and 5-year neurodevelopmental outcome of very preterm infants. Pediatrics. 2013;132(2): e372-80.
- Miyajima M, Nakajima M, Motoi Y, et al. Leucine-rich alpha2-glycoprotein is a novel biomarker of neurodegenerative disease in human cerebrospinal fluid and causes neurodegeneration in mouse cerebral cortex. PloS One 2013; 8: e74453.
- Moehle MS, Webber PJ, Tse T, et al. LRRK2 inhibition attenuates microglial inflammatory responses. J Neurosci. 2012;32(5):1602-11
- Moore LD, Le T, Fan G. DNA Methylation and Its Basic Function. Neuropsychopharmacology. 2013;38(1):23-38.
- Moore T, Hennessy EM, Myles J, et al. Neurological and developmental outcome in extremely preterm children born in England in 1995 and 2006: The EPICure studies. BMJ 2012; 345: e7961.
- Morizono H, Caldovic L, Shi D, et al. Mammalian N-acetylglutamate synthase. Mol Genet Metab. 2004;81 Suppl 1: S4-11.

- Moyon S, Huynh JI, Dutta D, et al. Functional Characterization of DNA Methylation in the Oligodendrocyte Lineage. Cell Reports, Elsevier Inc, 2016, 15, pp.1-13.
- Mueller BR, Bale TL. Sex-specific programming of offspring emotionality after stress early in pregnancy. J Neurosci. 2008;28(36):9055-65.
- Mukherjee P, Berman JI, Chung SW, et al. Diffusion tensor MR imaging and fiber tractography: theoretic underpinnings. AJNR Am J Neuroradiol. 2008;29(4):632-41.
- Mukherjee P, Miller JH, Shimony JS, et al. Normal brain maturation during childhood: developmental trends characterized with diffusion-tensor imaging. Radiology 2001;221: 349–358
- Muller MJ, Mazanek M, Weibrich C, et al. Distribution characteristics, reproducibility, and precision of region of interest-based hippocampal diffusion tensor imaging measures. Am J Neuroradiol 2006; 27:440–6
- Nagata-Kuroiwa R, Furutani N, Hara J, et al. Critical Role of Neuropeptides B/W Receptor 1 Signaling in Social Behavior and Fear Memory. PLoS ONE. 2011;6(2): e16972.
- Naidu S, Kaufmann WE, Abrams MT, et al. Neuroimaging studies in Rett syndrome. Brain Dev 23 Suppl 1: S62–S71, 2001
- Nakajima M, Miyajima M, Ogino I, et al. Brain localization of leucine-rich α2-glycoprotein and its role. Acta Neurochir Suppl. 2012; 113:97-101
- Naumova OY, Lee M, Koposov R, et al. Differential patterns of whole-genome DNA methylation in institutionalized children and children raised by their biological parents. Dev Psychopathol. 2012; 24:143–155
- Neil JJ, Shiran SI, McKinstry RC, et al. Normal brain in human newborns: apparent diffusion coefficient and diffusion anisotropy measured by using diffusion tensor MR imaging. Radiology 1998; 209:57-66
- Nemoda Z, Horvat-Gordon M, Fortunato CK, et al. Assessing genetic polymorphisms using DNA extracted from cells present in saliva samples BMC Medical Research Methodology 2011, 11:170
- NessAvier M. Basic Nuclear Magnetic Resonance 2008. www.simplyphysics.com
- Neubauer V, Junker D, Griesmaier E, et al. Bronchopulmonary dysplasia is associated with delayed structural brain maturation in preterm infants. Neonatology. 2015;107(3):179-84.
- Niebler S, Bosserhoff AK. The transcription factor activating enhancer-binding protein epsilon (AP-2ε) regulates the core promoter of type II collagen (COL2A1). FEBS J. 2013;280(6):1397-408.
- Nishida M, Makris N, Kennedy DN et al. Detailed semi automated MRI based morphometry of the neonatal brain: Preliminary results. NeuroImage 2006; 32 1:041 – 1049
- Nohesara S, Ghadirivasfi M, Mostafavi S, et al. DNA hypomethylation of MB-COMT promoter in the DNA derived from saliva in schizophrenia and bipolar disorder. J Psychiatr Res. 2011;45(11):1432–8.
- Nosarti C, Reichenberg A, Murray RM, et al. Preterm birth and psychiatric disorders in young adult life. Arch Gen Psychiatry 2012; 69: E1–E8.

- Nossin-Manor R, Card D, Morris D et al. Quantitative MRI in the very preterm brain: assessing tissue organization and myelination using magnetization transfer, diffusion tensor and T (1) imaging. Neuroimage. 2013; 64:505-16
- Novetsky AP, Zighelboim I, Thompson DM Jr, et al. Frequent mutations in the RPL22 gene and its clinical and functional implications. Gynecol Oncol. 2013;128(3):470-4.
- Nugent BM and McCarthy MM. Epigenetic influences on the developing brain: effects of hormones and nutrition. Advances in Genomics and Genetics 2015:5 215–225
- Odell ID, Newick K, Heintz NH, et al. Non-specific DNA binding interferes with the efficient excision of oxidative lesions from chromatin by the human DNA glycosylase, NEIL1. DNA Repair (Amst). 2010;9(2):134-43.
- O'Gorman RL, Bucher HU, Held U. Tract-based spatial statistics to assess the neuroprotective effect of early erythropoietin on white matter development in preterm infants. Brain. 2015;138(Pt 2):388-97.
- O'Kane RL, Hawkins RA. Na+-dependent transport of large neutral amino acids occurs at the abluminal membrane of the blood-brain barrier. Am J Physiol Endocrinol Metab 2003; 285: E1167–E1173.
- O'Mahony SM, Clarke G, Borre YE, et al. Serotonin, tryptophan metabolism and the brain-gut-microbiome axis. Behav Brain Res. 2015; 277:32-48.
- Pandit AS, Ball G, Edwards AD, Counsell SJ. Diffusion magnetic resonance imaging in preterm brain injury. Neuroradiology. 2013;55 Suppl 2:65-95.
- Pang Y, Campbell L, Zheng B et al. Lipopolysaccharide-activated microglia induce death of oligodendrocyte progenitor cells and impede their development. Neuroscience. 2010;166(2):464-75
- Papile LA, Burstein J, Burstein R et al. Incidence and evolution of subependymal and intraventricular hemorrhage: A study of infants with birth weight less than 1,500 gm. J Pediatr 1978;92:529-34.
- Paquette AG, Lesseur C, Armstrong DA, et al. Placental HTR2A methylation is associated with infant neurobehavioral outcomes. Epigenetics. 2013;8(8):796-801.
- Paquette AG, Lester BM, Koestler DC, et al. Placental FKBP5 Genetic and Epigenetic Variation Is Associated with Infant Neurobehavioral Outcomes in the RICHS Cohort. Potash JB, ed. PLoS ONE. 2014;9(8): e104913.
- Partridge S, Mukherjee P, Berman J et al. Tractography-Based Quantitation of Diffusion Tensor Imaging Parameters in White Matter Tracts of Preterm Newborns. Journal of Magnetic Resonance Imaging. 2005; 22:467–474
- Paul LK. Developmental malformation of the corpus callosum: a review of typical callosal development and examples of developmental disorders with callosal involvement. Journal of neurodevelopmental disorders. 2011;3(1):3-27.
- Piyasena C, Cartier J, Provençal N, et al. Dynamic Changes in DNA Methylation Occur during the First Year of Life in Preterm Infants. Frontiers in Endocrinology. 2016; 7:158.
- Plaisier A, Govaert P, Lequin M.H, and Dudink J. Optimal Timing of Cerebral MRI in Preterm Infants to Predict Long-Term Neurodevelopmental Outcome: A Systematic Review. AJNR 2013; 35:841– 47

- Porter RH, Eastwood SL, Harrison PJ et al. Distribution of kainate receptor subunit mRNAs in human hippocampus, neocortex and cerebellum, and bilateral reduction of hippocampal GluR6 and KA2 transcripts in schizophrenia. Brain Res 1997; 751: 217–231
- Poulter MO, Du L, Weaver IC, et al. GABAA receptor promoter hypermethylation in suicide brain: implications for the involvement of epigenetic processes. Biol Psychiatry 2008; 64: 645–652
- Provencal N, Suderman MJ, Guillemin C, et al. The signature of maternal rearing in the methylome in rhesus macaque prefrontal cortex and T cells. J Neurosci 2012; 32: 15626–15642.
- Provenzale JM, Liang L, DeLong D et al. Diffusion tensor imaging assessment of brain white matter maturation during the first postnatal year. AJR 2007; 189:476–486
- Rahman A, Ting K, Cullen KM, et al. The excitotoxin quinolinic acid induces tau phosphorylation in human neurons. PloS One 2009; 4: e6344
- Rajatileka S, Odd D, Robinson MT et al. Mol Neurobiol (2017). doi:10.1007/s12035-017-0462-1
- Ramprasad MP, Terpstra V, Kondratenko N, et al. Cell surface expression of mouse macrosialin and human CD68 and their role as macrophage receptors for oxidized low density lipoprotein. Proc Natl Acad Sci U S A. 1996;93(25):14833-8.
- Ravelli GP, Stein ZA, Susser MW. Obesity in young men after famine exposure in utero and early infancy. N Engl J Med 1976; 295:349-53.
- Ray KN, Lorch SA. Hospitalization of early preterm, late preterm, and term infants during the first year of life by gestational age. Hosp Pediatr. 2013;3(3):194-203.
- Rhein M, Hagemeier L, Klintschar M, et al. DNA methylation results depend on DNA integrity—role of post mortem interval. Front. Genet. 2015; 6:182.
- Ripellinoa JA, Neveb RL, and Howe JR et al. Expression and heteromeric interactions of non-N-methyl-d-aspartate glutamate receptor subunits in the developing and adult cerebellum. Neuroscience 1997; 82 (2): 485–497
- Ritchie K, Bora S, Woodward LJ. Social development of children born very preterm: a systematic review. Dev Med Child Neurol. 2015;57(10):899-918.
- Rogers CE, Smyser T, Smyser CD, et al. Regional White Matter Development in Very Preterm Infants: Perinatal Predictors and Early Developmental Outcomes. Pediatric research. 2016;79(1-1):87-95.
- Roloff TC, Ropers HH, Nuber UA. Comparative study of methyl-CpG-binding domain proteins. BMC Genomics. 2003; 4:1.
- Rose J, Butler EE, Lamont LE, et al. Neonatal brain structure on MRI and diffusion tensor imaging, sex and neurodevelopment in very-low-birthweight preterm children. Devel Med Child Neurol 2009; 51: 526–35.
- Rose J, Mirmiran J, Butler EE, et al. Neonatal microstructural development of the internal capsule on diffusion tensor imaging correlations with severity of gait and motor deficits. Devel Med Child Neurol 2007; 49: 745–50.
- Rose J, Vassar R, Cahill-Rowley K, et al. Neonatal physiological correlates of near-term brain development on MRI and DTI in very-low-birth-weight preterm infants. NeuroImage: Clinical. 2014; 5:169-177.

- Roth TL, Lubin FD, Funk AJ, et al. Lasting epigenetic influence of early-life adversity on the BDNF gene. Biol Psychiatry. 2009 May 1;65(9):760-9.
- Royal College of Obstetricians and Gynaecologists. Antenatal Corticosteroids to Reduce Neonatal Morbidity and Mortality. Green–top Guideline No. 7. October 2010.
- Roze E, Benders MJ, Kersbergen KJ, et al. Neonatal DTI early after birth predicts motor outcome in preterm infants with periventricular hemorrhagic infarction. Pediatr Res. 2015;78(3):298-303
- Rutherford M. MRI of the Neonatal Brain. 2012-2013. http://www.mrineonatalbrain.com/index.php
- Sakurai T. NPBWR1 and NPBWR2: Implications in Energy Homeostasis, Pain, and Emotion. Frontiers in Endocrinology. 2013; 4:23.
- Sass JO, Fischer K, Wang R, et al. D-glyceric aciduria is caused by genetic deficiency of D-glycerate kinase (GLYCTK). Hum Mutat. 2010;31(12):1280-5.
- Saunders NR, Liddelow SA, Dziegielewska KM. Barrier Mechanisms in the Developing Brain. Frontiers in Pharmacology. 2012; 3:46.
- Savman K, Nilsson UA, Blennow M et al. Non-protein-bound iron is elevated in cerebrospinal fluid from preterm infants with post hemorrhagic ventricular dilatation. Pediatric research 2001; 49(2):208-12.
- Schlapbach LJ, Aebischer M, Adams M. Impact of sepsis on neurodevelopmental outcome in a Swiss National Cohort of extremely premature infants. Pediatrics. 2011;128(2): e348-57.
- Schlapbach LJ, Ersch J, Adams M et al. Impact of chorioamnionitis and preeclampsia on neurodevelopmental outcome in preterm infants below 32 weeks gestational age. Acta Paediatr. 2010;99(10):1504-9
- Schmahmann JD, Smith EE, Eichler FS, et al. Cerebral White Matter: Neuroanatomy, Clinical Neurology, and Neurobehavioral Correlates. Annals of the New York Academy of Sciences. 2008; 1142:266-309.
- Schutyser E, Struyf S, Menten P, et al. Regulated production and molecular diversity of human liver and activation-regulated chemokine/macrophage inflammatory protein-3 alpha from normal and transformed cells. J Immunol. 2000;165(8):4470-7
- Shao L, Vawter MP. Shared gene expression alterations in schizophrenia and bipolar disorder. Biol Psychiatry 2008; 64: 89–97
- Shatrov JG, Birch SC, Lam LT et al. Chorioamnionitis and cerebral palsy: a meta-analysis. Obstet Gynecol. 2010; 116: 387-92
- Sheldon AL, Robinson MB. The role of glutamate transporters in neurodegenerative diseases and potential opportunities for intervention. Neurochem Int 2007; 51: 333–355.
- Shi L, Wu J. Epigenetic regulation in mammalian preimplantation embryo development. Reproductive Biology and Endocrinology: RB&E. 2009; 7:59.
- Shields A, Thomson M, Winter V et al. Repeated courses of antenatal corticosteroids have adverse effects on aspects of brain development in naturally delivered baboon infants. Pediatr Res. 2012;71(6):661-7
- Shirai R, Hirano F, Ohkura N et al. Up-regulation of the expression of leucine-rich alpha (2)-glycoprotein in hepatocytes by the mediators of acute-phase response. Biochem Biophys Res Commun. 2009;382(4):776-9.

- Shyu RY, Hsieh YC, Tsai FM, et al. Cloning and functional characterization of the HRASLS2 gene. Amino Acids. 2008;35(1):129-37
- Silbereis JC, Huang EJ, Back SA, et al. Towards improved animal models of neonatal white matter injury associated with cerebral palsy. Disease Models & Mechanisms. 2010;3(11-12):678-688.
- Simmons RK, Stringfellow SA, Glover ME, et al. DNA methylation markers in the postnatal developing rat brain. Brain Res.2013; 1533:26-36.
- Skiöld B, Horsch S, Hallberg B, et al. White matter changes in extremely preterm infants, a population-based diffusion tensor imaging study. Acta Paediatrica, 2010; 99: 842–849.
- Skiold B, Vollmer B, Bohm B, et al. Neonatal magnetic resonance imaging and outcome at age 30 months in extremely preterm infants. J Pediatr 2012; 160:559-566.
- Smith AK, Kilaru V, Klengel T, et al. DNA extracted from saliva for methylation studies of psychiatric traits: evidence tissue specificity and relatedness to brain. Am J Med Genet B 2015; 168B: 36–44.
- Smyth GK 2005. Limma: Linear models for microarray data. In: Gentleman R, Carey V, Huber W et al. Bioinformatics and Computational Biology Solutions using R and Bioconductor. Springer: New York, USA, 2005, pp 397–420.
- Soares JM, Marques P, Alves V, et al. A hitchhiker's guide to diffusion tensor imaging. Front Neurosci. 2013; 7:31.
- Song F, Mahmood S, Ghosh S, et al. Tissue specific differentially methylated regions (TDMR): Changes in DNA methylation during development. Genomics. 2009; 93(2):130-139.
- Soraisham AS, Trevenen C, Wood S, et al. Histological chorioamnionitis and neurodevelopmental outcome in preterm infants. J Perinatol. 2013;33(1):70-5.
- Sotiriadis A, Tsiami A, Papatheodorou S, et al. Neurodevelopmental Outcome After a Single Course of Antenatal Steroids in Children Born Preterm: A Systematic Review and Meta-analysis. Obstet Gynecol. 2015;125(6):1385-96.
- St Clair D, Xu M, Wang P, et al. Rates of adult schizophrenia following prenatal exposure to the Chinese famine of 1959-1961. JAMA 2005; 294:557-62.
- Stepanow S, Reichwald K, Huse K, et al. Allele-Specific, Age-Dependent and BMI-Associated DNA Methylation of Human MCHR1. Suter CM, ed. PLoS ONE. 2011;6(5): e17711.
- Stewart AL, Rifkin L, Amess PN et al. Brain structure and neurocognitive and behavioral function in adolescents who were born very preterm. Lancet 1999; 353: 1653–57
- Stewart AL, Thorburn RJ, Hope PL et al. Ultrasound appearance of the brain in very preterm infants and neurodevelopmental outcome at 18 months of age. Arch Dis Child 1983; 58:598-604.
- Stoll BJ, Hansen NI, Adams-Chapman I, et al. Neurodevelopmental and Growth Impairment Among Extremely Low-Birth-Weight Infants with Neonatal Infection. JAMA. 2004;292(19):2357-2365.
- Stoll BJ, Hansen N, Fanaroff AA, et al. Late-onset sepsis in very low birth weight neonates: the experience of the NICHD Neonatal Research Network. Pediatrics. 2002;110(2 Pt 1):285-91.

- Strunk T, Currie A, Richmond P, et al. Innate immunity in human newborn infants: prematurity means more than immaturity. J Matern Fetal Neonatal Med. 2011;24(1):25-31.
- Sucksdorff M, Lehtonen L, Chudal R, et al. Preterm Birth and Poor Fetal Growth as Risk Factors of Attention-Deficit/ Hyperactivity Disorder. Pediatrics. 2015;136(3): e599-608.
- Sundrani DP, Reddy US, Joshi AA, et al. Differential placental methylation and expression of VEGF, FLT-1 and KDR genes in human term and preterm preeclampsia. Clinical Epigenetics 2013, 5:6
- Susser E and Lin SP. Schizophrenia after prenatal exposure to the Dutch Hunger Winter of 1944-1945. Arch Gen Psychiatry 1992; 49:983-988
- Suter M, Abramovici A, Showalter L, et al. In utero tobacco exposure epigenetically modifies placental CYP1A1 expression. Metabolism. 2010;59(10):1481-1490
- Tanaka-Arakawa MM, Matsui M, Tanaka C, et al. Developmental Changes in the Corpus Callosum from Infancy to Early Adulthood: A Structural Magnetic Resonance Imaging Study. PLoS ONE 2015: 10(3): e0118760.
- Teschendorff AE, Marabita F, Lechner M et al. A beta-mixture quantile normalization method for correcting probe design bias in Illumina Infinium 450 k DNA methylation data. Bioinformatics 2013; 29:189–196
- Thompson DK, Inder TE, Faggian N et al. Corpus callosum alterations in very preterm infants: perinatal correlates and 2 year neurodevelopmental outcomes. Neuroimage 2012; 59:3571–81
- Thompson DK, Inder TE, Faggian N, et al. Characterization of the corpus callosum in very preterm and full-term infants utilizing MRI. NeuroImage 55, 2011; 479–490
- Thompson DK, Chen J, Beare R et al. Structural connectivity relates to perinatal factors and functional impairment at 7years in children born very preterm. Neuroimage. 2016; 134:328-37.
- Thummel KE, Wilkinson GR. In vitro and in vivo drug interactions involving human CYP3A. Annu. Rev. Pharmacol. Toxicol., 38 1998; pp. 389–430
- Tobi EW, Lumey LH, Talens RP, et al. DNA methylation differences after exposure to prenatal famine are common and timing- and sex specific. Hum Mol Genet 2009; 18:4046-53.
- Toulza E, Mattiuzzo NR, Galliano MF, et al. Large-scale identification of human genes implicated in epidermal barrier function. Genome Biol. 2007;8(6): R107.
- Tyrka AR, Parade SH, Welch ES, et al. Methylation of the leukocyte glucocorticoid receptor gene promoter in adults: associations with early adversity and depressive, anxiety and substance-use disorders. Transl Psychiatry. 2016;6(7): e848.
- Tyrka AR, Price LH, Marsit C, et al. Childhood adversity and epigenetic modulation of the leukocyte glucocorticoid receptor: preliminary findings in healthy adults. PLoS One. 2012;7: e30148.
- Ursini G, Bollati V, Fazio L, et al. Stress-related methylation of the catechol-O-methyltransferase Val 158 allele predicts human prefrontal cognition and activity. J. Neurosci. 2011; 31:6692–6698.
- Valkama AM, Paakko EL, Vainionpaa LK, et al. Magnetic resonance imaging at term and neuromotor outcome in preterm infants. Acta Paediatr 2000; 89:348-355.

- van Kooij BJ, de Vries LS, Ball G et al. Neonatal tract-based spatial statistics findings and outcome in preterm infants. AJNR 2012;33: 188–19
- van Kooij BJ, van Pul C, Benders MJ et al. Fiber tracking at term displays gender differences regarding cognitive and motor outcome at 2 years of age in preterm infants. Pediatr Res. 2011;70(6):626-32
- Van Raemdonck K, Berghmans N, Vanheule V, et al. Angiostatic, tumor inflammatory and anti-tumor effects of CXCL447–70 and CXCL4L147–70 in an EGF-dependent breast cancer model. Oncotarget. 2014;5(21):10916-10933.
- Volpe JJ, Kinney HC, Jensen FE, et al. The developing oligodendrocyte: key cellular target in brain injury in the premature infant. Int J Dev Neurosci 2011; 29(4): 423–440.
- Volpe JJ. Neurobiology of periventricular leukomalacia in the premature infant. Pediatr Res. 2001;50(5):553-62.
- Walton E, Pingault JB, Cecil CA, et al. Epigenetic profiling of ADHD symptoms trajectories: a prospective, methylome-wide study. Mol Psychiatry. 2016; 22(2):250-256.
- Wan G, Zhaorigetu S, Liu Z, et al. Apolipoprotein L1, a Novel Bcl-2 Homology Domain 3-only Lipid-binding Protein, Induces Autophagic Cell Death. The Journal of Biological Chemistry. 2008;283(31):21540-21549.
- Wang H, Li Y, Wang Y, et al. C9orf100, a new member of the Dbl-family guanine nucleotide exchange factors, promotes cell proliferation and migration in hepatocellular carcinoma. Mol Med Rep. 2012;5(5):1169-74.
- Watanabe N, Wada M, Irukayama-Tomobe Y, et al. A single nucleotide polymorphism of the neuropeptide B/W receptor-1 gene influences the evaluation of facial expressions. PloS One 2012; 7: e35390.
- Weaver IC, Cervoni N, Champagne FA, et al. Epigenetic programming by maternal behavior. Nat Neurosci. 2004;7(8):847–854.
- Welker KM and Patton A. Assessment of Normal Myelination with Magnetic Resonance Imaging. Semin Neurol 2012; 32:15–28.
- Westin CF, Maier SE, Mamata H, et al. Processing and visualization for diffusion tensor MRI. Medical Image Analysis, 2002; 93–108
- Wice BM, Gordon JI. A tetraspan membrane glycoprotein produced in the human intestinal epithelium and liver that can regulate cell density-dependent proliferation. J Biol Chem. 1995;270(37):21907-18.
- Wimberger DM, Roberts TP, Barkovich AJ et al. Identification of ‘‘premyelination’’ by diffusion-weighted MRI. J Comput Assist Tomogr. 1995;19(1):28-33
- Witelson SF. Hand and sex differences in the isthmus and genu of the human corpus callosum: a postmortem morphological study. Brain 1989; 112:799–835.
- Wittmann G, Mohácsik P, Balkhi MY, et al. Endotoxin-induced inflammation down-regulates L-type amino acid transporter 1 (LAT1) expression at the blood-brain barrier of male rats and mice. Fluids Barriers CNS. 2015; 12:21.
- Wockner LF, Noble EP, Lawford BR, et al. Genome-wide DNA methylation analysis of human brain tissue from schizophrenia patients. Transl Psychiatry 2014; 4, e339
- Wojdacz TK, Møller TH, Thestrup BB, et al. Limitations and advantages of MS-HRM and bisulfite sequencing for single locus methylation studies. Expert Rev Mol Diagn. 2010; 10(5):575-80.

- Wolf R, Ruzicka T, Yuspa SH. Novel S100A7 (psoriasin)/S100A15 (koebnerisin) subfamily: highly homologous but distinct in regulation and function. Amino Acids. 2011;41(4):789-96.
- Wolfe I, Macfarlane A, Donkin A, et al. Why children die: death in infants, children and young people in the UK Part A. May 2014. Royal College of Paediatrics and Child Health, National Children's Bureau and British Association for Child and Adolescent Public Health
- Woodward LJ, Anderson PJ, Austin NC, et al. Neonatal MRI to Predict Neurodevelopmental Outcomes in Preterm Infants. N Engl J Med 2006; 355:685-94
- Wright ML, Dozmorov MG, Wolen AR et al. Establishing an analytic pipeline for genome-wide DNA methylation. Clinical Epigenetics 2016; 8:45
- Yan Y, Sun X, Shen B. Contrast agents in dynamic contrast-enhanced magnetic resonance imaging. Oncotarget. 2017; 8(26):43491-43505.
- Ylijoki M, Lehtonen L, Lind A, et al; PIPARI Study Group. Chorioamnionitis and Five-Year Neurodevelopmental Outcome in Preterm Infants. Neonatology. 2016;110(4):286-295.
- Yoon BH, Romero R, Moon JB, et al. Clinical significance of intra-amniotic inflammation in patients with preterm labor and intact membranes. Am J Obstet Gynecol. 2001; 185:1130.
- Zanin E, Ranjeva JP, Confort-Gouny S et al. White matter maturation of normal human fetal brain. An in vivo diffusion tensor tractography study. Brain Behav. 2011;1(2):95-108
- Zhang ZM, Wang Y, Huang R, et al. TFAP2E hypermethylation was associated with survival advantage in patients with colorectal cancer. J Cancer Res Clin Oncol. 2014;140(12):2119-27
- Zhao J, Liem RK. α-Internexin and Peripherin: Expression, Assembly, Functions, and Roles in Disease. Methods Enzymol. 2016; 568:477-507.
- Zhao X, Ueba T, Christie BR, et al. Mice lacking methyl-CpG binding protein 1 have deficits in adult neurogenesis and hippocampal function. Proc Natl Acad Sci U S A. 2003; 100(11):6777-82.
- Zhaorigetu S, Wan G, Kaini R et al. ApoL1, a BH3-only lipid-binding protein, induces autophagic cell death. Autophagy. 2008;4(8):1079-82.
- Zhou L, Azfer A, Niu J, et al. Monocyte chemoattractant protein-1 induces a novel transcription factor that causes cardiac myocyte apoptosis and ventricular dysfunction. Circ. Res. 2006; 98: 1177-1185